

# TEHNIČKI GLASNIK

TEHNIČKI GLASNIK / TECHNICAL JOURNAL – GODIŠTE / VOLUME 12 – BROJ / NUMBER 2

LIPANJ 2018 / JUNE 2018 – STRANICA / PAGES 62-123



SVEUČILIŠTE SJEVER / UNIVERSITY NORTH – CROATIA – EUROPE

ISSN 1846-6168 (PRINT) / ISSN 1848-5588 (ONLINE)

# TECHNICAL JOURNAL

**TEHNIČKI GLASNIK - TECHNICAL JOURNAL**

Scientific-professional journal of University North

Volume 12

Number 2

Varaždin, April-June 2018

Pages 62–123

**Editorial Office:**

Sveučilište Sjever – Tehnički glasnik  
Sveučilišni centar Varaždin  
104. brigade 3, 42000 Varaždin, Hrvatska  
Tel. ++385 42 493 328, Fax. ++385 42 493 333  
E-mail: [tehnickiglasnik@unin.hr](mailto:tehnickiglasnik@unin.hr)  
<https://tehnickiglasnik.unin.hr>  
<https://www.unin.hr/djelatnost/izdavastvo/tehnicki-glasnik/>  
<https://hrcak.srce.hr/tehnickiglasnik>

**Founder and Publisher:**

Sveučilište Sjever / University North

**Council of Journal:**

Marin MILKOVIĆ, Chairman; Anica HUNJET, Member; Goran KOZINA, Member; Mario TOMIŠA, Member;  
Vlado TROPŠA, Member; Damir VUSIĆ, Member; Milan KLJAJIN, Member; Anatolii KOVROV, Member

**Editorial Board:**

Chairman Damir VUSIĆ (1), Milan KLJAJIN (2)/(1), Marin MILKOVIĆ (1), Krešimir BUNTAK (1), Anica HUNJET (1), Živko KONDIĆ (1), Goran KOZINA (1), Ljudevit KRPAN (1), Marko STOJIC (1), Božo SOLDI (1), Mario TOMIŠA (1), Vlado TROPŠA (1), Vinko VIŠNJIĆ (1), Duško PAVLETIĆ (5), Branimir PAVKOVIĆ (5), Mile MATIJEVIĆ (3), Damir MODRIĆ (3), Nikola MRVAC (3), Klaudio PAP (3), Ivana ŽILJAK STANIMIROVIĆ (3), Krešimir GRILEC (6), Biserka RUNJE (6), Predrag ČOSIĆ (6), Sara HAVRLIŠAN (2), Dražan KOZAK (2), Roberto LUJIĆ (2), Leon MAGLIĆ (2), Ivan SAMARDŽIĆ (2), Antun STOIC (2), Katica ŠIMUNOVIĆ (2), Goran ŠIMUNOVIĆ (2), Ladislav LAZIĆ (7), Ante ČIKIĆ (8)/(1)/(2), Darko DUKIĆ (9), Gordana DUKIĆ (10), Srđan MEDIC (11), Sanja KALAMBURA (12), Marko DUNĐER (13), Zlata DOLÁČEK-ALDUK (4), Dina STÖBER (4)

**International Editorial Council:**

Boris TOVORNIK (14), Milan KUHTA (15), Nenad INJAC (16), Džafer KUDUMOVIC (17), Marin PETROVIĆ (18), Salim IBRAHIMEFENDIĆ (19), Zoran LOVREKOVIĆ (20), Igor BUDAK (21), Darko BAJIĆ (22), Tomáš HANÁK (23), Nikolaj SURIANINOV (24), Evgenij KLIMENKO (24), Oleg POPOV (24), Ivo ČOLAK (25)

**Editor-in-Chief:**

Milan KLJAJIN

**Technical Editor:**

Goran KOZINA

**Graphics Editor:**

Snježana IVANČIĆ VALENKO, Anja ZORKO

**Linguistic Advisers for English language:**

Ivana GRABAR, Iva GRUBJEŠIĆ

**IT support:**

Davor LEVANIĆ

**Print:**

Centar za digitalno nakladništvo, Sveučilište Sjever

**All manuscripts published in journal have been reviewed.****Manuscripts are not returned.****The journal is free of charge and four issues per year are published.****Circulation:** 100 copies**Journal is indexed and abstracted in:**

Web of Science Core Collection (Emerging Sources Citation Index - ESCI), EBSCOhost Academic Search Complete, EBSCOhost – One Belt, One Road Reference Source Product, ERIH PLUS, CITEFACTOR – Academic Scientific Journals, Hrcak - Portal znanstvenih časopisa RH

**Registration of journal:**

The journal "Tehnički glasnik" is listed in the HGK Register on the issuance and distribution of printed editions on the 18<sup>th</sup> October 2007 under number 825.

**Preparation ended:**

June 2018

**Legend:**

(1) University Nord, (2) Mechanical Engineering Faculty in Slavonski Brod, (3) Faculty of Graphic Arts Zagreb, (4) Faculty of Civil Engineering Osijek, (5) Faculty of Engineering Rijeka, (6) Faculty of Mechanical Engineering and Naval Architecture Zagreb, (7) Faculty of Metallurgy Sisak, (8) Bjelovar University of Applied Sciences, (9) Department of Physics of the University of Josip Juraj Strossmayer in Osijek, (10) Faculty of Humanities and Social Sciences Osijek, (11) Karlovac University of Applied Sciences, (12) University of Applied Sciences Velika Gorica, (13) Department of Polytechnics - Faculty of Humanities and Social Sciences Rijeka, (14) Faculty of Electrical Engineering and Computer Science - University of Maribor, (15) Faculty of Civil Engineering - University of Maribor, (16) University College of Teacher Education of Christian Churches Vienna/Krems, (17) Mechanical Engineering Faculty Tuzla, (18) Mechanical Engineering Faculty Sarajevo, (19) University of Travnik - Faculty of Technical Studies, (20) Higher Education Technical School of Professional Studies in Novi Sad, (21) University of Novi Sad - Faculty of Technical Sciences, (22) Faculty of Mechanical Engineering - University of Montenegro, (23) Brno University of Technology, (24) Odessa State Academy of Civil Engineering and Architecture, (25) Faculty of Civil Engineering - University of Mostar

<b>CONTENT</b>	<b>I</b>
<b>NOTE FROM THE EDITOR-IN-CHIEF</b>	<b>II</b>
Andrija BERNIK, Dinko GALETIC <b>REMOTE RENDERING CONTROL USING PYTHON SCRIPTS AND DROPBOX TECHNOLOGY</b>	<b>62</b>
Željko BARAČ, Ivan PLAŠČAK, Tomislav JURIĆ, Mladen JURIŠIĆ, Domagoj ZIMMER, Ivan VIDAKOVIĆ, Davor PETROVIĆ, Vinko DUVNJAK, Monika MARKOVIĆ <b>OPERATOR'S WHOLE BODY VIBRATIONS DEPENDENT OF AGROTECHNICAL SURFACE, SPEED OF MOVEMENT AND SEAT UPHOLSTERY</b>	<b>68</b>
Seval UYANIK, Hatice Kübra KAYNAK <b>A COMPARATIVE STUDY ON THE PERFORMANCE PROPERTIES OF BREATHABLE AND NON-BREATHABLE BABY DIAPER BACK SHEET</b>	<b>74</b>
Kamil Neyfel ÇERÇİ, Özge SÜFER, Mustafa SÖYLER, Ertuç HÜRDOĞAN, Coşkun ÖZALP <b>THIN LAYER DRYING OF ZUCCHINI IN SOLAR DRYER LOCATED IN OSMANIYE REGION</b>	<b>79</b>
Branko TOMIČIĆ, Ladislav HAVAŠ, Dunja SRPAK <b>INFLUENCE OF STRANDS TRANSPOSITION ON CURRENT DISTRIBUTION AND POWER LOSSES IN WINDINGS OF AC MACHINES</b>	<b>86</b>
Volodymyr VOLCHUK, Ievgenii KLYMENKO, Sergii KROVIAKOV, Matija OREŠKOVIĆ <b>METHOD OF MATERIAL QUALITY ESTIMATION WITH USAGE OF MULTIFRACTAL FORMALISM</b>	<b>93</b>
Simon MUHIČ, Ante ČIKIĆ, Jadran PIŠTAN, Marinko STOJKOV, Mladen BOŠNJAKOVIĆ <b>TRANSPORT EMISSIONS AND ELECTRIC MOBILITY IN PRIVATE TRANSPORT IN THE REPUBLIC OF SLOVENIA</b>	<b>98</b>
Yusuf FEDAI, Funda KAHRAMAN, Hediye KIRLI AKIN, Gokhan BASAR <b>OPTIMIZATION OF MACHINING PARAMETERS IN FACE MILLING USING MULTI-OBJECTIVE TAGUCHI TECHNIQUE</b>	<b>104</b>
Emine AVŞAR AYDIN <b>A PRELIMINARY STUDY FOR EARLY BREAST CANCER DETECTION WITH MICROWAVES</b>	<b>109</b>
Ivica KANIŠKI, Ivan VINCEK <b>SUCCESS MEASUREMENT OF BUSINESS PROCESSES</b>	<b>113</b>
Nataša LONČARIĆ, Damira KEČEK, Marko KRALJIĆ <b>MATRICES IN COMPUTER GRAPHICS</b>	<b>120</b>
<b>INSTRUCTIONS FOR AUTHORS</b>	<b>IV</b>



## Note from the Editor-in-Chief

Dear readers,

In order for the journal to be included in some other index databases (e.g. INSPEC, Scopus, Ei Compendex, etc.), much work needs to be done regarding the Editorial Board and the International Editorial Council, as well as the membership in CrossRef which enables the use of the DOI numbers and brings other benefits.

Instead of the usual foreword I have decided to repeat some important things about duties of reviewers which you can find also on

<https://tehnickiglasnik.unin.hr/reviewers.php>.

Peer reviews assist the editor in making editorial decisions and through the editorial communications with the author may also assist the author in improving the paper. Any selected reviewer who feels unqualified to review the research reported in a manuscript or knows that its prompt review will be impossible should notify the editor and excuse himself from the review process. Any manuscripts received for review must be treated as confidential documents. They must not be shown to or discussed with others unless authorized by the editor. Under double-blind review the identity of the reviewers and the authors are hidden from each other. This level of anonymity is designed to encourage fairness, with papers being considered on their individual merits. Reviews should be conducted objectively. Personal criticism of the author is inappropriate. Reviewers should express their views clearly with supporting arguments.

Reviewers should identify relevant published work that has not been cited by the authors. Any statement that an observation, derivation, or argument had been previously reported should be accompanied by the relevant citation. A reviewer should also call to the editor's attention any substantial similarity or overlap between the manuscript under consideration and any other published paper of which they have personal knowledge.

Privileged information or ideas obtained through peer review must be kept confidential and not used for personal

advantage. Reviewers should not consider manuscripts in which they have conflicts of interest resulting from competitive, collaborative, or other relationships or connections with any of the authors, companies, or institutions connected with the papers.

Why review? When your time is stretched it is tempting to say no to the requests for a review, but there are a number of very valid reasons why review should be accepted:

- Help the author to improve the paper – in the light of your own professional expertise.
- Make the author aware of any additional literature that may provide useful comparison, or clarification of an approach.
- Assist in a rigorous process to ensure only the best research is published.
- Maintain your awareness of current research emerging within the discipline.

You've agreed to referee a paper, so what should you do next? Start by visiting the Journal homepage to get a sense of the Journal's usual contents and house style to help decide whether the paper being reviewed is suitable. Refer to the Instructions for Authors to see if the paper meets the submission criteria of the Journal (e.g. length, scope, and presentation). At the request of the Editor-in-Chief the reviewers are invited to make online review using the Paper Submission Tool (PST) – the section for reviewers.

Fill in the review questions or score sheet to indicate the relative strengths or weaknesses of the paper. Remember that authors will welcome positive feedback as well as constructive criticism from you. Key questions to ask: Is the paper original? Is the relative contribution made to the existing literature good enough? Will the paper be interesting to the readership of the Journal?

Once you have read the paper and assessed its quality, you need to make a recommendation to the editor regarding publication. Should it be accepted? Revised and resubmitted? Rejected pending revision? Supply some comments suitable for transmission to the author as an

opportunity to seek clarification on any unclear points and for further elaboration. If you have time, make suggestions as to how the author can improve clarity, succinctness, and the overall quality of the presentation. Confirm whether you feel the subject of the paper is sufficiently interesting to justify its length. If you recommend shortening of the paper it is useful to the author(s) if you can indicate specific areas where you think that shortening is required.

Unable to review? It will prove impossible for you to accept every invitation to review. In this situation it is very helpful if you are able to recommend an alternative expert or someone whose opinion you trust. If you are unable to complete your report on a paper then inform the editorial office as soon as possible so that the reviewing process is not delayed. Make the editors aware of any potential conflict of interest that may affect the paper under review. We are always very grateful for the contribution made to our Journal by our reviewers and would be pleased to hear any comments or suggestions on our current peer review procedures.

With great efforts of the authors, reviewers and the editorial team, we have managed to complete this regular second journal issue with ten selected papers. Following the reviewers' remarks, the authors edited the papers in the form in front of you.

In the end, as always, we welcome you, our dear readers, to use your input to contribute to our joint work and permanent endeavour to retain the quality of our joint journal.

Best regards,

A handwritten signature in blue ink, appearing to read 'M. Kljajin', with a stylized flourish at the end.

Full. Prof. Milan Kljajin, Ph.D.

Editor-in-Chief

**Tehnički Glasnik-Technical Journal**

# REMOTE RENDERING CONTROL USING PYTHON SCRIPTS AND DROPBOX TECHNOLOGY

Andrija BERNIK, Dinko GALETIC

**Abstract:** The process of rendering a 3D animation often takes a very long time to complete. In situations where it would take several hours or even many days, it is inconvenient to spend that time near the rendering computer in order to control and oversee the process. Through the work with 3D computer graphic technologies, the authors realized that there is no simple solution on the market that facilitates the monitoring of the remote computer that is running the rendering process. This paper deals with developing a system to enable those tasks to be done from a remote computer or any mobile device. The developed proof-of-concept system consists of two Python programs communicating over the Dropbox service and a computer that is running the Autodesk Maya software.

**Keywords:** Autodesk Maya; Dropbox; Python; remote rendering

## 1 INTRODUCTION

Rendering is a process in which a dynamic environment is stored as a 2D image. To create an image, it is necessary to use a system for calculating the position of a model and sources of light in a 3D space. The Autodesk Maya software solution was used in this paper for the purposes of 3D modeling and rendering. Since the process of rendering can take a very long time, sometimes even up to several hours for a single image [1] (usually called a frame), it is often inconvenient to be physically present by the rendering computer in order to oversee and control the process.

As for example, Jonah Lehrer said for the Wired Magazine regarding the making of Toy Story 3: "The average frame (a movie has 24 frames per second) takes about seven hours to render, although some can take nearly 39 hours of computing time. The Pixar building houses two massive render farms, each of which contains hundreds of servers running 24 hours a day." [1]

This paper addresses this problem by creating a system which enables the user to remotely control the process. The goal is to have a simple, portable system with as few dependencies as possible.

## 2 EXISTING RENDERING CONTROL SOFTWARE AND SETTING UP THE SCENE

The scene is created in Autodesk Maya and the focus is based on setting up the render preferences. Important to note is that there are two types of inputs for the complete setting up of the preferences and those are connected to the output file and quality of the rendering calculations.

Fig. 1 has some important options that directly influence the size and the type of rendering. Image format is set to jpg because of file size. The quality of an image is slightly lower but for the animation it is not a problem since we have 24 FPS (frames per second).

Frame extension is set to the "name.#.ext" format. This format is a must because of the Operating and file type (FAT / NTFS) system. [4]

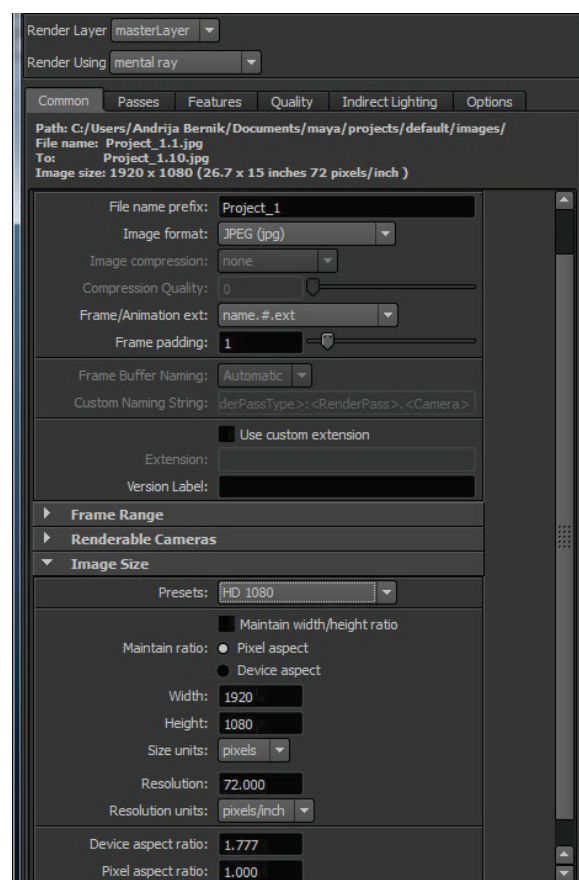


Figure 1 Common Render Settings

Rendered frames are meant to be used in the compositing software such as Adobe After Effects and that is why we also have to set the first and last frame for the rendering process. The last part of Common attributes is image size, which is determined by the use of animation. The other important feature is connected to the Quality itself. The user has the ability to choose from Quality presets if he or she does not have enough knowledge to

manually set the rendering stats. Rendering is not the main subject for this article which is why any further analysis will not be made.

There are several existing solutions for rendering available. The 3D Buzz's "Maya Renderer" application is created for the Windows Phone 7 mobile platform. This choice of platform imposes a limit on the application's usability: it cannot be used from a PC, and the Android and iOS platforms are more widely used when it comes to mobile platforms [2].

The "Mental Ray Satellite Tech" software can be used to control the rendering process through a Local Area Network (LAN), making it suitable for remote control only if Virtual Private Network (VPN) technology is used. Since such systems require some setting up and are often commercial, the authors did not find this solution appropriate.

The "Team Viewer" and similar screen casting applications give full control of the computer to a remote user by transmitting the controlled computer's entire screen over the network to the remote user's computer, and the remote user's mouse and keyboard input to the controlled computer. The authors find this solution inappropriate because its broad approach uses a lot of network bandwidth, while an application focused specifically on the control of the rendering process would use a significantly smaller amount. Such an application would be usable even in situations where bandwidth is severely limited, such as accessing Internet via a mobile phone while in roaming.

### 3 OVERVIEW OF THE DEVELOPED RENDERING CONTROL SYSTEM

The Python 2.7. Programming language was chosen to develop the solution. Python interpreters exist for a wide array of platforms [3], making the code written in Python almost entirely platform independent. Python's high-level approach is particularly suitable for solving a high-level problem such as this. Lastly, a large amount of Python modules [5] [6] greatly increases the functionality of the language.

The system consists of three parts:

- a) The client application,
- b) The server application,
- c) The Dropbox server.

The client application runs on the computer from which one wishes to control the rendering process. The server application runs on the computer which does the rendering (referred to as 'the rendering server' in this paper). While the rendering computers are usually very strong computers, the client computer can be any computer capable of running Python 2.7. To allow communication between the client and the server computer, the Dropbox service was used. Dropbox is an online storage service which allows a user to store up to 2 GB of files for free and easily synchronizes them between different computers [7]. The Dropbox service can be used with a Dropbox application, through a browser or through their Application Programming Interface (API).

The API is available in Python through the Dropbox's official python module.

In this solution, the rendering server uses the Dropbox application, and the client computer uses the Dropbox Python module in order to access the Dropbox server. This was used to show how both approaches can be used to allow such communication; alternatives where both computers use either the API or the application can similarly be made.

The server and client applications communicate by uploading and downloading files to and from each other via the Dropbox server. Those files are used to exchange commands for the server ("commands.txt"), to keep track of the Maya project currently being rendered ("active\_rend.txt") and to keep track of all the projects available for rendering ("projects\_to\_rend.txt"). Additionally, the server uses a log file ("LOG.txt") to keep track of the commands it has already executed.

The server application does three basic tasks:

- a) Check the commands file for updates,
- b) Execute new commands,
- c) Maintain the available project file.

Since a) and c) are input-output tasks that need to run continuously, each of the three tasks runs in its own thread of execution. Upon any updates to the command file, the commands are read and accordingly executed or queued for execution. If a new Maya project is added to the designated projects directory, the project name is added to the available project file.

The client application mostly runs in a single thread since it only needs to communicate with the Dropbox server upon the user's request and has no tasks it needs to run perpetually. It displays the data from the active rendering and available project files, and updates the command file when the user sends a new command. It briefly invokes a second thread to upload the updated command file in order to avoid the application from blocking while the file is being uploaded.

### 4 DROPBOX API SPECIFICS

In order for an application to be able to use the Dropbox API, it needs to be registered on the Dropbox website, where it receives two pieces of information unique to it, called "APP\_KEY" and "APP\_SECRET". The creator of the application has to choose whether the application will have access only to a single directory in the user's Dropbox account, called the "Apps" directory, or to everything in the account. The latter requires a special permission from the Dropbox staff, but the former was sufficient for this application. The key, the secret and the access type information are required to use the API.

The user of the application allows the application to connect to their Dropbox account by following a link to the Dropbox website (called the 'authorization url') specially generated by the application and agreeing to permit the application to connect to their account. Once the application is permitted, the Dropbox server returns the "access token", which is an object containing the credentials signifying the

permission. The authorization can be remembered for future uses by saving the token to a hard drive and loading it when needed. [11] The required parts of the Dropbox module can be imported with the following:

```
from dropbox import client, rest, session
```

In order to start a Dropbox session, the application needs to run the following code:

```
sess = session.DropboxSession (APP_KEY,
APP_SECRET, ACCESS_TYPE)
```

In order to create the authorization url, the application must first obtain a "request token" from the Dropbox server and use it to create the url:

```
request_token = sess.obtain_request_token()
url = sess.build_authorize_url
(request_token)
```

The url thus obtained is a plain text string. Once the user follows it and allows the application to access their Dropbox account, the following line of code is used to fetch the authorization credentials from the Dropbox server:

```
sess.obtain_access_token (request_token)
```

The credentials are stored in the `sess` object as the `sess.key` and `sess.secret` variables. Note that these are unrelated to the before mentioned `APP_KEY` and `APP_SECRET` variables. Finally, the `sess.set_token` method needs to be called with the `key` and `secret` variables before we can use the rest of the API.

```
key, secret = sess.token.key,
sess.token.secret
sess.set_token(key, secret)
```

If the access token was saved to the hard drive, only the last step is required. One would load the `key` and `secret` variables from a file and call the `set_token` as shown above.

Uploading a file to the Dropbox server and downloading a file from it can each be accomplished by one line of code. First, a "client" object is required.

```
klijent = client.DropboxClient(sess)
```

The `client.get_file` method returns an open file object which can be read or saved as a file object returned by the Python's built-in `open` function. The `client.get_file`.

The method requires an argument specifying the path to the file in the user's account, with the root directory being the one the application is allowed to use. The Dropbox API uses the Unix notation of forward slashes ("/") for paths.

```
dat = klijent.get_file ("/path/to/file.txt")
```

To upload a file, the `client.put_file` method needs to be called with the remote path (the name and the location under which to save the file) and an open local file object parameters specified. By default, the file will be automatically renamed to avoid overwriting an existing file with the same name. The function returns an object containing the uploaded file's metadata. This operation is synchronous and will block the program until the file is uploaded.

```
response = klijent.put_file (remotepath,
local_file)
```

## 5 IMPLEMENTATION DETAILS FOR THE CLIENT SIDE APPLICATION

The rendering process can be invoked by using a command line interface (CLI) program called "render" without starting the Maya Software. [8] The parameters passed to "render" can be used to set various rendering details. This approach was very suitable for this solution because sending, receiving and processing a line of text can easily be done and requires very little network bandwidth. This solution allows the user to choose which rendering algorithm to use and to set which frames are to be rendered by choosing the first and the last frame. The necessary variables for the CLI command are determined by the user's choices and added to the command file, after which a new thread is started to upload the file. [9]

```
write_me = "rend:render -r " + render + " -s
" + start_frame + end_frame + " " +
project_file + "\n"
dat = open(COMMANDS_FILE, "a")
dat.write(write_me)
dat.close()
Thread(target = self.send_work).start()
```

The `Thread` object comes from the Python `threading` module. The `send_work` method wraps around a generic uploading function and calls it to upload a specific file. While this is the only instance in the application where the generic function is used, that function was written with future expansions in mind.

```
def send_work(self):
    """ Upload the commands file to the
    Dropbox server. """
    self.__upload__(COMMANDS_FILE,
remotepath = "/Maya/commands.txt", overwrite
= True)
```

In the `__upload__` method, the API `put_file` method is called in the following way. The `overwrite` parameter is set to `True` because the API does not offer a way to append to a file, making it necessary to overwrite the existing one. The `expanduser` method provides a portable way to use file names.



```
local_file = open(os.path.expanduser
(localpath))
response = self.klijent.put_file
(remote_path, local_file, overwrite)
```

Besides the command to initiate the rendering process, the application supports the "progress" command. The command requests the server to upload the latest rendered image to Dropbox so the user can check how far the rendering process got and whether the scene looks as expected.

The list of available tasks is downloaded by the `fetch_tasks` method. A similar method called `fetch_active_rend` does the same thing, with the only difference of opening a different file and saving in a different variable.

```
def fetch_tasks(self):
    """ Download a list of projects awaiting
    rendering."""
    dat = self.klijent.get_file
    ("/Maya/projects_to_rend.txt")
    try:
        data = dat.read()
        # Each element of "data" is
        a string representing a project file
        (*.mb or *.ma).
        data = data.rstrip().split("\n")
    except:
        data = []
    self.task_list = data
```

## 6 IMPLEMENTATION DETAILS FOR THE SERVER SIDE APPLICATION

Once started, the server side application asks the user to enter the paths to the required directories and files: the Dropbox directory the application is allowed to use, the directory where the Maya projects are stored, the path to the directory where the rendered images are stored and the path to the log file. Afterwards, the application initiates the required threads and runs in the background, requiring no further user input. The main thread continuously checks the command file for updates. A portable way to do that is to keep checking the file modification time, stored in the `st_mtime` variable.

```
old_modify_time = os.stat(dropbox_path +
"commands.txt").st_mtime
while(True):
    try:
        new_modify_time =
os.stat(dropbox_path +
"commands.txt").st_mtime
    except:
        # The exception will happen
if the file is beign written to while
attempting to read it;
        # waiting 15 seconds should be
sufficient for the writing to finish.
        time.sleep(15)
```

```
new_modify_time =
os.stat(dropbox_path +
"commands.txt").st_mtime
if new_modify_time != old_modify_time:
    old_modify_time = new_modify_time
    dat = open(dropbox_path +
"commands.txt", "r")
    commands =
dat.read().split("\n")
    dat.close()
```

Since the command file contains every command that was ever sent to the rendering server, a log is maintained to keep track of what commands were executed. The new commands are now read and processed. The lines starting with "rend:" represent the commands to render a project, and those commands are appended to a queue variable, to be read by the rendering thread. The lines saying "progress:" are requests for progress updates. Since these are just a matter of finding and copying the latest image to the Dropbox directory, they can be executed quickly and thus do not require a specific thread to execute them.

```
for com in commands_to_run:
    last_command_number += 1
    if com[0:4] == "rend":
        q.append(com[5:])
    elif com[0:8] == "progress":
        progress()
```

The rendering thread runs the following code. Since the `subprocess.call` blocks the calling thread until the sub process finishes, the thread will be blocked until the rendering process is complete.

```
def render_thread():
    """ Perpetually checks the queue.
    Executes commands one by one."""
    while True:
        while len(q) > 0:
            command = q.pop(0)
            print command
            dat = open(dropbox_path +
"active_rend.txt", "w")
            # Write the name of the
            file being rendered.
            dat.write(command.split()[-1])
            dat.close()
            # Run the command as the
            CLI command.
            result =
subprocess.call(command.split())
            # Clear the active_rend.txt
            file.
            dat = open(dropbox_path +
"active_rend.txt", "w")
            dat.close()
            time.sleep(5)
```

## 7 PROBLEMS ENCOUNTERED DURING DEVELOPMENT

The Dropbox API documentation [10] contained an error regarding the `obtain_access_token` method at

the time of writing of this paper. The method does not return a tuple object containing the key and the secret as the documentation states; it stores the token in the session variable.

```
# key, secret =
sess.obtain_access_token(request_token) #
Error!
sess.obtain_access_token(self.request_token)
print sess.token.key, sess.token.secret #
Correct.
```

Various bugs occurred due to the differences in how the GNU/Linux and Windows operating systems treat text files and file paths. GNU/Linux separates the lines in text files using the line feed (LF) character, while Windows uses both the carriage return (CR) and the LF characters, thus separating the lines with CRLF (depicted in Python as `"\\r\\n"`). Both the server and the client application expect the lines to be separated with just the LF. While this works fine, Windows text editing applications may show all the text from this solution's files as a single line. The difference in how the OSs treat file paths (Windows separates directories with a backslash ("`\\`"), and GNU/Linux with a slash ("`/`")) were avoided by using the `os.path.expanduser` method instead of using file paths directly.

## 8 FUTURE DEVELOPMENT POSSIBILITIES

As a proof-of-concept application, it contains a very basic set of just two commands that can be passed to the rendering server. It can easily be expanded to include other commands, such as stopping the rendering process or changing the priority of the queued tasks. Advanced options such as allowing multiple machines per user or controlling an entire rendering cluster could be added as well.

Concurrency issues are possible if a thread attempts to read its file while the file is not done downloading. This was avoided by using a try-except block which delays the reading if an error occurs, but a proper solution would be to use semaphores and possibly the file metadata to determine when the downloading was finished.

Semaphores could also be used to keep the rendering thread inactive when there are no tasks waiting instead of using `time.sleep(5)` to have it checked for new tasks every five seconds.

The application could be expanded to support more platforms. Mobile phones would be particularly suited for the purpose of remotely controlling the rendering computer. Finally, support for a 3D rendering software besides Maya could be added.

## 9 CONCLUSION

This article shows that even though there is not a single PC solution that enables the user to remotely control Maya's batch render, authors have successfully combined the given technology. Dropbox is essential and required for transferring and triggering python scripts which then

communicate with Maya's batch render in the background process of the Windows platform. The problems were based on the differences between the two operating systems. Moreover, there is a flaw inside the Dropbox documentation which needs to be corrected for future user readings.

If running the code samples from the article, please note that the article formatting often broke longer lines into two or more lines and should be adjusted accordingly.

Maya's CLI interface is suitable for use by another program to control the rendering process. A rudimentary application which remotely controls the process can be developed in a few days and there is much potential for expanding its functionality.

## 10 REFERENCES

- [1] Lehrer, J. (2010). Animating a Blockbuster: How Pixar Built Toy Story 3, [http://www.wired.com/magazine/2010/05/process\\_pixar/all/](http://www.wired.com/magazine/2010/05/process_pixar/all/) (Accessed: 06.04.2017).
- [2] van der Meulen, R. & Rivera, J. (2013). Gartner Says Worldwide Mobile Phone Sales Declined 1.7 Percent in 2012, <http://www.gartner.com/newsroom/id/2335616> (Accessed: 10.04.2017).
- [3] Python Software Foundation: Download Python for Other Platforms, <http://www.python.org/getit/other/>, Accessed 11.04.2017.
- [4] Preda, M., Villegas, P., Morán, F., Lafruit, G., & Berretty, R. P. (2008). A model for adapting 3D graphics based on scalable coding, real-time simplification and remote rendering. *The Visual Computer*, 1, 24(10), 881-888. <https://doi.org/10.1007/s00371-008-0284-2>
- [5] The Python Standard Library, Python Software Foundation, 2013, <http://docs.python.org/2/library/> (Accessed: 13.04.2017).
- [6] PyPI - the Python Package Index, Python Software Foundation, 2013, <https://pypi.python.org/pypi> (Accessed: 13.04.2017).
- [7] Dropbox, Inc.: Dropbox - Tour, <https://www.dropbox.com/tour> (Accessed: 11.04.2017).
- [8] Palamar, T. & Keller, E. (2011). *Mastering Autodesk Maya 2012*. Wiley Publishing, Inc. Indianapolis, Indiana, 657-664.
- [9] Autodesk Maya: Maya User's Guide: Start Maya from the command line, available at [http://download.autodesk.com/global/docs/maya2013/en\\_us/index.html?url=files/Interface\\_o\\_verview\\_Start\\_Maya\\_from\\_the\\_command\\_line\\_.htm,topicNumber=d30e12859](http://download.autodesk.com/global/docs/maya2013/en_us/index.html?url=files/Interface_o_verview_Start_Maya_from_the_command_line_.htm,topicNumber=d30e12859), Accessed 07.02.2017.
- [10] Dropbox Inc.: Dropbox Client - Dropbox Documentation, [https://www.dropbox.com/static/developers/dropbox-python-sdk-1.5.1-docs/index.html#dropbox.session.DropboxSession.obtain\\_access\\_token](https://www.dropbox.com/static/developers/dropbox-python-sdk-1.5.1-docs/index.html#dropbox.session.DropboxSession.obtain_access_token) (Accessed: 06.02.2017).
- [11] Drago, I., Mellia, M., Munafo, M., Sperotto, A., Sadre, R., & Pras, A. (2012). Inside Dropbox: understanding personal cloud storage services. *Proceedings of the 2012 ACM conference on Internet measurement conference*, 481-494. <https://doi.org/10.1145/2398776.2398827>

**Authors' contacts:**

**Andrija BERNIK, Ph.D.**  
University North,  
42000 Varazdin, Croatia  
andrija.bernik@unin.hr

**Dinko GALETIC, Mag. inf.**  
Self-employed programmer,  
47000 Karlovac, Croatia  
dinko.galetic@gmail.com

# OPERATOR'S WHOLE BODY VIBRATIONS DEPENDENT OF AGROTECHNICAL SURFACE, SPEED OF MOVEMENT AND SEAT UPHOLSTERY

Željko BARAČ, Ivan PLAŠČAK, Tomislav JURIĆ, Mladen JURIŠIĆ, Domagoj ZIMMER, Ivan VIDA KOVIĆ,  
Davor PETROVIĆ, Vinko DUVNJAK, Monika MARKOVIĆ

**Abstract:** The paper presents the recorded vibrations that affect the operator's body when an agricultural tractor moves along three types of agrotechnical surfaces, i.e. asphalt, an alfalfa field, and a field path, and when seven different tractor seat upholsteries are used. The research was performed in accordance with the HRN ISO 2631-1 and HRN ISO 2631-4 standards. The tractor used in the research was an IMT 560 and the duration of the measurement was 30 minutes, which was repeated three times for every tractor seat upholstery type. The research was exploitative. The measurements were performed using an MMF VM30 meter. The paper reveals a different level of vibrations in dependence with different surfaces and seat upholsteries. The fewest vibrations were produced by asphalt, and the best upholsteries are memory foam and sponge.

**Keywords:** agricultural tractor; agrotechnical surfaces; seat upholstery; vibrations

## 1 INTRODUCTION

Vibrations are generally considered to be oscillatory motions of a mechanical system. Oscillation is a periodical motion around an equilibrium point, i.e. a motion that repeats itself after a certain period. Vibrations are a result of dynamic forces in machines with moving parts, as well as in the structures linked to machines. In the beginning, the insignificant vibrations can cause a resonance in some other parts of the structure and they can increase and become the main and rather serious source of increased vibrations and noise. Different machine parts vibrate at different amplitudes and frequencies. Vibrations cause material fatigue and wear. They are often a cause of machine defects [1].

The vibrations transferred to the operator's body, i.e. whole-body vibrations occur when the body leans against a vibrating surface, e.g. when the driver is sitting on a vibrating chair, standing on a vibrating floor, or lying on a vibrating surface [2].

The authors [3] posit that the most important machine component regarding the influence of vibrations is the seat as operators spend most of their time in a seated position. Seat construction, the back of the operator, the depth of the seat, and the upholstery of the seat can exert a complex impact on the operator's ability to operate the machine, as well as on the occurrence of occupational diseases. The same authors claim that the seat upholstery wears out in time so that it is necessary to mend it. A defective seat cannot ensure proper sitting posture, which can cause occupational diseases. Overexposure to mechanical vibrations can have a negative impact on the human body, e.g. overexposure to high vibrational frequencies can lead to physical problems such as spinal dysfunction [3].

The authors [4] in their research claim that a suspended front axle of a tractor generally dampens the vibrations transferred to the operator's seat. The vibrations decrease on average from 13% to 15% but they may be reduced as much

as 30%. The authors [5] suggest that a seat suspension has been almost a universal feature of agricultural tractors during the last 30 years. The suspension system was introduced to enable the operator to manage the machine in a more comfortable and easier way, which has resulted in increased work productivity. The authors [6] argue that operators might drive tractors for as long as twelve hours a day, which can cause back problems. The analysis of vibrations produced by agricultural machinery is complex as it depends on many factors. The abovementioned authors emphasize that tyre pressure and seat suspension affect vibrations. The authors [7] posit that tractor speed, tyre pressure and the distribution of the transported weight are the most crucial factors that affect the comfort of a tractor operator riding on a tractor that moves along an asphalt surface. Lower tyre pressure is more comfortable for the operator; however, it is not always possible to lower tyre pressure for distinct reasons, one of the most important being the quality of the surface along which the tractor is moving. The authors [8] claim that air seat reduces both high and low vibration frequencies. The same authors argue that low vibration frequencies can be reduced by assembling an air container next to the seat or onto the cabin. The authors [9] suggest that the sitting posture of the driver, i.e. the position of his legs during driving is in significant connection with the sitting comfort.

The authors [10] conducted a research on Masey Ferguson tractors using the limits of vibration exposure as a criterion. They established that after an eight-hour exposure to vibrations, the allowed limit was not exceeded. Additionally, they claim that it is important to bear in mind that in certain situations, some frequencies pertaining to axles do exceed the permitted limits. Thus, it was concluded that seats can absorb vibrations and create ergonomically proper work conditions. The study was performed on an asphalt surface. The authors [11] conducted a study on vibrations on two tractors. One tractor was a newer model with a cabin, whereas the other was an older model without

a cabin. It was concluded that it is easier to measure vibrations on a tractor without a cabin and that the engine itself is the greatest source of vibrations in both tractors. The cabin was emphasized as an important part of tractor equipment because it protects the operator from vibrations, dust, and the objects that might appear in the operator's vicinity. Higher vibration levels were established on the older tractor.

The aim of the research is to measure the levels of vibrations that affect the operator's body when an agricultural tractor moves on various agrotechnical surfaces at various speeds in dependence with different upholstery of the tractor seat. Additionally, the aim is to establish potential interdependencies. It is hypothesized that due to a tractor's movement along various agrotechnical surfaces in dependence with different seat upholstery, the level of vibrations affecting the operator's body will increase.

## 2 MATERIALS AND METHODS

MMF VM30-H is the measuring device used for the measurement of mechanical vibrations that affect the body of the operator when an IMT 558 agricultural tractor is in motion. The tractor moved along three different surfaces, namely asphalt, an alfalfa field, and a field path. The following are the seat upholstery on which the driver sat: a seat without an upholstery (i.e. only a metal seat framework), cork, styrofoam, sponge, memory foam, cotton wool, and air cushion, Tab. 1. Each measurement was repeated three times. The motion speed was 4, 5 and 6 km/h. The research shown here was exploitative. The measurements were performed in 2017 in a period of 20 days. The average daytime air temperature in the days when the measurements took place ranged between 18° and 19°, whereas the relative humidity was between 58% and 60%.

**Table 1** Characteristic of the seat upholstery material

Type	Main characteristic	Thickness
Industrial Cork	density 110-120 kgm <sup>-3</sup>	100 mm
Viscoelastic polyurethane memory foam	density 80 kgm <sup>-3</sup>	100 mm
Expanded polystyrene (EPS) – Styrofoam	density 15 kgm <sup>-3</sup>	100 mm
Polyuretan sponge	density 35 kgm <sup>-3</sup>	100 mm
Cotton wool cushion	density 120 gm <sup>-3</sup>	100 mm
Orthopedic PVC air cushion	diameter 330 mm	100 mm

The research was performed in accordance with the standards [12] and [13]. The measurements were performed while the driver was sitting in accordance with the standard [12]. The seat therefore represents the contact point between the operator and the tractor. The measuring device was set in the exact position in accordance with the operators sitting position. It was set onto the seat so that the axes were recorded in the following directions [12]: *x* axis: longitudinally (along the axis of motion – forward (positive) / backward (negative)), *y* axis: laterally (at the right angle to the motion direction) and *z* axis: vertically, upward (positive) / downward, vertically to the surface (negative). The vibrations were recorded based on a coordinate system

for particular body parts. The device recorded the vibrations that were directly transferred through the seat to the operator's body.

According to [14], the limit values for the daily level of vibration exposure were established. The limit value for the vibration transferred to the body of the operator is 1.15 m/s<sup>2</sup>. *W<sub>d</sub>* and *W<sub>k</sub>* are the weight filters used in the measurements. *W<sub>d</sub>* is used for vibration measurement in the direction of the *x* and *y* axes in the sitting position, whereas *W<sub>k</sub>* refers to the vibrations in the direction of the *x* axis.

The R.M.S. measurement method used for the measurement in motion accounts for the occasional impulse and transient vibrations. It applies a short integral time constant. The size of vibrations is defined as a maximum transient vibration value (*MTVV*), which is the maximum for *a<sub>w</sub>(t<sub>0</sub>)*.

$$a_w(t_0) = \left\{ \frac{1}{\tau} \int_{t_0-\tau}^{t_0} [a_w(t)]^2 dt \right\}^{\frac{1}{2}} \quad (1)$$

*a<sub>w</sub>(t)* – the current frequency of the recorded acceleration (m/s<sup>2</sup>),

*τ* – time of integration for the current averaging,

*t* – time (s),

*t<sub>0</sub>* – time of observation (s).

$$MTVV = \max [a_w(t_0)] \quad (2)$$

*MTVV* - maximum transient vibration value (m/s<sup>2</sup>)

The measured values were statistically analyzed using an application for statistical analysis in the MS Office Excel 2013, and IBM SPSS Statistics v.19.0.1. The paper shows the descriptive statistical values and multiple analysis of variance (MANOVA). Multiple correlations and the regression equation in this analysis were performed.

## 3 RESULTS AND DISCUSSION

The measurement of vibrations for the upholstery-free seat produced on the asphalt surface resulted in the occurrence of the maximum vibration value recorded in the direction of the *y* axis at all motion speeds. The lowest recorded value was established in the direction of the *x* axis at all speeds (Fig. 1). Furthermore, a conspicuously highest level of vibrations was recorded on the alfalfa field in the direction of the *x* axis at all speeds, whereas the lowest level was recorded in the direction of the *z* axis at 4 km/h, with all other values being the same. The vibrations recorded on the field path were the lowest in the direction of the *z* axis at all speeds, whereas the highest value was recorded in the direction of the *x* axis at 4 km/h. All other values were identical.

The highest level of vibrations for the cork seat (Fig. 2) was established in the direction of the *y* axis at all motion speeds on the asphalt surface, whereas the lowest recorded value for the same surface occurred in the direction of the *x* axis at 4 km/h, while all other values were the same.

Additionally, the highest recorded values on the field path happened in the direction of the  $z$  axis at 5 km/h) and at 6 km/h in the direction of all three axes.

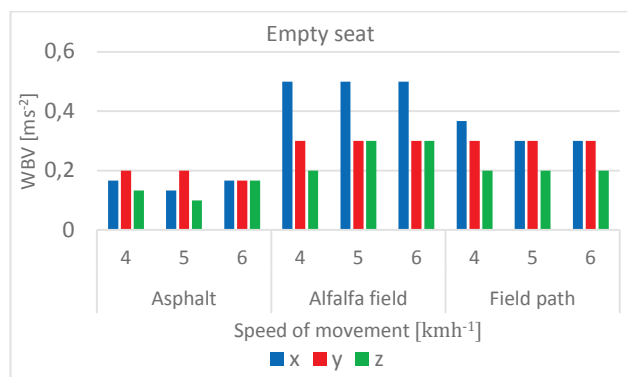


Figure 1 Measured vibration data – empty seat

Fig. 3 shows the highest levels of vibrations recorded on the asphalt surface in the direction of the  $y$  axis at all motion speeds, whereas the lowest values were recorded in the direction of the  $x$  axis at all motion speeds as well as in the direction of the  $z$  axis at 5 and 6 km/h.

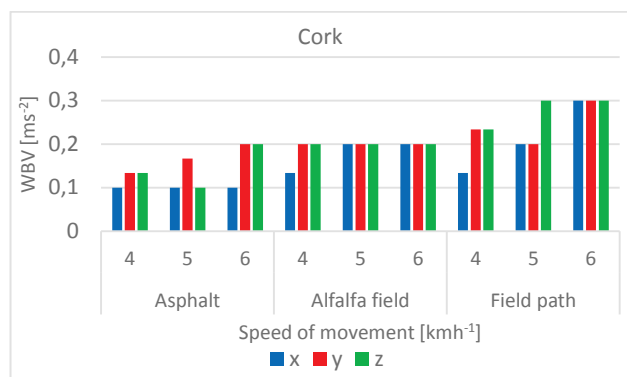


Figure 2 Measured vibration data – cork seat

The highest values of vibrations on the alfalfa field were found in the direction of the  $z$  axis at all speeds, while all other vibration values were the same.

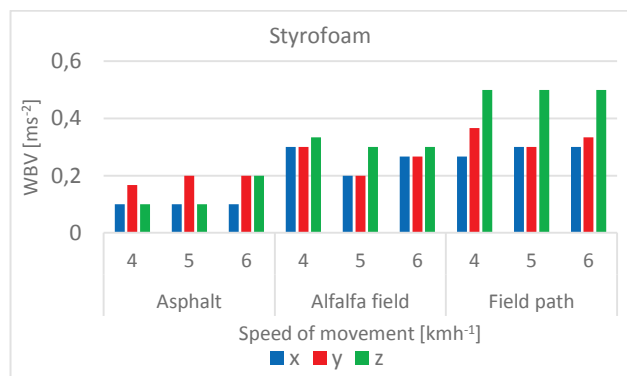


Figure 3 Measured vibration data – Styrofoam seat

The vibration measurement for sponge (Fig. 4) resulted in the highest values on the asphalt surface in the direction of the  $x$  axis at 4 km/h, while the lowest value was recorded

in the direction of the  $y$  axis at 4 and 5 km/h, while all other values were the same. Moreover, the highest level of vibrations was recorded on the alfalfa field in the direction of the  $x$  axis at all speeds as well as in the direction of the  $z$  axis at 5 and 6 km/h, whereas the lowest value was recorded in the direction of the  $y$  axis at 4 km/h, while all other values were the same. The vibrations recorded on the field path are the lowest in the direction of the  $y$  axis at all speeds, whereas the highest value was recorded in the direction of the  $z$  axis at all motion speeds and in the direction of the  $x$  axis at 6 km/h. All other vibration values were the same.

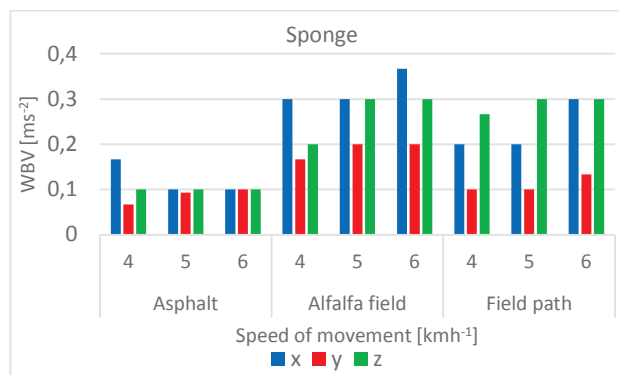


Figure 4 Measured vibration data – sponge seat

The vibrations recorded on memory foam (Fig. 5) have the same values on the asphalt surface in the direction of all three axes and at all motion speeds. The highest vibration value was recorded on the alfalfa field in the direction of the  $z$  axis at all speeds and in the direction of the  $x$  axis at 5 km/h, while all other values were the same. The lowest level of vibrations on the field path was recorded in the direction of the  $y$  axis at all speeds, whereas the highest value was recorded in the direction of the  $z$  axis at 6 km/h. All other vibrations had the same values.

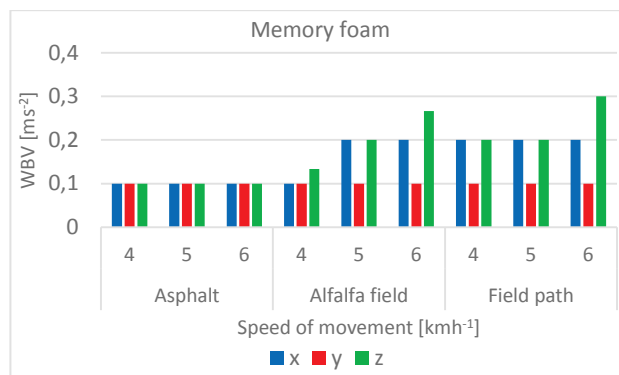


Figure 5 Measured vibration data – memory foam seat

The vibrations recorded on cotton wool (Fig. 6) have the same values on the asphalt surface in the direction of all three axes and at all motion speeds. The highest vibration value was recorded on the alfalfa field in the direction of the  $x$  axis at all speeds and in the direction of the  $z$  axis at 6 km/h, while the lowest value was recorded in the direction of the  $y$  axis at all speeds and in the direction of the  $z$  axis at

4 km/h. Moreover, the lowest level of vibration was recorded on the field path in the direction of the  $y$  axis at all speeds, while the highest values were recorded in the direction of the  $z$  axis at all speeds and in the direction of the  $x$  axis at 5 and 6 km/h.

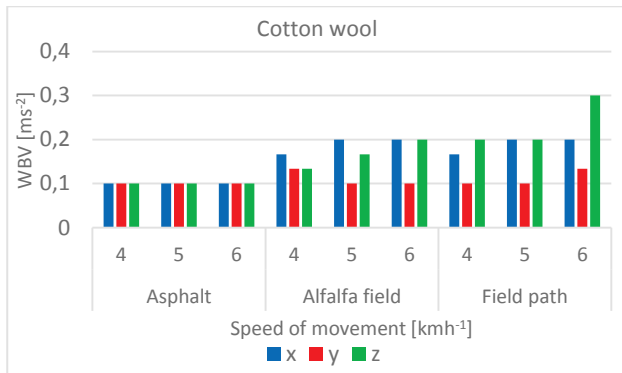


Figure 6 Measured vibration data – cotton wool seat

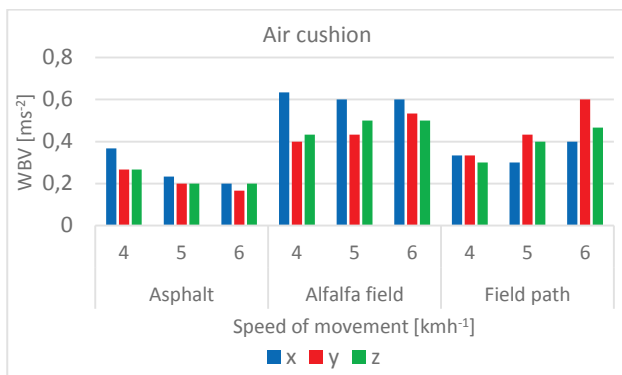


Figure 7 Measured vibration data – air cushion seat

The vibrations recorded on the air cushion (Fig. 7) on an asphalt surface show the highest values in the direction of the  $x$  axis at all speeds and in the direction of the  $z$  axis at 6 km/h, while the lowest level was recorded in the direction

of the  $y$  axis at 6 km/h at all speeds, while all other values were the same. Furthermore, the highest vibration level was recorded on the alfalfa field in the direction of the  $x$  axis at all speeds, whereas the lowest was recorded in the direction of the  $y$  axis at 4 and 5 km/h, as well as in the direction of the  $z$  axis at 6 km/h. The vibrations recorded on the field path show the lowest value in the direction of the  $z$  axis at 4 km/h and in the direction of the  $x$  axis at 5 and 6 km/h. The highest value was recorded in the direction of the  $x$  axis at 4 km/h and in the direction of the  $y$  axis at all speeds.

Tab. 2 shows the statistical significance of all tested effects and their interaction in the direction of the  $x$  axis, with the impact of the independent variables 'seat upholstery' and 'agrotechnical surface' being highly significant, and the impact of the independent variable 'motion speed' being significant. The mutual interaction of all three independent variables is highly significant.

The impact of all independent variables in the direction of the  $y$  axis is highly significant. The interaction of the independent variables ('agrotechnical surface', 'motion speed') is significant, whereas it is highly significant for all other variables (Tab. 3).

The impact of all three independent variables in the direction of the  $z$  axis is generally highly significant, which is shown in Tab. 4. Moreover, the interaction of the independent variables ('seat upholstery', 'motion speed') is significant, while it is highly significant for all other variables.

Tab. 5 shows the correlation coefficient, the connection between a dependent and independent variable (i.e. the vibrations that impact the body of the operator in the direction of the  $x$ ,  $y$ , and  $z$  axes). Additionally, according to [15], the actual significant connection in the direction of the  $z$  axis is discernible, whereas the connection in the direction of the  $x$  and  $y$  axis is slight.

Table 2 Tests of Between - Subjects Effects - Dependent Variable: xos

Source	Type III Sum of Squares	df	Mean Square	F	Sig.	Partial Eta Squared	Noncent. Parameter	Observed Power <sup>b</sup>
Corrected Model	3.340 <sup>a</sup>	62	0.054	42.423	0.000	0.954	2630.250	1.000
Intercept	10.290	1	10.290	8103.375	0.000	0.985	8103.375	1.000
Seat_upholstery	1.533	6	0.256	201.250	0.000	0.906	1207.500	1.000
Agrotechnical_surface	1.007	2	0.503	396.500	0.000	0.863	793.000	1.000
Motion_speed	0.012	2	0.006	4.625	0.012	0.068	9.250	0.772
Seat_upholstery * Agrotechnical_surface	0.609	12	0.051	39.938	0.000	0.792	479.250	1.000
Seat_upholstery * Motion_speed	0.066	12	0.006	4.333	0.000	0.292	52.000	1.000
Agrotechnical_surface * Motion_speed	0.045	4	0.011	8.875	0.000	0.220	35.500	0.999
Seat_upholstery * Agrotechnical_surface * Motion_speed	0.068	24	0.003	2.240	0.002	0.299	53.750	0.995
Error	0.160	126	0.001					
Total	13.790	189						
Corrected Total	3.500	188						

**Table 3** Tests of Between - Subjects Effects - Dependent Variable: yos

Source	Type III Sum of Squares	df	Mean Square	F	Sig.	Partial Eta Squared	Noncent. Parameter	Observed Power <sup>b</sup>
Corrected Model	2.472 <sup>a</sup>	62	0.040	22.161	0.000	0.916	1373.951	1.000
Intercept	7.957	1	7.957	4421.901	0.000	0.972	4421.901	1.000
Seat upholstery	1.653	6	0.276	153.129	0.000	0.879	918.772	1.000
Agrotechnical surface	0.301	2	0.150	83.571	0.000	0.570	167.141	1.000
Motion speed	0.023	2	0.011	6.299	0.002	0.091	12.599	0.891
Seat upholstery * Agrotechnical surface	0.305	12	0.025	14.140	0.000	0.574	169.682	1.000
Seat upholstery * Motion speed	0.055	12	0.005	2.547	0.005	0.195	30.558	0.967
Agrotechnical surface * Motion speed	0.022	4	0.005	3.053	0.019	0.088	12.213	0.793
Seat upholstery * Agrotechnical surface * Motion speed	0.113	24	0.005	2.624	0.000	0.333	62.986	0.999
Error	0.227	126	0.002					
Total	10.656	189						
Corrected Total	2.699	188						

**Table 4** Tests of Between - Subjects Effects - Dependent Variable: zos

Source	Type III Sum of Squares	df	Mean Square	F	Sig.	Partial Eta Squared	Noncent. Parameter	Observed Power <sup>b</sup>
Corrected Model	2.546 <sup>a</sup>	62	0.041	59.697	0.000	0.967	3701.231	1.000
Intercept	10.478	1	10.478	15232.692	0.000	0.992	15232.692	1.000
Seat upholstery	0.890	6	0.148	215.538	0.000	0.911	1293.231	1.000
Agrotechnical surface	1.020	2	0.510	741.769	0.000	0.922	1483.538	1.000
Motion speed	0.078	2	0.039	56.385	0.000	0.472	112.769	1.000
Seat upholstery * Agrotechnical surface	0.407	12	0.034	49.308	0.000	0.824	591.692	1.000
Seat upholstery * Motion speed	0.017	12	0.001	2.000	0.029	0.160	24.000	.905
Agrotechnical surface * Motion speed	0.029	4	0.007	10.462	0.000	0.249	41.846	1.000
Seat upholstery * Agrotechnical surface * Motion speed	0.106	24	0.004	6.423	0.000	0.550	154.154	1.000
Error	0.087	126	0.001					
Total	13.110	189						
Corrected Total	2.632	188						

**Table 5** Coefficient of variation dependent variable x, y and z axes

Model	r	r <sup>2</sup> Square	Adjusted r <sup>2</sup> Square	Std. Error of the estimate
xos				
1	0.379	0.144	0.130	0.12727
yis				
2	0.309	0.095	0.081	0.11488
zos				
3	0.633	0.401	0.391	0.09233

## 4 CONCLUSION

The two-way variance analysis generally shows that the impact of the two independent variables 'seat upholstery' and 'agrotechnical surface' in the direction of the x axis is highly significant in relation to the dependent variable. The impact of the independent variable 'motion speed' is significant. The interaction of all independent variables is highly significant.

Additionally, the impact of all three independent variables in the direction of the y axis is highly significant, the interaction of the independent variables 'agrotechnical surface' and 'motion speed' is significant, and the impact of all other independent variables is highly significant. The impact of all three independent variables in the direction of the z axis is highly significant, while the interaction of the

independent variables 'seat upholstery' and 'speed motion' is significant. For all other independent variables, the impact is highly significant.

The correlation coefficient shows a connection among dependent variables (i.e. the vibrations that affect the operator's body in the direction of the x, y, and z axes) and the independent variables for which an actual significant correlation in the direction of the z axis was established, while a slight correlation was established in the direction of the x and y axes.

The published research shows that none of the recorded vibration values that affect the operator's body exceeded the limit value of 1.15 m/s<sup>2</sup>.

## 5 REFERENCES

- [1] Tanković, A., Suljić-Beganović, F., Talajić, M., Lutvica, S., Lutvica, E., & Goletić, A. (2015). Effect of vibrations on human body. *Bulletin of Medical Chamber*, 20, 33-40
- [2] Fahy, F. & Thompson, D. (2016). *Fundamentals of sounds and vibration*, 2<sup>nd</sup> ed. Institute of sounds and vibration research, Southampton, U. K. Bergs, J. & Kanaska, D. (2012). Motor vehicle seats and their defect classification. *Engineering for rural development, Proceedings of the 11<sup>th</sup> International scientific conference*, Jelgava, May 2012, 314-318



- [3] Marsili, A., Ragni, L., Santuro, G., Servadio, P., & Vassalini, G. (2002). PM—Power and Machinery: Innovative Systems to reduce Vibrations on Agricultural Tractors: Comparative Analysis of Acceleration transmitted through the Driving Seat. *Biosystems Engineering*, 81(1), 35-47. <https://doi.org/10.1006/bioe.2001.0003>
- [4] Scarlett, A. J., Price, J. S., & Stayner, R. M. (2007). Whole-body vibration: Evaluation of emission and exposure levels arising from agricultural tractors. *Journal of Terramechanics*, 44, 65-73. <https://doi.org/10.1016/j.jterra.2006.01.006>
- [5] Deboli, R., Calvo, A., & Preti, C. (2017). Whole-body vibration: Measurement of horizontal and vertical transmissibility of an agricultural tractor seat. *International Journal of Industrial Ergonomics*, 58, 69-78. <https://doi.org/10.1016/j.ergon.2017.02.002>
- [6] Cutini, M., Romano, E., & Bisaglia, C. (2010). Effect of tyre pressure and wheel loads on whole-body vibration characteristics of tractors. *International Conference, Work Safety and Risk Prevention in Agro-Food and Forest Systems*, Ragusa, September 2010, 431-436.
- [7] Hostens, I., Deprez, K., & Ramon, H. (2004). An improved design of air suspension for seats of mobile agricultural machines. *Journal of sound and vibration*, 276(1-2), 141-156. <https://doi.org/10.1016/j.jsv.2003.07.018>
- [8] Grujicic, M., Pandurangan, B., Arakeres, G., Bell, W. C., He, T., & Xiw, X. (2009). Seat-cushion and soft-tissue material modeling and a finite element investigation of the seating comfort for passenger-vehicle occupants. *Materials and Design*, 30(10), 4273-4285. <https://doi.org/10.1016/j.matdes.2009.04.028>
- [9] Baesso, M. M., Martins, G. A., Barsso, R. C. E., & Fischer, S. J. C. (2014). Noise and Vibration of Tractors: An Ergonomic Evaluation. *International Journal of Applied Science and Technology*, 4(4), 46-54.
- [10] Almeida, S. V., Sperotto, F. C. S., Doimo, L. S., Correia, T. P. S., Santos, J. E. G., & Silva, P. R. A. (2015). Analysis of vibration levels in agricultural tractor with and without cabin. *African Journal of Agricultural Research*, 53(10), 4945-4949.
- [11] HZN (1999). Mechanical vibration and shock -- Evaluation of human exposure to whole-body vibration -- Part 1: General requirements, HRN ISO 2631-1. Croatian Standards Institute, Zagreb, 1999.
- [12] HZN (2010). Mechanical vibration and shock -- Evaluation of human exposure to whole-body vibration -- Part 4: Guidelines for the evaluation of the effects of vibration and rotational motion on passenger and crew comfort in fixed-guideway transport systems, HRN ISO 2631-4. Croatian Standards Institute, Zagreb, 2010.
- [13] EC (2002). Council Directive on the minimum health safety requirements regarding the exposure of workers to the risks arising from physical agents (vibration), J Eur Commun, EEC 89/391, 2002/44.
- [14] Petz, B., Kolesarić, V., & Ivanec, D. (2012). *Petz Statistics – Basic Statistical Methods for Non-mathematicians*. Senat Sveučilišta u Zagrebu, Zagreb.

#### Authors' contacts:

**Željko BARAČ**, MSc, Assistant  
Faculty of Agriculture  
Vladimira Preloga 1, 31000 Osijek  
zbarac@pfos.hr

**Ivan PLAŠČAK**, PhD, Assistant Professor  
Faculty of Agriculture  
Vladimira Preloga 1, 31000 Osijek  
iplascak@pfos.hr

**Tomislav JURIC**, PhD, Full Professor  
Faculty of Agriculture  
Vladimira Preloga 1, 31000 Osijek  
tjuric@pfos.hr

**Mladen JURISIĆ**, PhD, Full Professor  
Faculty of Agriculture  
Vladimira Preloga 1, 31000 Osijek  
mjuriscic@pfos.hr

**Domagoj ZIMMER**, MSc, Assistant  
Faculty of Agriculture  
Vladimira Preloga 1, 31000 Osijek  
dzimmer@pfos.hr

**Ivan VIDA KOVIĆ**, MSc, Assistant  
Faculty of Agriculture  
Vladimira Preloga 1, 31000 Osijek  
ividakovic@pfos.hr

**Davor PETROVIĆ**, MSc, Assistant  
Faculty of Agriculture  
Vladimira Preloga 1, 31000 Osijek  
dpetrovic@pfos.hr

**Vinko DUVNJAK**, PhD, Scientific Adviser  
Agricultural Institute Osijek  
Južno predgrađe 17, 31000 Osijek  
vinko.duvnjak@poljinos.hr

**Monika MARKOVIĆ**, PhD, Assistant Professor  
Faculty of Agriculture  
Vladimira Preloga 1, 31000 Osijek  
mmarkovic@pfos.hr

# A COMPARATIVE STUDY ON THE PERFORMANCE PROPERTIES OF BREATHABLE AND NON-BREATHABLE BABY DIAPER BACK SHEET

Seval UYANIK, Hatice Kübra KAYNAK

**Abstract:** Disposable diapers are very important in terms of babies' health because they are in touch with the baby's skin. Disposable diapers have sheets with different functions from each other. The main layers of disposable diapers are as follows: top sheet, absorbent layer and back sheet. The function of the top sheet is to pass the liquid to the lower absorbent layer whereas the function of the absorbent layer is to absorb the liquid. As for the back sheet, this layer keeps the liquid inside and prevents it from leaving the diaper. The back sheet is usually a nonwoven/ polyethylene (PE) film composite. Considering the babies' health, breathable back sheets are mostly used in baby diapers to keep the skin drier. These have a positive effect on the baby's skin, especially in terms of occlusion, diaper dermatitis. In this study, the performance properties of some commercial baby diaper back sheet layers have been investigated. For this purpose, weight, thickness, air permeability, water vapor permeability and water resistance tests were applied to back sheet samples with different fabric mass as breathable and non-breathable films. All back sheet samples are SMS nonwoven/ polyethylene (PE) film composites. Breathable samples have a larger fabric mass than non-breathable samples. For breathable samples, while increasing mass, air permeability and water vapor permeability decrease, water resistance increases. On the other hand, the same tendency is not seen in non-breathable samples. Breathable samples have higher air permeability, water vapor permeability, water resistance, and bursting strength than non-breathable samples. Consequently, the using of a baby diaper containing breathable back sheet is more proper in terms of baby's skin health.

**Keywords:** air permeability; back sheet; breathable; bursting strength; non-breathable; water resistance; water vapor permeability

## 1 INTRODUCTION

The disposable diaper is one of the most significant consumer product developments of the twentieth century. Baby diapers are safely used every day by parents all over the world. Disposable diapers affect the skin's health directly because they are in close contact with the baby's skin [1]. Since single-use diapers were invented in the 1930s, they have constantly improved and become lighter over the years. Now, baby diapers are easily used, have higher comfort, better hygiene, and improvement in the number and quality [2].

The layers in a typical disposable diaper are namely: top sheet, core, breathable film, and back sheet (Fig. 1). These layers have different effects on the baby diaper thermal comfort property [3].

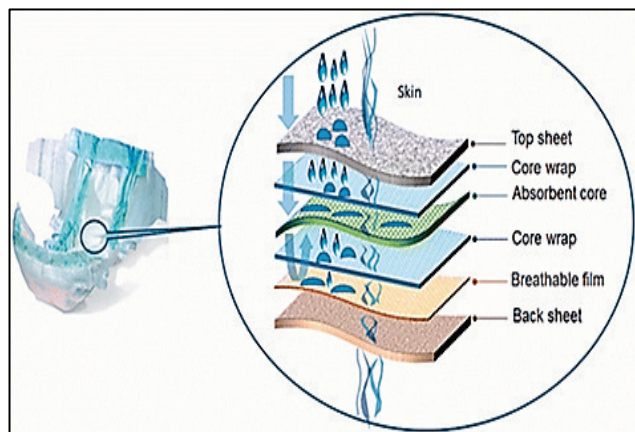


Figure 1 Diaper layers [3]

All sheets forming disposable diapers have different functions. The main layers of disposable diapers are a top

sheet, absorbent layer and back sheet. The function of the top sheet is to pass the liquid to the lower absorbent layer whereas the function of the absorbent layer is to absorb the liquid. In addition, coverstock between the top sheet and the absorbent layer does not let the liquid return to the top sheet. On the other hand, the function of the back sheet is to keep the liquid inside.

In the late 1980s and early 1990s, baby diapers became thinner and a lot of innovations were made. The innovations have improved leakage control (control shields and guards, curved elastic leg openings, waste barriers); comfort (stretch sides and waist bands, cloth-like covers, breathable materials); and aesthetics (cover prints and designs, pleasing scents) [2].

Polyethylene (PE) film or a nonwoven/film composite may be used for the back sheet. This layer contributes to the product performance by preventing the liquid transfer to the outer side of the diaper. Thus this layer has a vital role by the containment of the whole structure. Also, this is the first material that the consumer comes in touch with, therefore a soft touch is an important factor. It is also required from this layer to be robust enough to fulfill its functions. On the other hand, this layer is expected to be thin and noiseless. Breathable film back sheets are widely used in the modern-day absorbent products manufacture. These can help keep the skin drier, which has been shown to have a positive impact on the skin condition in the diapered area, particularly in terms of occlusion, diaper dermatitis [4].

Since the mid-90s when the "breathable" feature was first launched, many brands of baby diapers have been using permeable laminated back sheets (Fig. 2).

The easiest way to manufacture them is by adding calcium carbonate, a very fine mineral just like talc. The  $\text{CaCO}_3$  powder is added to the PE pellets and

homogeneously mixed before the melting screw. Once the film is being extruded, it is stretched with a group of rollers while the film is still warm. This stretching results in millions of micro holes that are made into the film (Fig. 3) [6].

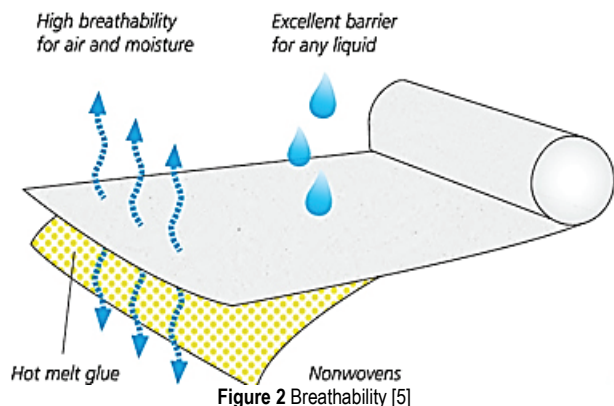


Figure 2 Breathability [5]

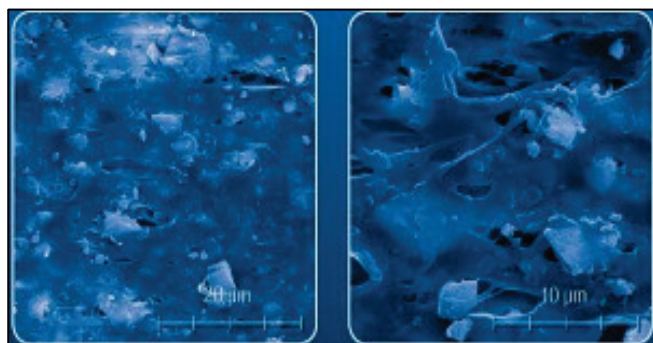


Figure 3 Breathable film after adding  $\text{CaCO}_3$  [7]

The water vapor can pass through the film, but not a drop of water, so it is liquid impervious (Fig. 4) [6].

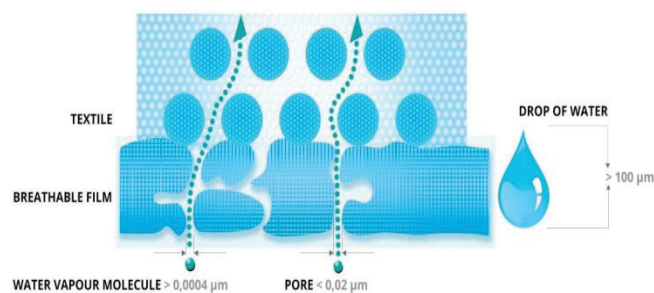


Figure 4 Breathable film [7]

This breathable film can be laminated with a nonwoven sheet using hot melt (Fig. 5) (also commonly called "hot melt lamination breathable laminate"); or extruded directly into a nonwoven sheet (also called "melt embossed breathable laminate") to create the breathable textile back sheet [6].

Typical weights for baby diaper Textile Back sheet range between 20 gsm (as a minimum for direct melt embossed extrusion) to around 28 gsm (as a minimum for hot melt lamination) [6].

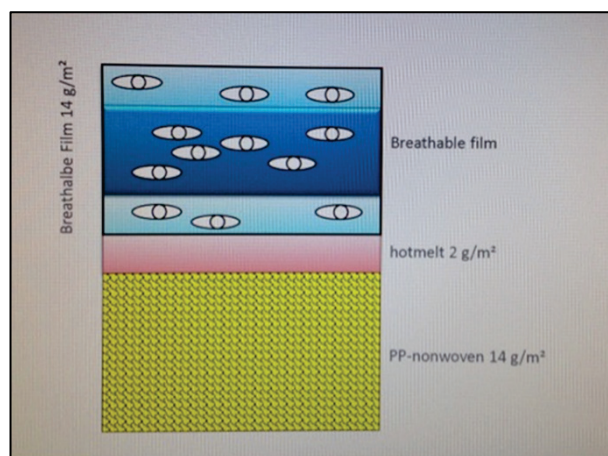


Figure 5 Breathable back sheet [6]

In the majority of previous works [8-11], thermal comfort properties i.e., thermal conductivity, heat, air, and water transport properties of one layer of diapers were investigated especially for top sheet layer.

In this study, the purpose is determining the performance properties of breathable and non-breathable baby diaper back sheet.

## 2 MATERIALS AND METHODS

All back sheet samples are SMS nonwoven/polyethylene (PE) film composites. Fabric mass and thickness values of the samples were determined according to the standards of TS 12127 and TS 7128 EN ISO 5084 and given in Tab. 1. As seen from Tab. 1, breathable samples have a higher mass than non-breathable samples. For all samples, 1 g hot-melt was used for the lamination of film and nonwoven. On the other hand, there is no difference between thickness values of breathable and non-breathable samples. Likewise, the increase in weight does not affect the thickness of the samples when breathable and non-breathable samples are examined without discrimination.

Table 1 Fabric mass and thickness values of the back sheet samples

	Samples	Mass, gsm	Thickness, mm
Non-breathable	1	23	0.09
	2	23	0.11
	3	24	0.11
Breathable	4	25	0.10
	5	26	0.10
	6	28	0.11

In the context of this study, air permeability, water vapor permeability, water resistance and bursting strength tests were applied to back sheet samples having different fabric mass as breathable and non-breathable films in accordance with TS 391 EN ISO 9237, BS 7209, TS 257 EN 20811, and EN ISO 13938-2 standards, respectively. Moreover, independent samples T-test and Pearson correlation tests were performed via SPSS 21 package program in order to understand the statistical importance of breathability on the back sheet properties. The program was



also used to determine the relationship between independent and dependent variables.

Air permeability test was done with digital air permeability test device at a 100 Pa pressure drop and a 20 cm<sup>2</sup> test area with 5 specimens from each sample (Fig. 6).

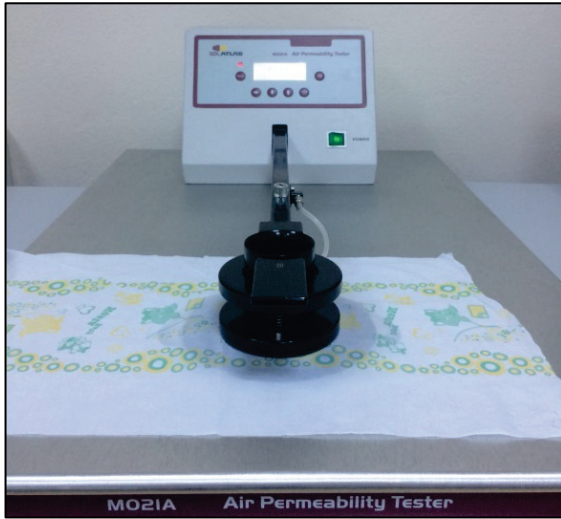


Figure 6 Air permeability test

Water vapor permeability test was done according to the evaporative dish method BS 7209:1990. Three test specimens were mounted over the test dishes containing distilled water at 20±2°C. These dishes were placed on a rotating turntable. The samples were rotated with a turntable for one hour to establish equilibrium of water vapor pressure gradient across the sample (Fig. 7). Then, the masses of the dishes were determined. The turntable with dishes was rotated for a further 5-hour time-period. The masses of the dishes were weighed after this period. The weight difference was found.

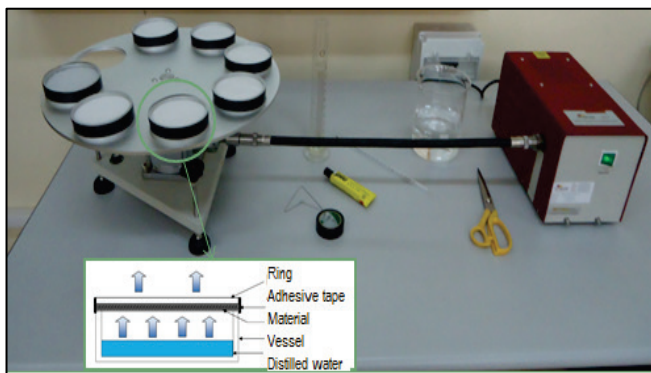


Figure 7 Water vapor permeability test (evaporative dish method)

The water vapor permeability (*WVP*) in g/m<sup>2</sup>/day is given by the equation:

$$WVP = \frac{24M}{At} \quad (1)$$

where,

*M* = loss in mass of the dish over the time period in grams

*t* = time between successive weighing of the assembly in hours

*A* = area of the exposed sample, 5.41×10<sup>-3</sup> m<sup>2</sup>

Water resistance test was done with Hydrostatic head tester by Dynamic test (Fig. 8). Test head of 100 cm<sup>2</sup> was used and the tests were performed with 10 cm water column/min (mbar/min) pressure increase. Five specimens were tested from each sample.



Figure 8 Water resistance test (dynamic test)



Figure 9 Bursting strength test (pneumatic method)

The bursting strength test was done by a pneumatic bursting strength test device (Fig. 9) in five different places per sample, and test results were evaluated in kPa. The test area used in the instrument was 7.3 cm<sup>2</sup>. The tests were performed using a pneumatic method where the sample was

placed on an elastic diaphragm and increased pneumatic pressure was applied beneath the diaphragm until the specimen burst. It should also be noted that nonwoven surfaces of the specimens were placed at the bottom.

### 3 RESULTS AND DISCUSSION

The results were analyzed under 4 headings as air permeability, water vapor permeability, water resistance, and bursting strength.

#### 3.1 Air permeability

From Fig. 10, different tendencies were seen between breathable and non-breathable samples. Increase in weight increased air permeability values of the samples unexpectedly. On the contrary, increase in weight reduced these values in breathable samples.

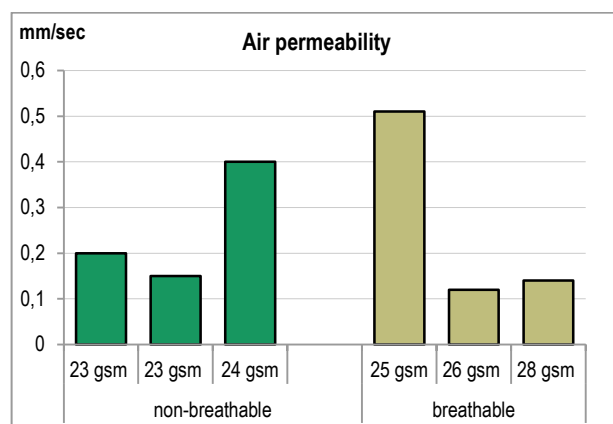


Figure 10 Air permeability

Breathability as a factor has no effect on air permeability of back sheet, since 2- tailed sig. value (0.944)>0.05 according to Tab. 2. Furthermore, Pearson correlation test results show that there is no relationship between breathability and air permeability.

#### 3.2 Water Vapor Permeability

Breathability is a water vapor transmission with diffusion of a material and it is important for healthy skin as determined above. In terms of water vapor permeability properties of the samples, there is a very clear difference between breathable and non-breathable samples (Fig. 11). Breathable samples have noticeably higher water vapor permeability than non-breathable samples. In addition to this, water vapor permeability values decreased with increasing mass for breathable samples.

T-test results display that breathability ( $p$  value is  $0.07 < 0.05$ ) has a significant effect on water vapor permeability of back sheet. According to Pearson correlation, there is a very strong and positive relationship between breathability and water vapor permeability.

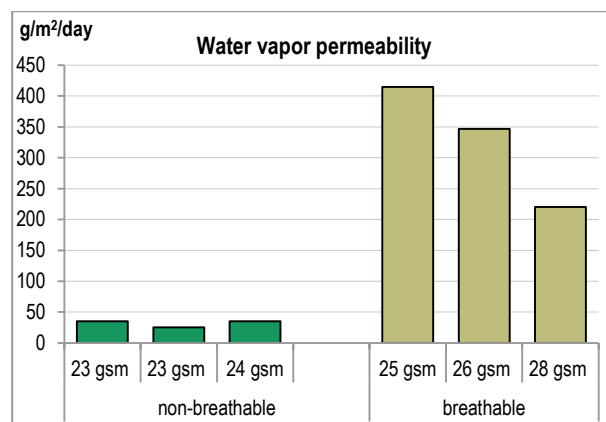


Figure 11 Water vapor permeability

#### 3.3 Water Resistance

According to Fig. 12, breathable samples have higher water resistance than non-breathable samples. For breathable samples, increasing mass increased water resistance. On the other hand, the same tendency is not seen for non-breathable samples.

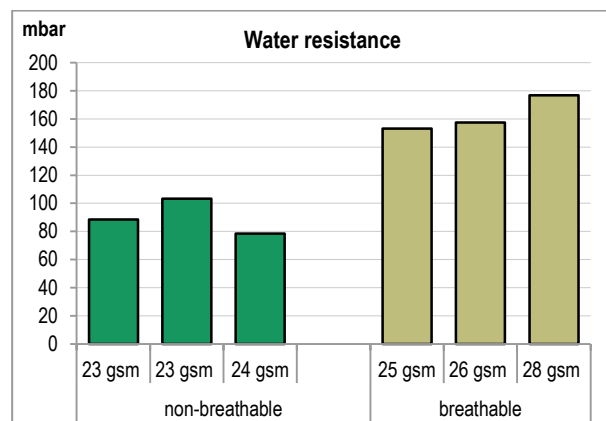


Figure 12 Water resistance

According to t-test results, breathability ( $p$  value is  $0.02 < 0.05$ ) has a significant effect on water resistance of back sheets. As for Pearson correlation, it is visible that there are very strong and positive relationships between breathability and water resistance, and between mass and water resistance. However, the relationship between breathability and water resistance is stronger than the relationship between the mass and water resistance.

#### 3.4 Bursting strength

It is seen that bursting strength values of breathable samples are higher than that of non-breathable samples from Fig. 13. There is no clear tendency of increasing bursting strength with higher mass for non-breathable samples. On the contrary, it is clear that the bursting strength values of samples increase by increasing mass for breathable samples.

T-test results show that breathability ( $p$  value is  $0.026 < 0.05$ ) has a significant effect on bursting strength of the back sheet. There are very strong and positive

relationships between breathability and bursting strength, and between mass and bursting strength according to the Pearson correlation analysis. This means that bursting strength increases with breathability and increasing mass.

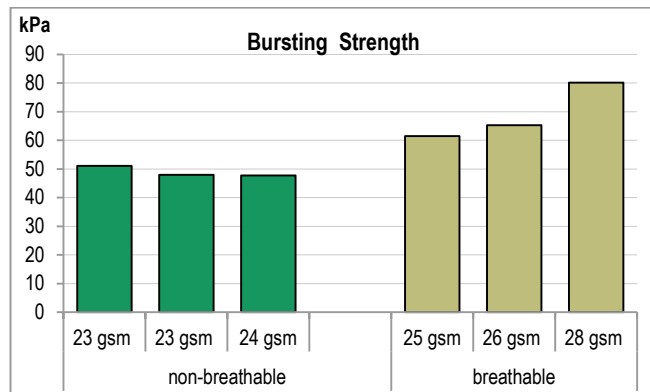


Figure 13 Bursting strength

Independent samples T-test and Pearson test results are shown in Tabs. 2 and 3, respectively. According to Tab. 2, group variances were assumed as equal for all variables since all significance values  $>0.05$  in Levene's test. 2-tailed significance values displayed with \* symbol were considered for the interpretation of t-test.

Table 2 Independent Samples T-test results

	Levene's test for equality of variances		T-test for equality of means	
	F	Sig.	T	Sig. (2-tailed)
Air permeability	1.791	0.252	-0.045	0.966*
			-0.045	0.967**
Water vapor permeability	6.384	0.065	-5.167	<b>0.007*</b>
			-5.167	<b>0.035**</b>
Water resistance	0.025	0.881	-7.094	<b>0.002*</b>
			-7.094	<b>0.002**</b>
Bursting strength	7.515	0.052	-3.454	<b>0.026*</b>
			-3.454	<b>0.067**</b>

\*Equal variances assumed

\*\* Equal variances not assumed

Table 3 Pearson correlation test results

	Type	Mass	Thickness
Air permeability	0.023	-0.195	-0.025
Water vapor permeability	<b>0.933**</b>	0.612	-0.161
Water resistance	<b>0.962**</b>	<b>0.880*</b>	0.103
Bursting strength	<b>0.865*</b>	<b>0.965**</b>	0.132

\*Correlation is significant at 0.05 level.

\*\* Correlation is significant at 0.01 level.

The definition of 'type' expresses breathability or non-breathability for back sheet in Tab. 4.

## 4 CONCLUSIONS

For breathable samples, while increasing mass, air permeability and water vapor permeability decrease, water resistance and bursting strength increase. On the other hand, the same tendency is not seen for non-breathable samples. Breathability is a water vapor transmission with diffusion of a material and it is important for healthy skin as determined

above. Breathable samples have higher air permeability, water vapor permeability, water resistance and bursting strength than non-breathable samples.

T-test results display that breathability ( $p$  value is  $0.07 < 0.05$ ) has significant effect on water vapor permeability of back sheet. According to Pearson correlation, there is very strong and positive relationship between breathability and water vapor permeability. This means that breathability increases water vapor permeability in parallel.

## 5 REFERENCES

- [1] Yaman, N., Senol, M. F., & Tayyar, A. E. (2007). Alternative Test Methods for Assessing Mechanical Properties of Disposable Diapers. *Fibres & Textiles in Eastern Europe*. 15(2) (61), 80-84.
- [2] See <http://edana.org>
- [3] Ozen, I., Cincik, E., & Simsek, S. (2016). Thermal Comfort Properties of Simulated Multilayered Diaper Structures in Dry and Wet Conditions. *Journal of Industrial Textiles*. 46(1), 256-278. <https://doi.org/10.1177/1528083715580521>
- [4] <http://disposablediaper.net/files/dictionary.pdf>
- [5] <http://www.plastik.it/en/product/breathable-textile-back-sheet/>
- [6] <https://www.linkedin.com/pulse/how-choose-correct-breathability-disposable-diaper-carlos-pdf>
- [7] <http://www.fatra.cz/en/products/breathable-films-and-laminates/breathable-films-sontek-f/>
- [8] Vakili, M. H., Ebadi-Dehaghani, H., & Haghshenas-Fard, M. (2011). Crystallization and Thermal Conductivity of  $\text{CaCO}_3$  Nanoparticle Filled Polypropylene. *J Macromol Sci B*, 50, 1637-1645. <https://doi.org/10.1080/00222348.2010.543033>
- [9] Jakubowska, P. & Sterzyński, T. (2012). Thermal Diffusivity of Polyolefin Composites Highly Filled with Calcium Carbonate. *Polimery*, 57, 271-275. <https://doi.org/10.14314/polimery.2012.271>
- [10] Yokura, H. & Sukigara, S. (2010). Evaluation of the Wetness of Pantliners. *Textile Research Journal*, 80, 1643-1647. <https://doi.org/10.1177/0040517510365955>
- [11] Guo, Y., Ng, F. S. F., Hui, P. C. L. (2013). Heat and Mass Transfer of Adult Incontinence Briefs in Computational Simulations and Objective Measurements. *International Journal of Heat and Mass Transfer*, 64, 133-144. <https://doi.org/10.1016/j.ijheatmasstransfer.2013.04.022>

### Authors' contacts:

Seval UYANIK, Dr.  
Gaziantep University,  
Technical Sciences High Vocational School,  
Textile Department  
Gaziantep/Turkey  
+90 342 3601200/3644, uyanik@gantep.edu.tr

Hatice Kübra KAYNAK, Assoc. Prof.  
Gaziantep University,  
Textile Engineering Department  
Gaziantep/Turkey  
+90 342 3172709, tuluce@gantep.edu.tr

# THIN LAYER DRYING OF ZUCCHINI IN SOLAR DRYER LOCATED IN OSMANIYE REGION

Kamil Neyfel ÇERÇİ, Özge SÜFER, Mustafa SÖYLER, Ertay HÜRDOĞAN, Coşkun ÖZALP

**Abstract:** In this study, the dehydration behavior of zucchini using solar assisted drying system was examined according to 22 thin layer drying models available in literature. The correlation coefficient ( $R^2$ ), chi-square ( $\chi^2$ ) and root mean square error (RMSE) values were calculated to check the suitability of models by non-linear regression analysis. It was found that Cubic and Modified Midilli-1 models were the most suitable equations and their  $R^2$  values were calculated as 0.99963.  $\chi^2$  and RMSE values of related mathematical expressions were  $1.89343 \times 10^{-5}$ ,  $1.91692 \times 10^{-5}$  and  $0.01685 \times 10^{-3}$ ,  $0.01721 \times 10^{-3}$  respectively. In addition, heat transfer, mass transfer and diffusion coefficients, which were important parameters in design of drying systems were also determined as  $5.18124 \text{ W/m}^2\text{°C}$ ,  $1.57129 \times 10^{-7} \text{ m/s}$  and  $2.335718 \times 10^{-9} \text{ m}^2/\text{s}$  respectively.

**Keywords:** diffusion coefficient; heat and mass transfer coefficient; mathematical modeling

## 1 INTRODUCTION

Drying basically starts with the solution of coupling forces between water and material which will be dried. There is a specific energy requirement and this must be given to material continuously as heating for the evaporation of moisture to the surface and pores of the layer. In this sense, the drying process is the heat and mass transfer processes that take place at the same time [1,2]. If product is not dried up sufficiently, it affects the quality of the food negatively due to changes in chemical, biochemical and physical characteristics [3,4].

In this context, scientists have been working on mathematical models and computer simulations to design and develop dryers for efficient dehydration. In order to accurately describe the drying kinetics of food products, mathematical modeling is one of the most appropriate approaches. Factors affecting heat and mass transfer between food product and drying air, deviations in case of equilibrium between product and dry air, the change of physical properties of product, water vapor and air by changing humidity and temperature are considered by using these models [5-10].

In the literature, there are many studies about the determination of heat and mass transfer, mathematical modeling, computer simulations in order to design and develop drying systems for different types of fruit and vegetables [11-16]. Midilli and Kucuk [17] carried out drying experiments for nuts under natural and forced convection in solar assisted drying. The scientists found that the logarithmic model could be the most appropriate model to define thin layer forced solar drying. However, they saw that the two-term model was more appropriate in natural solar drying. Younis et al. [18] carried out experiments for the drying of garlic slices; infrared drying was applied at different air velocities and radiation intensities onto materials. The results indicated that decreasing air velocity and rising radiation intensity caused an increase in drying rate and a decrease in drying time. Bozkır [19] developed a mathematical model in thin film formation of washed

apricots. The experiments carried out at different temperatures and velocities. Data from experiments was analyzed by Page's drying equations.

In this work, air solar collector assisted drying system was used for modelling zucchini drying. The zucchini contains mineral elements such as potassium, phosphorus, calcium, magnesium, sodium, iron. There is a great difference in nutritional values between consuming the same amount of fresh zucchini and dried zucchini, but when the benefits are compared, the dried zucchini is almost as useful as the fresh zucchini. Dried zucchini can be used for ready-made sacks, bulgur, rice mixtures, bird and pet food. [20]. To investigate the availability of models, correlation coefficient ( $R^2$ ), root mean square error (RMSE) and chi-square ( $\chi^2$ ) values were calculated. In addition, convective mass and heat transfer coefficients were calculated for contributing to the literature in drying design.

**Table 1** The devices used for measurements and their specifications

Device	Measurement parameters	Accuracy
Testo 435 air speed probe	Air velocity	0.1 m/s
Ledmer digital temperature measurement probe	Temperatures	0.1 °C
Dikomsan Model electronic balance	Product weight	0.1 gr
Testo 435 humidity measuring probe	Relative humidity	2-3 %
Eko model MS-410 type pyranometer	Radiation	-
Laboratory type oven (JSR, 400, England)	Initial and final moisture contents of samples	-

## 2 EXPERIMENTAL STUDY

Schematic illustration and the image of the solar assisted drying system are shown in Fig. 1. The ambient air enters the solar collector (state 1) and leaves the collector (state 2) hotter. Then, hot air is passed to the drying cabinet for drying the products. The drying chamber was designed specifically to distribute hot air uniformly. Finally, the air exits the cabinet with more moisture than when entered the cabinet. More



detailed information about the system is given in reference [21].

Zucchini samples were procured from Erzin region, Hatay/ Turkey. They were cut into average 47 mm of diameter

and 5 mm thickness and lined up on the tray.

Tab. 1 shows the devices used for measurements and their specifications.

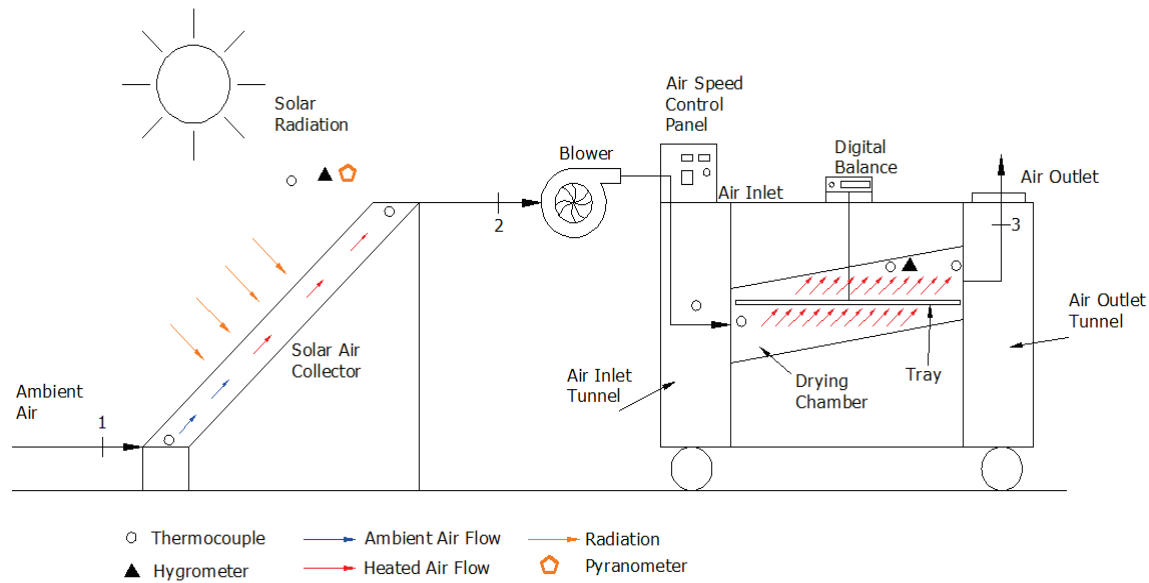


Figure 1 Schematic illustration (a) and the image (b) of the solar-assisted drying system

## 2.1 Computation Procedure

The data obtained from the drying process were fitted to 22 thin layer models given in Tab. 2.  $k$ ,  $k_0$ ,  $k_1$  and  $n$  denote drying constants and  $a$ ,  $b$ ,  $c$ ,  $d$  are statistical parameters.

$MR$  is moisture ratio and it was calculated by using Eq. (1).

$$MR = \frac{M - M_e}{M_0 - M_e} \quad (1)$$

In the related equation,  $M$  is the amount of moisture at

any time,  $M_e$  is the amount of moisture in equilibrium, and  $M_0$  is initial moisture content. To simplify  $MR$ , it can be expressed by  $M/M_0$ , because of  $M_e$  is lower than  $M$  and  $M_0$  values [42, 43].

Regression analysis was done by using Origin pro program 2016 (Origin Lab, USA).

Correlation coefficients ( $R^2$ ) were taken as the basic criteria to select the best equation that describes the drying curves of the products [44].

The most suitable model was determined using root mean square error ( $RMSE$ ) and chi-square ( $\chi^2$ ) values after  $R^2$  and calculated as:



$$RMSE = \left[ \frac{1}{N} \sum_{i=1}^N (MR_{exp,i} - MR_{pre,i})^2 \right]^{1/2} \quad (2)$$

$$\chi^2 = \frac{\sum_{i=1}^N (MR_{exp,i} - MR_{pre,i})^2}{N - z} \quad (3)$$

$MR_{exp,i}$  is an  $MR$  value in  $i$ ,  $MR_{pre,i}$  value is an estimated  $MR$  value.  $N$  is experiments number,  $z$  is constant number. The  $MR_{exp,i}$  is an  $MR$  value in  $i$ ,  $MR_{pre,i}$  value is an estimated  $MR$  value.  $N$  is experiments number,  $z$  is constant number.

**Table 2** Different thin layer drying models available in literature

Model Name	Equation	Reference
Lewis	$MR = \exp(-kt)$	[22]
Page	$MR = \exp(-kt^n)$	[23]
Modified Page	$MR = \exp(-kt^n)$	[24]
Henderson & Pabis	$MR = a \exp(-kt)$	[25]
Logarithmic	$MR = a \exp(-kt) + c$	[26]
Two-term	$MR = a \exp(-k_0t) + b \exp(-k_1t)$	[27]
Wang and Singh	$MR = 1 + at + bt^2$	[28]
Weibull	$MR = \exp\left(-\left(\frac{t}{b}\right)^a\right)$	[29]
Midilli et al.	$MR = a \exp(-kt^n) + bt$	[30]
Parabolic	$MR = a + bt + ct^2$	[30]
Cubic	$MR = a + bt + ct^2 + dt^3$	[31]
Sigmoid	$MR = a + \frac{b}{1 + e^{k(t-c)}}$	[32]
Thompson	$t = a \ln(MR) + b [\ln(MR)^2]$	[33]
Vega-Lemus	$MR = (a + bt)^2$	[34]
Rational	$MR = \frac{a+bt}{1+ct+dt^2}$	[35]
Vega Galvez-1	$MR = n + k\sqrt{t}$	[36]
Vega Galvez-2	$MR = \exp(n+kt)$	[36]
Hii et al.	$MR = a \exp(-k_0t^n) + b \exp(-k_1t^n)$	[37]
Mod. Midilli-1	$MR = \exp(-kt^n) + bt$	[38]
Mod. Midilli-2	$MR = \exp(-kt) + bt$	[39]
Sripinyowanich & Noomhorn	$MR = \exp(-kt^n) + bt + c$	[40]
Noomhorn & Verma	$MR = a \exp(-k_0t) + b \exp(-k_1t) + c$	[41]

The effective moisture diffusivity was computed with respect to Fick's second law. Some assumptions can be made within the framework of this law:

- The humidity distribution is uniform in the cylindrical geometry of the product.
- Mass transfer is symmetric according to the center of zucchini slice.
- The surface resistances in mass transfer can be ignored.
- The diffusion coefficient is assumed to be constant.

The correlation between  $MR$  and diffusion coefficient were indicated by Eq. (4):

$$MR = \frac{8}{\pi^2} \exp\left(-\pi^2 \frac{D'_{eff}}{r^2}\right) \quad (4)$$

$D'_{eff}$  is the diffusion coefficient ( $m^2/s$ ),  $r$  is the radius of the samples ( $m$ ),  $t$  is time ( $s$ ) [45].

Activation energy of zucchini samples was specified using Arrhenius type equations [14]:

$$D_{eff} = D_0 \exp\left(-\frac{E_a}{RT}\right) \quad (5)$$

$E_a$  is activation energy ( $kJ/mol$ ),  $R$  is universal gas constant ( $8.3143 J/mol K$ ),  $T$  is ambient temperature ( $K$ ), and  $D_0$  is predominant exponential factor ( $m^2/s$ ). The activation energy is formed of the slope of the linearized line of Eq. (5).

Besides, the convective mass transfer coefficient ( $\alpha$ ,  $m/s$ ) was obtained by Eq. (6) [46]:

$$\alpha = -\frac{V}{A_t} \ln(MR) \quad (6)$$

where,  $V$  is volume of product ( $m^3$ ),  $A_t$  is product area ( $m^2$ ).

The convective heat transfer coefficient ( $h_c$ ,  $W/m^2\text{°C}$ ) was calculated for forced convection by Eq. (7) [47].

$$h_c = \frac{Nu K_v}{x} \quad \text{or} \quad h_c = \frac{K_v}{x} C(Re Pr)^n \quad (7)$$

where,  $Nu$  is Nusselt Number,  $K_v$  is thermal conductivity ( $W/m\text{°C}$ ),  $Re$  is Reynolds Number,  $Pr$  is Prandtl Number,  $C$  and  $n$  are constants for calculating heat transfer coefficient value.

The rate of required heat to evaporate moisture ( $\dot{Q}_e$ ) was computed by Eq. (8) [48].

$$\dot{Q}_e = 0.016 h_c [P(T_c) - \gamma P(T_e)] \quad (8)$$

where,  $T_c$  is product temperature and  $T_e$  is exit air temperature.

The moisture evaporated was calculated by Eq. (9). Here, Eq. (8) was divided with latent heat of vaporization ( $\lambda$ ), and multiplied with the area of tray ( $A_t$ ) and time interval ( $t$ ).

$$\dot{m}_{ev} = \frac{\dot{Q}_e}{\lambda} A_t t \quad (9)$$

where,  $Z = 0.016 \frac{K_v}{x\lambda} [P(T_c) - \gamma P(T_e)] A_t t$

$$\frac{\dot{m}_{ev}}{Z} = C(Re Pr)^n \quad (10)$$

The logarithms of both sides of Eq. (10) are taken,

$$\ln\left[\frac{\dot{m}_{ev}}{Z}\right] = \ln C + n \ln(Re Pr) \quad (11)$$

Eq. (11) similar to an equation of straight line,  
 $Y = b_1 X + b_0$

where,  $Y = \ln \left[ \frac{\dot{m}_{ev}}{z} \right]$ ,  $b_1 = n$ ,  $X = \ln(Re Pr)$ ,  $b_0 = \ln C$

$C$  and  $n$  values were determined using linear regression analysis with the obtained experimental data of exit air relative humidity, the product and exit air temperatures and moisture evaporated at the specific time intervals.

The different physical properties of humid air, such as density ( $\rho_v$ ), thermal conductivity ( $K_v$ ), specific heat ( $C_v$ ) and viscosity ( $\mu_v$ ), were calculated by using  $T_i$ , which is taken as an average of product temperature ( $T_c$ ) and exit air temperature ( $T_e$ ) for calculating Reynolds number ( $Re$ ) and Prandtl number ( $Pr$ ) [49].

$$\rho_v = \frac{353.44}{(T_i + 273.15)} \quad (12)$$

$$K_v = 0.0244 + 0.6773 \times 10^{-4} T_i \quad (13)$$

$$C_v = 999.2 + 0.1434 T_i + 1.101 \times 10^{-4} T_i^2 - 6.7581 \times 10^{-8} T_i^3 \quad (14)$$

$$\mu_v = 1.718 \times 10^{-5} + 4.620 \times 10^{-8} T_i \quad (15)$$

$$P(T) = \exp \left[ 25.317 - \frac{5144}{T_i + 273.15} \right] \quad (16)$$

### 3 RESULTS AND DISCUSSION

In the study, the drying behaviors of the zucchini samples were investigated by using experimental data collected from the solar energy-assisted dryer.

The highest correlation coefficient ( $R^2$ ) values were found as 0.99963 for Spirinyowanich and Noomhorn, Cubic, Rational, Modified Midilli-1 and Midilli models. The best results of  $\chi^2$  values were seen in Cubic and Modified Midilli-1 models because of the lowest levels. The values obtained from indicated models were  $1.89343 \times 10^{-5}$  and  $1.91692 \times 10^{-5}$ , respectively. In addition, RMSE values for Cubic and Modified Midilli-1 models were calculated as  $0.01685 \times 10^{-3}$  and  $0.01721 \times 10^{-3}$  respectively. The values of Spirinyowanich and Noomhorn, Cubic, Rational, Modified Midilli-1 and Midilli models were shown in Table 3 since they have the best correlation coefficient values ( $R^2$ ).

The variation of the convective mass transfer coefficient (m/s) and  $\ln MR$  values with time were shown in Fig. 2 and 3 respectively.

According to Fig. 2, the convective mass transfer coefficient values varied between  $8.65264 \times 10^{-8}$  and  $1.97664 \times 10^{-7}$  m/s. The average convective mass transfer coefficient was calculated as  $1.57129 \times 10^{-7}$  m/s. The average diffusion coefficient of zucchini samples was obtained as  $2.33572 \times 10^{-9}$  m<sup>2</sup>/s. It is seen that the diffusion coefficient

values calculated in this study are in accordance with the literature [50, 51, 52, 53].

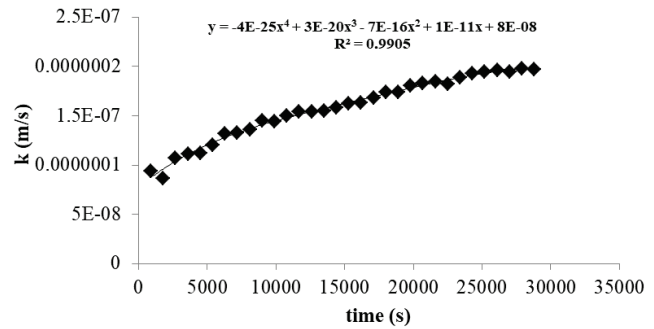


Figure 2 Variation of mass transfer coefficient with drying time

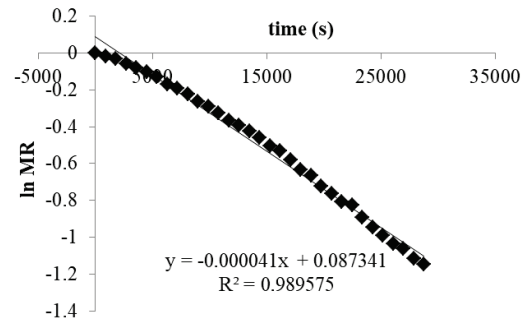


Figure 3  $\ln MR$  with drying time

The variations in convective heat transfer coefficient with time are presented in Fig. 4.

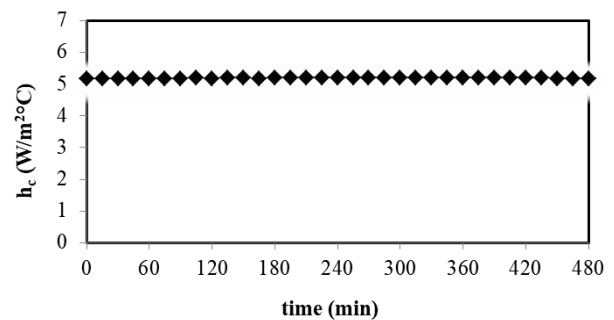


Figure 4 Variation of heat transfer coefficient with drying time

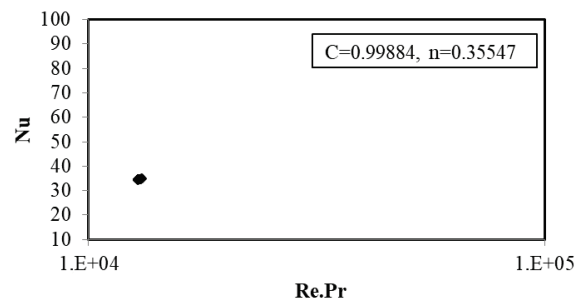


Figure 5 The relation between  $Nu-Re.Pr$  for zucchini samples drying at forced convection

The convective heat transfer coefficient values varied between 5.16841-5.18672 W/m<sup>2</sup>°C during drying process. The variation remained almost constant during drying. The air

velocity, which is an important parameter in forced convection is kept constant during the experiment. Akpınar [50, 54], evaluated convective heat transfer coefficient values for different food products for forced convection in literature. The convective heat transfer coefficient values varied at between 0.644 and 10.94 W/m<sup>2</sup>°C. It was seen that these values are in accordance with the literature [50, 54].

The relation between Nusselt and Reynolds-Prandtl numbers were given in the following graph (Fig. 5).

It could be seen from the figure that the heat transfer carried out under the laminar regime because of  $Re \cdot Pr \leq 10^5$  [55]. The Nusselt number values of the zucchini samples were found between 34.29895-34.76936. Also, C and n constants were found 0.99884 and 0.35547 respectively. Similar results were found by Jain and Tiwari [56]. They indicated laminar regime on drying of peas in greenhouse dryer for forced convection.

**Table 3** The statistical parameters of Spirinyowanich and Noomhorn, Cubic, Rational, Modified Midilli-1 and Midilli models

Model name	$R^2$	$\chi^2$	SSE	RMSE	k	n	a	b	c	d
Midilli et al.	0.99963	$0.00193 \times 10^{-2}$	0.00056	$0.01698 \times 10^{-3}$	0.00038	1.29122	0.99809	-	-	-
Mod. Midilli-1	0.99963	$0.00189 \times 10^{-2}$	0.00057	$0.01721 \times 10^{-3}$	0.00041	1.27906	-	-0.00005	-	-
Spirinyowanich & Noomhorn	0.99963	$0.00193 \times 10^{-2}$	0.00056	$0.01698 \times 10^{-3}$	0.00038	1.29093	-	-0.00004	-0.00192	-
Cubic	0.99963	$0.00191 \times 10^{-2}$	0.00056	$0.01685 \times 10^{-3}$	-	-	1.00634	-0.00137	$0.00001 \times 10^{-1}$	0
Rational	0.99963	$0.00196 \times 10^{-2}$	0.00057	$0.01729 \times 10^{-3}$	-	-	1.00347	-0.00081	0.00042	0

## 4 CONCLUSIONS

In this work, air solar collector assisted drying system was used to investigate the availability of the models for zucchini drying. The correlation coefficient ( $R^2$ ), root mean square error (RMSE) and chi-square ( $\chi^2$ ) were calculated. It was seen that the highest values for the correlation coefficient were found as 0.99963 in Spirinyowanich and Noomhorn, Cubic, Rational, Modified midilli-1 and Midilli models. Besides, the lowest values of the chi-square were obtained in Cubic and Modifid Midilli-1 models. Also, RMSE values of those models were computed as  $0.01685 \times 10^{-3}$  and  $0.01721 \times 10^{-3}$  respectively. Finally, the convective mass and heat transfer coefficients and diffusion coefficient, which are important parameters in determining the drying performance, have been calculated. The average convective mass transfer coefficient and diffusion coefficient were calculated as  $1.57129 \times 10^{-7}$  m/s and  $2.33572 \times 10^{-9}$  m<sup>2</sup>/s respectively. The average convective heat transfer coefficient for forced convection was calculated as 5.18124 W/m<sup>2</sup>°C. Also, C and n values, which are used for calculating convective heat transfer coefficient, were found as 0.99884 and 0.35547 respectively.

## Acknowledgment

This work was supported by the Department of Energy Systems Engineering under OKÜ scientific research project unit (project no: OKÜBAP-2014-PT3-032), Turkey.

**Note:** This research was presented at the International Advanced Researches and Engineering Congress, IAREC 2017 (16-18 November 2017, Osmaniye, Türkiye).

## 5 REFERENCES

- [1] Yaşartekin, Y. (1991). Kabinet tipi güneş enerjili kurutucunun tasarımı ve tarımsal ürünlerin kurutulmasında denemesi, *MSc Thesis*, Ege University, İzmir.
- [2] Çınar, H. (2009). Muğla iklim koşullarında havalı güneş toplacı ısı pompalı kereste kurutma tesisinde kurutma ekonomisinin araştırılması. *MSc Thesis*, Muğla University, Muğla.
- [3] Fellows, P. (2000). Food processing technology principles and practice, 2<sup>nd</sup> Edition, Boca Raton and Cambridge, CRC Press.
- [4] Yemmireddy, V. K., Chinnan, M. S., Kerr, W. L., & Hung, Y. C. (2006). Effect of drying method on drying time and physico-chemical properties of dried rabbiteye blueberries. *LWT-Food Science and Technology*, 50(2), 739-745. <https://doi.org/10.1016/j.lwt.2012.07.011>
- [5] Brooker, D. B., Bakker-Arkema, F. W., & Hall, C. W. (1982). *Drying cereal grains*, Westport, CT: AVI Publishing Co.
- [6] Courtois, F., Lebert, A., Lasseran, J. C., & Bimbenet, J. J. (1991). Simulation of industrial dryers: solving numerical and computer problems. *Drying Technology*, 9(4), 927-945. <https://doi.org/10.1080/07373939108916728>
- [7] Khatchatourian, O. A., Borges, P. A. P., & Vielmo, H. A. (2003). Simulation of soy grains drying Dynamics in camera of fixed bed. *Proceeding of the 17<sup>th</sup> International Congress of Mechanical Engineering / Sao Paulo, Brazil*.
- [8] Khatchatourian, O. A. & Oliveira, F. A. (2006). Mathematical modelling of airflow and thermal state in large aerated grain storage. *Biosystems Engineering*, 95(2), 159-169. <https://doi.org/10.1016/j.biosystemseng.2006.05.009>
- [9] Parry, J. L. (1985). Mathematical modelling and computer simulation of heat and mass transfer in agricultural grain drying: a review. *Journal of Agricultural Engineering Research*, 32(1), 1-29. [https://doi.org/10.1016/0021-8634\(85\)90116-7](https://doi.org/10.1016/0021-8634(85)90116-7)
- [10] Celma, A. R., Rojas, S., & Lopez-Rodriguez, F. (2008). Mathematical modelling of thin-layer infrared drying of wet olive husk. *Chemical Engineering and Processing*, 47, 1810-1818. <https://doi.org/10.1016/j.cep.2007.10.003>
- [11] Khatchatourian, O. A. (2012). Experimental study and mathematical model for soya bean drying in thin layer. *Biosystems engineering*, 113, 54-64. <https://doi.org/10.1016/j.biosystemseng.2012.06.006>
- [12] White, G. M., Bridges, T. C., Loewer, O. J., & Ross, I. J. (1981). Thin-layer drying model for soybeans. *Transaction of ASAE*, 6, 1643-1646. <https://doi.org/10.13031/2013.34506>
- [13] Wang, C. Y. & Singh, R. P. (1978). A single layer drying equation for rough rice, *ASAE*, 78-3001.
- [14] Akpınar, E., Midilli, A., & Bicer, Y. (2003). Single layer drying behavior of potato slices in a convective cyclone dryer and mathematical modelling. *Energy Conversion and Management*, 44, 1689-1705. [https://doi.org/10.1016/S0196-8904\(02\)00171-1](https://doi.org/10.1016/S0196-8904(02)00171-1)

- [15] Akpinar, E. K., Bicer, Y., & Yıldız, C. (2003). Thin layer drying of red pepper. *Journal of Food Engineering*, 59, 99-104. [https://doi.org/10.1016/S0260-8774\(02\)00425-9](https://doi.org/10.1016/S0260-8774(02)00425-9)
- [16] Ross, I. J. & White, G. M. (1972). Thin-layer drying characteristics of white corn. *Transaction of ASAE*, 15, 175-179. <https://doi.org/10.13031/2013.37859>
- [17] Midilli, A. & Küçük, H. (2003). Mathematical modeling of thin layer drying of pistachio by using solar energy. *Energy Conversion and Management*, 44(7), 1111-1122. [https://doi.org/10.1016/S0196-8904\(02\)00099-7](https://doi.org/10.1016/S0196-8904(02)00099-7)
- [18] Younis, M., Abdelkarim, D., & El-Abdein, A. Z. (2017). Kinetics and mathematical modeling of infrared thin-layer drying of garlic slices. *Saudi Journal of Biological Sciences*.
- [19] Bozkir, O. (2006). Thin-layer drying and mathematical modelling for washed dry apricots. *Journal of Food Engineering*, 77, 146-151. <https://doi.org/10.1016/j.jfoodeng.2005.06.057>
- [20] <http://www.kurucum.com/kabak-kurusu.html> (Accessed: 05.09.2017)
- [21] Akman, H. (2017). Güneş Enerjisi Destekli Bir Kurutma Sisteminin Termodinamik Analizi, *MSc Thesis*, Osmaniye Korkut Ata University, Osmaniye.
- [22] Bruce, D. M. (1985). Exposed layer barley drying, three models fitted to new data up to 150 °C. *Journal of Agricultural Engineering Research*, 32, 337-47. [https://doi.org/10.1016/0021-8634\(85\)90098-8](https://doi.org/10.1016/0021-8634(85)90098-8)
- [23] Page, G. E. (1949). Factors influencing the maximum rates of air drying shelled corn in thin layers (*M.S. thesis*), Purdue, USA: Department of Mechanical Engineering, Purdue University.
- [24] White, G. M., Ross, I. J., & Ponekert, R. (1981). Fully-exposed drying of popcorn. *Transactions of the ASAE*, 24, 466-468. <https://doi.org/10.13031/2013.34276>
- [25] Henderson, S. M. & Pabis, S. (1961). Grain drying theory I: temperature effect on drying coefficient. *Journal of Agricultural Engineering Research*, 6, 169-74.
- [26] Toğrul, I. T. & Pehlivan, D. (2002). Mathematical modelling of solar drying of apricots in thin layers. *Journal of Food Engineering*, 55, 209-216. [https://doi.org/10.1016/S0260-8774\(02\)00065-1](https://doi.org/10.1016/S0260-8774(02)00065-1)
- [27] Henderson, S. M. (1974). Progress in developing the thin layer drying equation. *Transactions of the ASAE*, 17, 1167-1172. <https://doi.org/10.13031/2013.37052>
- [28] Wang, C. Y. & Singh, R. P. (1978). Use of variable equilibrium moisture content in modelling rice drying. *Transactions of the ASAE*, 11, 668-672.
- [29] Corzo, O., Bracho, N., Pereira, A., & Vasquez, A. (2008). Weibull distribution for modelling air drying of coroba slices. *LWT-Food Science and Technology*, 41, 2023-2028. <https://doi.org/10.1016/j.lwt.2008.01.002>
- [30] Sharma, G. P. & Prasad, S. (2004). Effective moisture diffusivity of garlic cloves undergoing microwave-convective drying. *Journal of Food Engineering*, 65, 609-617. <https://doi.org/10.1016/j.jfoodeng.2004.02.027>
- [31] Dalvand, M. J., Mohtasebi, S. S., & Rafiee, S. (2012). Determining the influence of drying conditions on EHD drying process. *Journal of Agricultural and Biological Science*, 7, 396-401.
- [32] Figiel, A. (2009). Drying kinetics and quality of vacuum-microwave dehydrated garlic cloves and slices. *Journal of Food Engineering*, 94, 98-104. <https://doi.org/10.1016/j.jfoodeng.2009.03.007>
- [33] Thompson, T. L., Peart, R. M., Foster, & G. H. (1968). Mathematical simulation of corn drying - a new model. *Transactions of ASAE*, 11, 582-586.
- [34] Vega-Galvez, A., Di Scala, K., & Rodriguez, K. (2009). Effect of air-drying temperature on physico-chemical properties, antioxidant capacity, colour and total phenolic content of red pepper (*Capsicum annum*, L. var. Hungarian). *Food Chemistry*, 117, 647-653. <https://doi.org/10.1016/j.foodchem.2009.04.066>
- [35] Haghi, A. K. & Angiz, F. Z. (2007). Heat and mass transfer in thermal drying of wool: A theoretical approach. *Proceedings of the 5<sup>th</sup> Asia-Pacific Drying Conference / Hong Kong*, 443-448. [https://doi.org/10.1142/9789812771957\\_0065](https://doi.org/10.1142/9789812771957_0065)
- [36] Lemus-Mondaca, R., Miranda, M., Grau, A. A., Briones, V., Villalobos, R., & Vega-Gálvez, A. (2009). Effect of osmotic pretreatment on hot air drying kinetics and quality of Chilean papaya (*Carica pubescens*). *Drying Technology*, 27(10), 1105-1115. <https://doi.org/10.1080/07373930903221291>
- [37] Hii, C. L., Law, C. L., & Cloke, W. (2009). Modeling using a new thin layer drying model and product quality of cocoa. *Journal of Food Engineering*, 90, 191-198. <https://doi.org/10.1016/j.jfoodeng.2008.06.022>
- [38] Ghazanfari, A., Emami, S., Tabil, L. G., Panigrahi, S. (2006). Thin-layer drying of flax fiber: II. Modeling drying process using semi-theoretical and empirical models. *Drying Technology*, 24, 1637-1642. <https://doi.org/10.1080/07373930601031463>
- [39] Erbay, Z. & İcier, F. (2010). A review of thin-layer drying of foods: theory, modeling, and experimental results. *Critical Reviews in Food Science and Nutrition*, 50(5), 441-464. <https://doi.org/10.1080/10408390802437063>
- [40] Sripinyowanich, J. & Noomhorm, A. (2011). A new model and quality of unfrozen and frozen cooked rice dried in a microwave vibro-fluidized bed dryer. *Drying Technology*, 29, 735-748. <https://doi.org/10.1080/07373937.2010.535399>
- [41] Noomhorm, A. & Verma, L. R. (1986) Generalized single-layer rice drying models. *Transactions of the ASAE*, 29(2), 587-591. <https://doi.org/10.13031/2013.30194>
- [42] Doymaz, I. (2004). Effect of pre-treatments using potassium metabisulphite and alkaline ethyl oleate on the drying kinetics of apricots. *Biosystems Engineering*, 89, 281-287. <https://doi.org/10.1016/j.biosystemseng.2004.07.009>
- [43] Kingsly, R. P. & Singh, D. B. (2007). Drying kinetics of pomegranate arils. *Journal of Food Engineering*, 79, 741-744. <https://doi.org/10.1016/j.jfoodeng.2006.02.033>
- [44] Doymaz, I. (2004). Effect of dipping treatment on air drying of plums. *Journal of Food Engineering*, 64, 465-470. <https://doi.org/10.1016/j.jfoodeng.2003.11.013>
- [45] Mota, C. L., Luciano, C., Dias, A., Barroca, M. J., & Guine, R. P. F. (2010). Convective drying of onion: Kinetics and nutritional evaluation. *Food and Bioproducts Processing*, 88, 115-123. <https://doi.org/10.1016/j.fbp.2009.09.004>
- [46] Kaya, A., Aydin, O., & Demirtas, C. (2007). Concentration boundary conditions in the theoretical analysis of convective drying process. *Journal of Food Process Engineering*, 30(5), 546-577. <https://doi.org/10.1111/j.1745-4530.2007.00131.x>
- [47] Pitts, D. R. & Sissom, L. E. (1977). *Theory and problems of heat transfer*. McGraw-Hill Book Company.
- [48] Malik, M. A. S., Tiwari, G. N., Kumar, A., & Sodha, M. S. (1982). *Solar distillation*. Pergamon Press, Oxford.
- [49] Tiwari, G. N. & Suneja, S. (1997). *Solar thermal engineering systems*. Narosa Publishing House, New Delhi.
- [50] Akpinar, E. & Toraman, S. (2016). Determination of drying kinetics and convective heat transfer coefficients of ginger slices. *Heat Mass Transfer*, 52, 2271-2281. <https://doi.org/10.1007/s00231-015-1729-6>
- [51] Thorat, I. D., Mohapatra, D., Sutar, R. F., Kapdi S. S., &

- Jagtap D. D. (2010). Mathematical modeling and experimental study on thin-layer vacuum drying of ginger (*Zingiber officinale* R.) slices. *Food Bioprocess Technol.* <https://doi.org/10.1007/s11947-010-0429-y>
- [52] Jayashree, E. & Visvanthan, R. (2013). Studies on thin layer drying characteristics of ginger (*Zingiber officinale*) in a mechanical tray drier journal of plantation crops. *J Spices Aromat Crops*, 41(1), 86-90.
- [53] Afolabi, J. T., Tunde-Akintunde, T. Y., & Oyelade, O. J. (2014). Influence of drying conditions on the effective moisture diffusivity and energy requirements of ginger slices. *J Food Res*, 3(5), 103-112. <https://doi.org/10.5539/jfr.v3n5p103>
- [54] Akpınar, E. K. (2004). Experimental determination of convective heat transfer coefficient of some agricultural product in forced convection drying. *Int Commun Heat Mass Transfer*, 31(4), 585-595. [https://doi.org/10.1016/S0735-1933\(04\)00038-7](https://doi.org/10.1016/S0735-1933(04)00038-7)
- [55] Holman, J. P. (1992). *Heat transfer*, 7<sup>th</sup> ed., SI Unit, McGraw-Hill Book Company, Berlin.
- [56] Jain, D. & Tiwari, G. N. (2004). Effect of greenhouse on crop drying under natural and forced convection I: Evaluation of convective mass transfer coefficient. *Energy Conversion and Management*, 45, 765-783. [https://doi.org/10.1016/S0196-8904\(03\)00178-X](https://doi.org/10.1016/S0196-8904(03)00178-X)

#### Authors' contacts:

**Kamil Neyfel ÇERÇİ**, Res. Assist.  
**Mustafa SÖYLER**, Res. Assist.  
**Ertuğ HÜRDOĞAN**, Assoc. Prof. Dr., Corresponding author  
**Coşkun ÖZALP**, Assoc. Prof. Dr.  
 Department of Energy Systems Engineering,  
 Osmaniye Korkut Ata University,  
 Osmaniye, 151-742, Turkey,  
 +90 328 8251818-3503/+90 328 825 00 97,  
 ehurdogan@osmaniye.edu.tr

**Özge SÜFER**, Res. Assist.  
 Department of Food Engineering,  
 Osmaniye Korkut Ata University,  
 Osmaniye, 151-742, Turkey,

# INFLUENCE OF STRANDS TRANSPOSITION ON CURRENT DISTRIBUTION AND POWER LOSSES IN WINDINGS OF AC MACHINES

Branko TOMIČIĆ, Ladislav HAVAŠ, Dunja SRPAK

**Abstract:** This paper analyses how the type of winding affects the current distribution and power losses in armature winding. Using finite element method, four different types of winding used in large asynchronous motors are analyzed: form-wound concentric, with and without transposition, and form-wound barrel, with and without transposition, for the stationary state. In two cases, the calculation shows clear differences between maximum currents in strands, a shift in their phases, and a resulting increase of AC resistance. In two other cases, minor deviations, smaller phase shift and smaller increase of AC resistance, are detected. It indicates that in certain types of armature winding of large motors the strands transposition leads to significant positive effects in terms of motor power, while in other cases it leads to unnecessary complications making the manufacture of large asynchronous machines more difficult, with relatively small positive effect on the motor power losses.

**Keywords:** AC machines; conductors; finite element method; losses; windings

## 1 INTRODUCTION

Manufacturers of electric machines are trying to increase the efficiency of their machines by reducing the losses with the appropriate design. Many articles present researches with slot shapes to perform better heat transfer from windings to stator core [1-3]. This improves the thermal behavior of machines and reduces their losses. Another possibility to reduce the unequal strands current distribution in the machine is by selecting the appropriate winding mode. Unequal current distribution is known as an eddy current. The main reason for an eddy current is the leakage flux, which crosses the conductors placed in slots. Authors in [4-8] analyze the influence of an eddy current on the losses in the induction motors, by using the finite element method (FEM). This method is often used for 2D or 3D analyses related with operation of electrical machines, as in [9-12]. The correlation between the eddy current losses and the winding geometry with solid or stranded conductors, woven or twisted, using the 2D finite elements model is analyzed in [13-15] for switched reluctance machine.

The influence of eddy currents on the increase of resistance was studied even in early works as [16] and [17]. Eddy currents cause additional losses in conductors, which may consist of one or more strands. The transposition of the insulated strands in a multi strand windings has the influence on AC losses, as described in [18-20]. Authors in [21] propose the windings transposition to reduce the additional eddy loss in permanent magnet synchronous motor (PMSM). Different transposition angles of armature windings using analytical model are studied to minimize eddy current losses in [22]. This paper shows the results of analyzing the influence of strands transposition for various types of windings used in AC machines to reduce the eddy current losses. Analytical methods that can be used to calculate leakage magnetic fields do not take into account the complex geometry of the magnetic circuit and the

nonlinear characteristics of the core material. Such imperfections can be eliminated by applying the FEM to the calculation of the magnetic field on the models corresponding to the actual state.

By calculating the magnetic field in the electric machines using the finite elements method (FEM), it is possible to determine the distribution of current in strands forming conductors. The amounts of currents in strands of conductor and the phase shift between them cause increase of losses. By choosing the appropriate type of winding, with or without transposition, the losses can be significantly reduced, as this research indicates.

This paper is organized as follows: First, a general description of the winding and the basis for AC losses calculation is given. In the next section, the used method of finite elements (FEM) for computing the increase of AC losses is described, as well as the model of tested induction motor. Then, the results of the analysis are presented for the different types of stator windings, including the winding performed on the concerned motor. Finally, the discussion and conclusion are presented.

## 2 GENERAL DESCRIPTION OF THE WINDING DESIGN

A stranded conductor consists of parallel paths that can be represented each by an equivalent resistance and inductance connected in series. The equivalent scheme of a conductor consisting of two strands is shown in Fig. 1.

Resistance of each parallel path has the same amount, because of equal cross section and length of strand. The inductance of the strand depends of the position in the slot. Strands that are positioned deeper in slot have higher inductance than the ones positioned closer to the air gap. The reason for the difference of the inductance is the component of magnetic flux, which passes transversely to the slots (Fig. 2). This is the leakage flux and it appears in the whole range of operation of asynchronous motor.

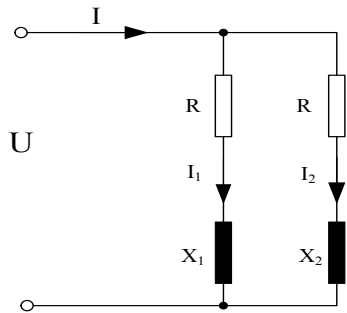


Figure 1 Equivalent scheme of parallel paths

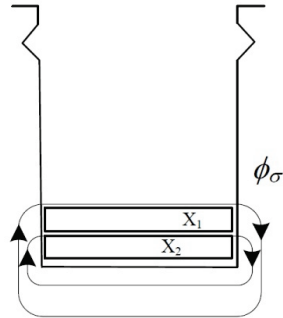


Figure 2 Leakage magnetic flux

The strands current will be distributed depending on the impedance in the parallel paths. The current in the strand with higher inductance will be lower and more phase-shifted in relation to voltage. The current in the strand with lower inductance will be higher and less phase-shifted in relation to voltage (Fig. 3).

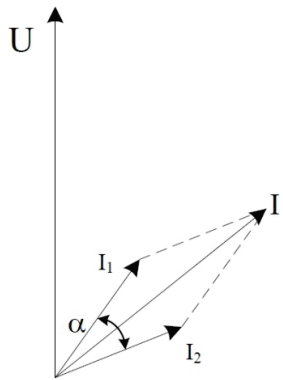


Figure 3 Phase diagram of motor currents

The total current through the winding is a sum of both currents. The losses in the winding are:

$$I_1^2 R + I_2^2 R = I^2 R_{\text{ekv}}, \quad (1)$$

where  $I_1$  – current through the first strand,  $I_2$  – current through the second strand,  $I$  – total current,  $R$  – strand resistance,  $R_{\text{ekv}}$  – equivalent resistance of conductor.

Then the equivalent resistance of winding is:

$$R_{\text{ekv}} = \frac{2(I_1^2 + I_2^2) R}{I^2}. \quad (2)$$

Resistance to direct current amounts  $R/2$ , therefore the factor of increase of AC resistance caused by the proximity and skin effects is:

$$k_r = \frac{2(I_1^2 + I_2^2)}{I^2}. \quad (3)$$

The square of the total current amounts is:

$$I^2 = I_1^2 + I_2^2 + 2I_1 I_2 \cos \alpha, \quad (4)$$

where  $\alpha$  is a phase-shift between currents in strands. If it is assumed that currents  $I_1$  and  $I_2$  are almost the same, the increase of AC resistance caused by proximity and skin effects can be calculated in the following way:

$$I_1 = I_2 = I_s \quad (5)$$

$$I^2 = I_s^2 + I_s^2 + 2I_s^2 \cos \alpha \quad (6)$$

$$I^2 = 2I_s^2 (1 + \cos \alpha) \quad (7)$$

By using Eq. (6) in Eq. (3) equation for the increase of AC resistance caused by proximity and skin effects becomes:

$$k_r = \frac{2(2I_s^2)}{2I_s^2 (1 + \cos \alpha)} = \frac{2}{1 + \cos \alpha}. \quad (8)$$

### 3 MODELLING OF STEADY STATE INDUCTION MOTOR WITH LOAD BY FIELD CALCULATION

The squirrel-cage induction motor analyzed in this paper is shown in Fig. 4, and the rated data of that motor are presented in Tab. 1.



Figure 4 The manufactured and tested motor

For FEM calculation of magnetic field, current distribution and thus increased AC resistance caused by



proximity and skin effects, a 2D model of one pole of the motor is created. The model is shown in Fig. 5, and it is composed of the static and the rotating part.

**Table 1** Data of tested induction motor

Rated parameter	Nominal value
Rated voltage	580 V
Rated output power	2200 kW
Rated current	2544 A
Rated frequency	50Hz
Rated speed	996 min <sup>-1</sup>
Total motor mass	8750 kg

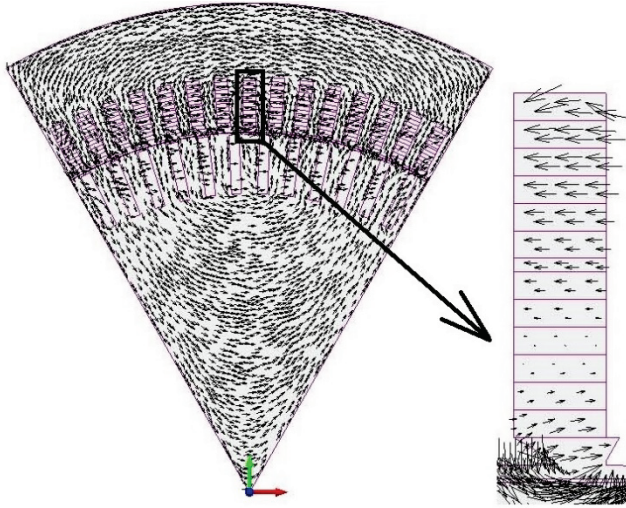


**Figure 5** Magnetic field at a steady state

The static part consists of a laminated core with slots in which there are conductors of a three-phase double layer winding. The shape of the slot is rectangular semi-closed and asymmetrical, adjusted to coils made of rectangular copper wire and insulation system for low voltage machines. The number of coils per pole and phase is 5, and the slot pitch is 12. Number of turns per coil is 3 and each conductor consists of 2 copper strands. The windings are star connected.

The rotating part consists of a laminated core made of dynamo sheets. Type of winding is squirrel-cage. Number of slots per pole is 12 and rectangular bars are made of copper. Rotor core is fixed on the shaft made of steel.

The program package MagNet® is used for FEM calculation of magnetic field [23]. The following assumptions are introduced:

- All machine windings are symmetrically distributed on each pole, have the same number of conductors and resistance, which enables analysis of a single pole;
- Electric conductivity of iron is neglected, which excludes the influence of eddy and stray currents;
- Characteristics of built-in material are isotopic, hysteresis loop is neglected, and iron permeability depends only on magnetic field strength;
- Windings of the machine are connected to the ideal current sources and the waveforms of currents feeding the armature windings are sinusoidal.

A software module that takes into account rotor speed is used for calculation of the magnetic field, and the field solution is based on the expressions [24]:

$$\oint_C \vec{E} \cdot d\vec{l} = - \frac{d}{dt} \int_S \vec{B} \cdot \vec{n} \cdot dS \quad (9)$$

$$\oint_C \vec{H} \cdot d\vec{l} = \int_S \vec{J} \cdot \vec{n} \cdot dS \quad (10)$$

$$\int_S \vec{B} \cdot \vec{n} \cdot dS = 0 \quad (11)$$

where the symbols represent:

$\vec{E}$  – electric field strength in conductors,

$\vec{B}$  – magnetic induction,

$\vec{H}$  – magnetic field strength,

$\vec{J}$  – current density,

$S$  – surface within which the field is computed,

$\vec{n}$  – unit vector of normal on surface  $S$ ,

$C$  – boundary curve of the surface  $S$ .

The conductor strands are coupled into two parallel paths and connected to the ideal power sources as shown in Fig. 6.

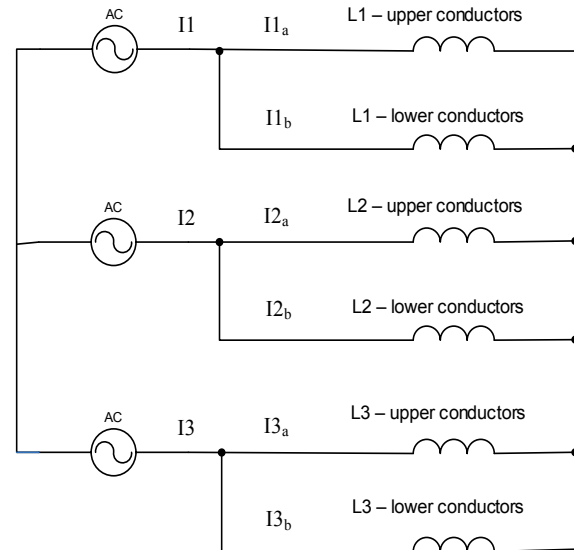


**Figure 6** Winding connection diagram

The calculation is made in the time from 0 to 1 s, i.e. until the steady state has been attained. All the time, the torque on the shaft is constant and adjusted to the nominal value. The calculation results of a magnetic field at a steady state with maximum current in phase placed in axis of the model are shown in Fig. 5. There it is visible that magnetic field has a main component, which passes around stator and rotor winding, but there is also a component which passes transversely to the slots.

The length of the arrow which shows the direction of the magnetic field is proportional to its value. The field has



the largest value at the bottom and the top of the slot, and the opposite direction in those places. This is the expected result as the magnetic field closes around the current which flows perpendicular to the drawing.

The next calculations are performed for the following variations of winding:

1. Form-wound concentric,
2. Form-wound barrel,
3. Form-wound concentric with transposition,
4. Form-wound barrel with transposition.

## 4 RESULTS OF TESTING OF VARIOUS WINDING DESIGN

Research has been carried out for different types of winding designs where the strands are insulated along the whole length of winding. For the total current  $I$ , currents in strands  $I_1$ , and  $I_2$ , are calculated. In addition, the phase shift between currents is taken into account. Then, the factor of increase  $k_r$  is calculated according to Eq. (3) and Eq. (8).

### 4.1 Form-Wound Concentric Type of Winding without Transposition

The form-wound concentric type of winding is characterized by the same order of conductors in upper and lower layers. Looking at the winding sequence in the top layer from the slot opening to the middle of the slot, the same conductors are located in the bottom layer from the slot middle towards the bottom. Thus, the conductor placed first under the slot opening in the upper layer is the first below the interlayer inlay in the bottom layer. This type of winding is applied on the machines where first copper is formed into the bars. After inserting the bars into the slots, the coils are formed by soldering the wires on the ends. These are usually older production machines.

Fig. 7 shows phase current and phase voltage in steady state. The phase shift between them is 2 ms which corresponds to the angle of  $36^\circ$ , i.e. the power factor of 0.81.

Fig. 8a shows the mode of connecting the conductors into the parallel paths of form-wound concentric type of winding for one phase. Conductors with the index 1 are connected in one path and with the index 2 in another.

The calculated values of currents in strands ( $I_1$ ,  $I_2$ ) and the total current ( $I$ ) are presented by multiple time series for the purpose of graphical analysis [25]. The amplitudes of the currents in conductor strands can be read from Fig. 8 (b) as 210 A and 180 A, while the amplitude of the total current is 350 A. The phase shift visible in Fig. 7b is 2.8 ms, which corresponds to the phase shift of  $50.4^\circ$ . Using the Eq. (3), increase in resistance from 1.224 is obtained. The waveform of the current in conductors, besides the base harmonic, also contains harmonics which are generated due to different magnetic conductivity at certain points of the calculation. Magnetic conductivity changes due to rotor rotation, and depends on the mutual position of the slots and tooth at certain points of the calculation. Harmonics in current can be avoided by using an FEM calculation without motion of rotor, e.g. by simulating a duty point with blocked rotor. In

this case, the actual magnetic field like in a machine under load would not be taken into account.

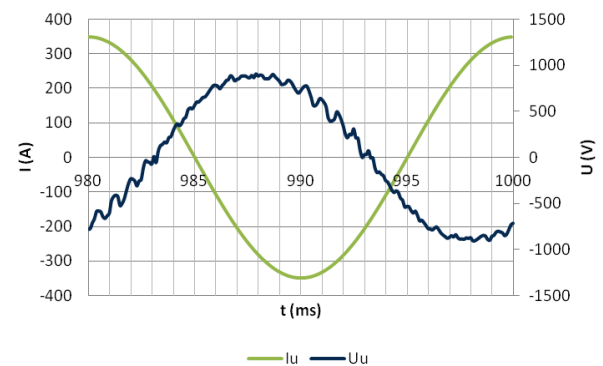


Figure 7 The phase current and phase voltage in steady state

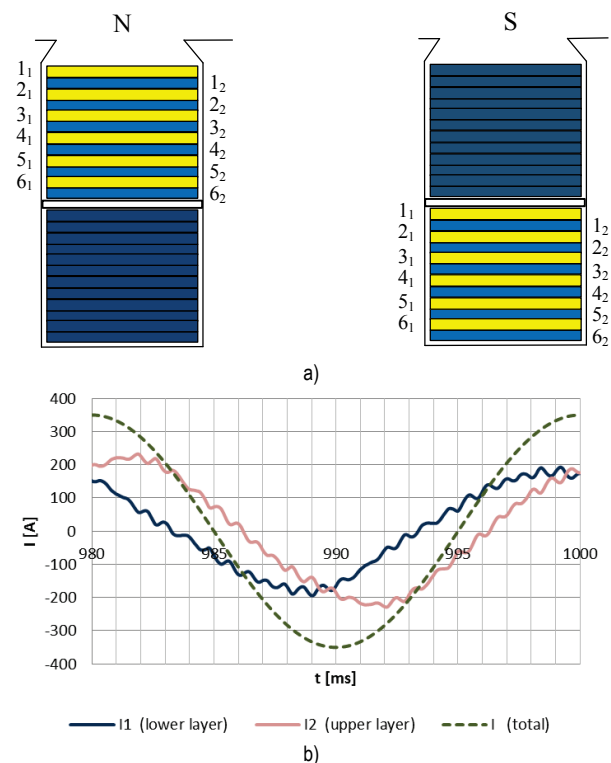
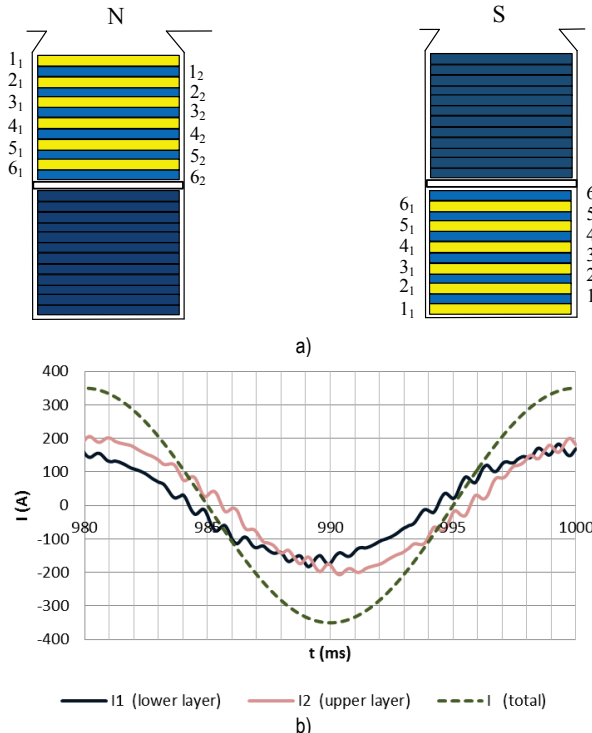


Figure 8 Form-wound concentric type windings without transposition  
(a) Connection of conductors in parallel paths,  
(b) Currents of the motor in the parallel paths of conductor

### 4.2 Form-Wound Barrel Type of Winding without Transposition

In case of form-wound barrel type of winding, the rotation of conductors is made. The conductors in upper and lower layer are in reverse order. The conductors placed in the top layer from the slot opening to the middle of the slot are located in the lower layer from the bottom of the slot towards the middle. Thus, the conductor placed first under the slot opening in the upper layer is the first from the bottom in the lower layer. This type of winding is most widely used in machines for general purposes with higher power. The coils are made by winding the wires, and the forming has to be made on a special device.

Fig. 9a shows the method of connecting the conductors into the parallel paths of barrel winding for one phase (with index 1 in one path and with the index 2 in another). The results of calculation of the current in conductor strands shown in Fig. 9b indicate that there is still a difference in current amplitudes, as well as the phase shift between them. However, the amounts are considerably more favorable than in the previous case. The current amplitudes read from the graphs are 190A and 170 A, while the phase shift is 1.5 ms corresponding to the electric angle of  $27^\circ$  at a frequency of 50 Hz. By including the values into the Eq. (3), an increase in resistance from 1.06 is obtained.



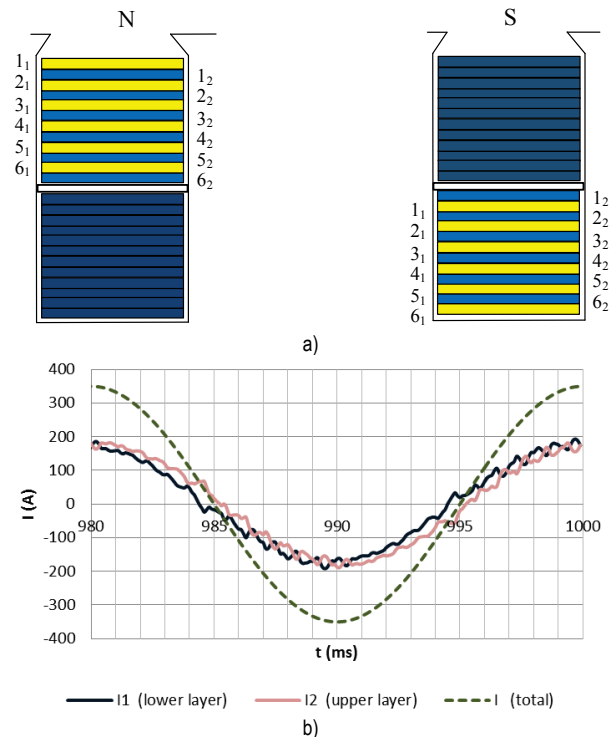
**Figure 9** Form-wound barrel type of windings without transposition  
(a) Connection of conductors in parallel paths,  
(b) Currents of the motor in the parallel paths of conductor.

### 4.3 Form-Wound Concentric Type of Winding with Transposition

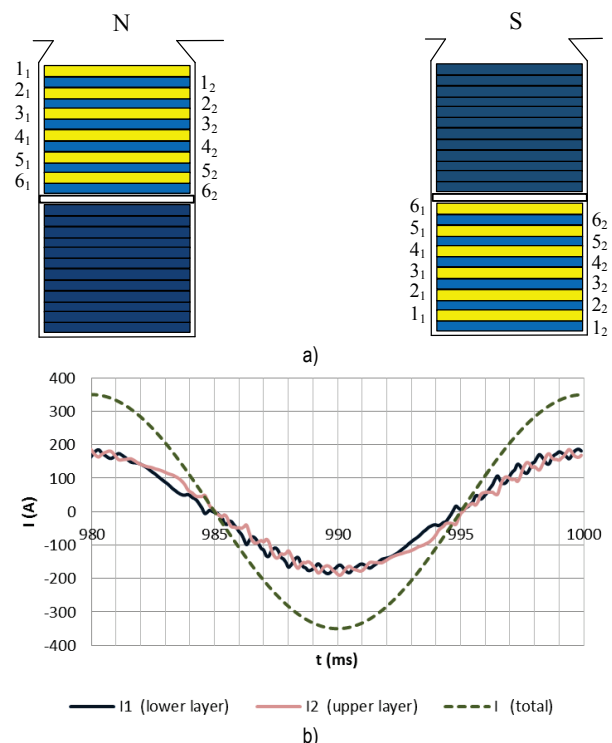
The form-wound concentric type of winding with transposition differs from the one without transposition in conductors placed in the lower layer. The upper conductors placed in the upper layer from the slot opening to the middle of the slot are connected with the lower conductors in the lower layer, from the middle of the slot towards the bottom, as shown in Fig. 10a.

Fig. 10b shows that the obtained results are more favorable than in the first and the second case. The differences in current amplitudes cannot be read from the graphs and the phase shift is 0.8 ms corresponding to the electric angle of  $12.6^\circ$ . In this case, the Eq. (8) must be applied to estimate the increase in resistance. By calculating using that phase angle, an increase factor of 1.012 is obtained. It can be concluded that the strands transposition

in the case of the form-wound concentric type of windings significantly contributes to the reduction of additional losses.



**Figure 10** Form-wound concentric type of windings with transposition  
(a) Connection of conductors in parallel paths,  
(b) Currents of the motor in the parallel paths of conductor



**Figure 11** Form-wound barrel type of windings with transposition  
(a) Connection of conductors in parallel paths,  
(b) Currents of the motor in the parallel paths of conductor.

#### 4.4 Form-Wound Barrel Type of Winding with Transposition

In the form-wound barrel type of winding with transposition, the upper conductors placed in the upper layer from the slot opening to the middle of the slot are connected in one path with the upper conductors in the lower layer, from the bottom of the slot towards the middle, as shown in Fig. 11a. Fig. 11b shows that the currents in the conductor strands are equal, and the phase shift between them has a small value. The value of 0.2 ms can be read, which corresponds to the phase angle of  $3.6^\circ$ . Calculation with that phase angle and the Eq. (8) gives an additional losses factor of increase from 1.001, which is negligible. It can be concluded that in the case of the form-wound barrel type of windings the strands transposition does not contribute significantly to the reduction of additional losses.

The results of calculations for these four types of windings are shown in Tab. 2.

Table 2 Results for tested types of windings

Type	$I_1$ (A)	$I_2$ (A)	$I$ (A)	$k_r$ Eq. (3)	$\alpha$ ( $^\circ$ )	$k_r$ Eq. (8)
4.1	210	180	350	1,248	50,4	1,22
4.2	190	170	350	1,061	27,0	1,058
4.3	180	180	350	-	12,6	1,012
4.4	180	180	350	-	3,6	1,001

#### 5 DISCUSSION

This research has shown that the amount of additional AC losses can be affected by the selected winding design. Additional losses are caused by the distribution of current in strands that have different amount and phase shift. The current distribution depends on the leakage magnetic field that can be calculated by using the FEM. The results of the calculation show that the form-wound barrel type of winding is more appropriate than form-wound concentric type, because of the reduced losses.

The strands transposition significantly contributes to the reduction of the additional losses at the concentric type of windings. In form-wound barrel type of windings, the contribution of strands transposition is not significant since the coil construction provides a favorable distribution of the conductors along the height in the slot.

#### 6 CONCLUSION

The implementation of transposition requires careful insulating process and connecting of the strands when forming the coils for windings, making the production of large electric machines more difficult. Considering the complexity of manufacturing the winding with transposition and the negligible reduction in losses in case of barrel type winding, it is concluded that the optimum type of winding is barrel winding without transposition. This design is carried out on the largest number of electric machines in modern production.

The analysis of results for different types of windings presented in this paper shows that transposition in windings can be very valuable in some cases, while in other

cases it is not justified, due to practical implementation problems or cost aspects (as concluded also in [20] and [22]). In addition, unlike mainly analytical approaches used in most of related works presented in the introduction, the results of the analysis with the FEM method presented in this paper were verified on the actually produced squirrel-cage induction motor (Fig. 4, Tab. 1).

Since conductors can be realized with a different number of strands, their optimal number has to be determined. Increasing the number of strands reduces additional losses and transposition can be avoided. At the same time, the effective cross-section of the conductor in the slot is decreased regarding to insulation. Therefore, this can be the aim of future researches.

#### 7 REFERENCES

- [1] Wrobel, R., Williamson, S. J., Simpson, N. et al. (2015). Impact of slot shape on loss and thermal behaviour of open-slot modular stator windings. *Energy Conversion Congress and Exposition (ECCE), 2015 IEEE*, 4433-4440.
- [2] Zhang, W. & Jahns, T. M. (2014). Analytical 2-D Slot Model for Predicting AC Losses in Bar-Wound Machine Winding due to Armature Reaction. *IEEE Transportation Electrification Conference and Expo, ITEC 2014*, Dearborn, MI, USA, 1-6. <https://doi.org/10.1109/ITEC.2014.6861825>
- [3] Gonzalez, D. A. & Saban, D. M. (2014). Study of the Copper Losses in a High-Speed Permanent-Magnet Machine with Form-Wound Windings. *IEEE Transactions on Industrial Electronics*, 61(6), 3038-3045. <https://doi.org/10.1109/TIE.2013.2262759>
- [4] Hamalainen, H., Pyrhonen, J., & Nerg, J. (2013). AC Resistance Factor in One-layer Form-Wound Winding Used in Rotating Electrical Machines. *IEEE Transactions on Magnetics*, 49(6), 2967-2973. <https://doi.org/10.1109/TMAG.2013.2240008>
- [5] Islam, M. J., Khang, H. V., Repo, A.-K., et al. (2010). Eddy-Current Loss and Temperature Rise in the Form-Wound Stator Winding of an Inverter-Fed Cage Induction Motor. *IEEE Transactions on Magnetics*, 46(8), 3413-3416. <https://doi.org/10.1109/TMAG.2010.2044387>
- [6] Islam, M. J. & Arkkio, A. (2008). Time-stepping finite-element analysis of eddy currents in the form-wound stator winding of a cage induction motor supplied from a sinusoidal voltage source. *IET Electric Power Applications*, 2(4), 256-265. <https://doi.org/10.1049/iet-epa:20070440>
- [7] Chen, W., Liu, Y., Islam, J., et al. (2012). Strand-level Finite Element Model of Stator AC Copper Losses in the High Speed Machines. *2012 XX<sup>th</sup> International Conference on Electrical Machines (ICEM)*, France, 477-482. <https://doi.org/10.1109/ICEIMach.2012.6349912>
- [8] Tassarolo, A., Agnolet, F., Luise, F., et al. (2012). Use of Time Harmonic Finite-Element Analysis to Compute Stator Winding Eddy-Current Losses Due to Rotor Motion in Surface Permanent-Magnet Machines. *IEEE transactions on energy conversion*, 27(3), 670-679. <https://doi.org/10.1109/TEC.2012.2192498>
- [9] Martinez, J., Belahcen, A., Detoni, J., et al. (2014). A 2D FEM analysis of electromechanical signatures in induction motors under dynamic eccentricity. *International Journal of Numerical Modelling: Electronic Networks, Devices and Fields*, 27(3), 555-571. <https://doi.org/10.1002/jnm.1942>

- [10] Gang, L., Dihui, Z., & Tong, Z. (2017). Influences on performance in 3D analysis of linear induction motors with different transverse m.m.f. models in winding end-regions. *IET Electric Power Applications*, 11(8), 1424-1431.
- [11] Jiang, W. & Jahns, T. M. (2015). Coupled Electromagnetic-Thermal Analysis of Electric Machines Including Transient Operation Based on Finite-Element Techniques. *IEEE Transactions on Industry Applications*, 51(2), 1880-1889. <https://doi.org/10.1109/TIA.2014.2345955>
- [12] Handgruber, P., Schernthanner, S., Biró, O., et al. (2015). Effects of inverter supply on the iron loss characteristics of doubly fed induction machines. *COMPEL*, 34(5), 1460-1474. <https://doi.org/10.1108/COMPEL-02-2015-0051>
- [13] Al Eit, M., Bouillault, F., Marchand, C., et al. (2015). 2-D Reduced Model for Eddy Currents Calculation in Litz Wire and Its Application for Switched Reluctance Machine. *IEEE Transactions on Magnetics*, 52(3), 1-4. <https://doi.org/10.1109/TMAG.2015.2486838>
- [14] Al Eit, M., Bouillault, F., Santandrea, L., et al. (2016). Calculation of Copper Losses in Case of Litz and Twisted Wires. 2D Modeling and Application for Switched Reluctance Machine. *European Journal of Electrical Engineering, Lavoisier*, 18, 3-4.
- [15] Al Eit, M., Dular, P., Bouillault, F., et al. (2017). 2D finite element model reduction for copper losses calculation in switched reluctance machines. *2017 IEEE Conference on Electromagnetic Field Computation (CEFC)*.
- [16] Lyon, W. V. (1928). Abridgment of heat losses in D-C armature conductors. *Journal of the A.I.E.E.* 47(4), 286-289. <https://doi.org/10.1109/JAIEE.1928.6538114>
- [17] Dowell, P. L. (1966). Effects of eddy currents in transformer windings. *Proceedings of the Institution of Electrical Engineers*, 113(8), 1387-1394. <https://doi.org/10.1049/piee.1966.0236>
- [18] Reddy, P. B., Jahns, T. M., & Bohn, T. P. (2009). Transposition Effects on Bundle Proximity Losses in High-Speed PM Machines. *Energy Conversion Congress and Exposition (ECCE), 2009 IEEE*, 1919-1926.
- [19] Vetuschi, M. & Cupertino, F. (2015). Minimization of Proximity Losses in Electrical Machines with Tooth-Wound Coils. *IEEE Transactions on Industry Applications*, 51(4), 3068-3076. <https://doi.org/10.1109/TIA.2015.2412095>
- [20] Petrov, I., Polikarpova, M., Ponomarev, P., et al. (2016). Investigation of Additional AC Losses in Tooth-Coils Winding PMSM with High Electrical Frequency. *2016 XXII<sup>nd</sup> International Conference on Electrical Machines (ICEM)*, 1841-1846. <https://doi.org/10.1109/ICELMACH.2016.7732774>
- [21] Zou, J. B., Zhao, B., Xu, Y. X., et al. (2012). A New End Winding Transposition to Reduce Windings Eddy Loss for 2 MW Direct Drive Multi Unit PMSM. *IEEE Transactions on Magnetics*, 48(11), 3323-3326. <https://doi.org/10.1109/TMAG.2012.2201701>
- [22] Abbaszadeh, K. & Alam, F. R. (2013). Circulating current analysis between strands in armature winding of a turbo-generator using analytical model. *Turkish Journal of Electrical Engineering & Computer Sciences*, 21, 55-70.
- [23] Magnet Version 6.5. Tutorials, Infolytica Corporation (2000)
- [24] Haznadar, Z. & Štih, Ž. (1990). *Electromagnetism* (in Croatian), Školska knjiga, Zagreb.
- [25] Bisgaard, S. & Kulahci, M. (2011). *Time series analysis and forecasting by example - Wiley series in probability and statistics*, Wiley. <https://doi.org/10.1002/9781118056943>

#### Authors' contacts:

**Branko TOMIČIĆ**, PhD, Senior lecturer  
University North, University Center Varaždin  
104. brigade 3, 42000 Varaždin, Croatia,  
Končar Generators and Motors Inc.,  
Fallerovo šetalište 22, Zagreb, Croatia  
e-mail: btomicic@koncar-gim.hr

**Ladislav HAVAŠ**, PhD, Senior lecturer  
University North, University Center Varaždin  
104. brigade 3, 42000 Varaždin, Croatia  
e-mail: ladislav.havas@unin.hr

**Dunja SRPAK**, PhD, Lecturer  
(Corresponding author)  
University North, University Center Varaždin  
104. brigade 3, 42000 Varaždin, Croatia  
e-mail: dunja.srpak@unin.hr

# METHOD OF MATERIAL QUALITY ESTIMATION WITH USAGE OF MULTIFRACTAL FORMALISM

Volodymyr VOLCHUK, Ievgenii KLYMENKO, Sergii KROVIAKOV, Matija OREŠKOVIĆ

**Abstract:** Feasibility of application of multifractal theory for evaluation of materials mechanical properties, cast iron in particular, has been considered. The proposed method enables evaluation of mechanical properties of materials based on determination of their sensitivity to dimensions of structure elements from the multifractal Renyi spectrum. Sensitivity of cast iron ultimate strength to informational dimension of carbides, ultimate bending strength to fractal dimension of carbides, impact strength to correlation dimension of carbides and hardness to fractal dimension of graphite have been determined. Fractal prediction models of quality characteristics of cast iron based on the analysis of the following its structure elements (carbides and graphite) have been received.

**Keywords:** cast iron; graphite; mechanical properties; sensitivity coefficient; spectrum of Renyi dimensions; theory of multifractals

## 1 INTRODUCTION

Establishing the connection between composition, structure and properties of materials is determined with application of different methods including mathematic simulation. For example, in works [1, 2], about the use of multifactor modeling, the residual load-bearing capacity of the damaged reinforced concrete structures is calculated and ways to strengthen them are considered; in [3, 4] the properties of concretes on lightweight porous fillers for thin-walled structures are evaluated.

Many elements of materials structure at different scale levels have a complex geometrical shape configuration which cannot always be appropriately described by the use of traditional methods. For example, based on analysis of quantitative and qualitative assessment of many iron-carbon alloys of real structures, there are some differences between the results of direct experiments on determination of their qualitative characteristics using predictive methods [5] that must be observed for usage in practical purposes.

This fact represents insufficiency of formal axiomatic which arises during approximation of metal structure elements using the traditional figures of Euclid's geometry; this emphasizes the necessity of usage of the other prospective approaches to its assessment.

Fractal approach is these days successfully used for the structure analysis [6-9]. Particularly, multifractal theory is used for estimation of heterogeneous structures of metals, concretes, polymers and other materials. Having that in mind, here is the proposed method of estimation of quantitative characteristics of different materials based on multifractal analysis of their structure.

## 2 MATERIALS AND METHODS

Cast iron for manufacture of casting roller with spherical form of graphite was used as test material (0.5...2.5%); its chemical composition is as follows: 3.00...3.40% C, 1.45...1.80% Si, 0.45...0.65% Mn,

0.040...0.200% P, 0.004...0.010% S, 0.60...0.90% Cr, 0.70...1.30% Ni, 0.035...0.056% Mg. Quantity of carbides (cementite,  $\text{Fe}_3\text{C}$ ) is 20-30%. Figs. 1 and 2 shows cast iron structure.

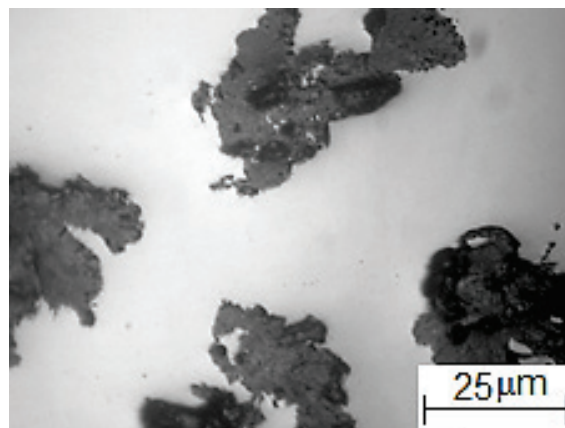


Figure 1 Structure of the working layer of cast iron roll: graphite eutectic

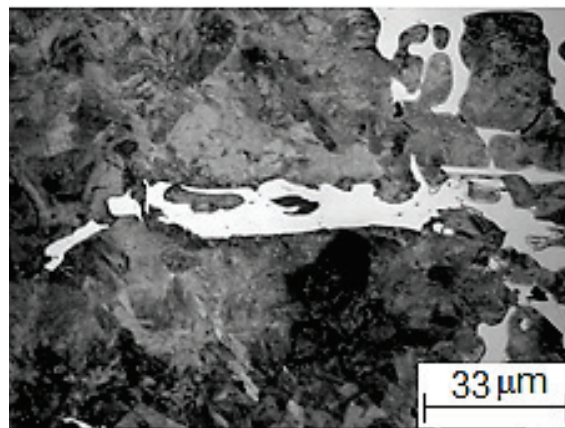


Figure 2 Colonies of Ledeburite, Graphite Eutectic, Pearlite Matrix, HNO<sub>3</sub> Etching in working layer of cast iron roll

Impact strength of cast iron KC was determined with groove of notch dimensions of 10×10×55 mm. For



estimating the strength level during bending,  $\sigma_B$  bars of  $10 \times 10 \times 90$  mm were used, and during tensile tests  $\sigma_B$  bars of 25 mm diameter were used with 50 mm gauge length. Hardness of cast iron bars,  $HSD$ , was defined according to Shore. For every structural component (cementite of ledeburite eutectic, pearlite, graphite) spectrum of statistical dimensions was counted as per Renyi formula [10]:

$$D(q) = \frac{1}{q-1} \cdot \lim_{\delta \rightarrow \infty} \frac{\ln \sum_{i=1}^N p_i^q}{\ln \delta} \quad (1)$$

where  $p_i$  is hit probability of point that is located on the test specimen to the  $i$  cell of square mesh with size  $\delta$ . Dimensions of spectrum  $D_0$ ,  $D_1$ ,  $D_2$ ,  $D_\infty$ ,  $D_{-\infty}$  were calculated:  $D_0$  is homogeneous fractal with  $q=0$  (Hausdorff-Besikovitch dimension);  $D_1$  is an informational dimension with  $q=1$  (informational entropy) characterizing growth rate of the amount of information and showing growth of information, necessary for determining the point location on the test specimen as cell size  $\delta$  tends to zero;  $D_2$  is a correlation dimension with  $q=2$ , characterizing probability of occurrence in the same mesh cell of two points on the test specimen;  $D_\infty$  is a dimension characterizing the most vacuum space in the test item (structure light segments);  $D_{-\infty}$  is a dimension characterizing the most concentrated space (structure dark segments).

Fig. 3 shows the example of calculated spectrum of dimensionalities  $D(q)$  of the structure, depending on interval of their variation  $q$ . In this case changes of index  $q$  were specified within limits from  $-100$  to  $100$ .

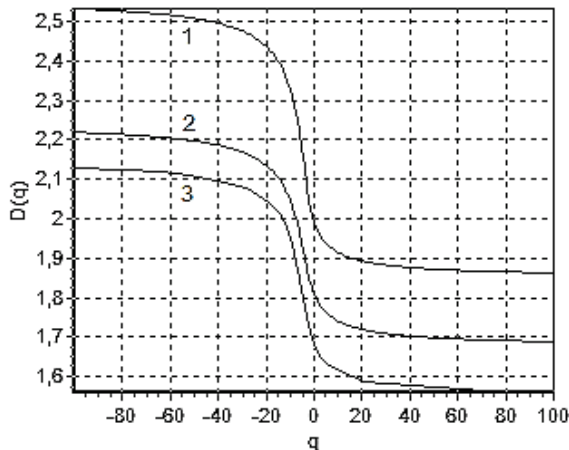


Figure 3 Spectrum of Dimensions of Cementite (1), Pearlite (2), Graphite (3)

### 3 RESULTS AND DISCUSSION

Method of material quality estimation with usage of multifractal theory comprises the following stages:

- Calculation of statistical dimensions' spectrum of structure elements according to Renyi formula.
- Determination of qualitative characteristics of the test material.

- Calculation of sensitivity of qualitative characteristics to statistical dimensions of structure elements.
- Description of relation between the most sensitive dimensions of the material structure elements and its qualitative characteristics.

For the materials science issues it is useful to study sensitivity of fractal or any other dimension of the material structure elements to changes of their qualitative characteristics through calculation of sensitivity coefficient  $K_i$  (2) according to the method [11]:

$$K_i = \frac{|Y_i - Y_{i+1}|}{|X_i - X_{i+1}|} \quad (2)$$

The sensitivity will be maximal at those points of the structure where the maximum change in the metal properties is observed. It is shown in use [12] that sensitivity of the dimension's spectrum of the elements of ferrite and perlite structure of low-carbon low-alloy steel to mechanical properties is relatively high. This indicates that dimensional evaluation may be applied as an indicator of the material's quality characteristics.

Figs. 4-6 show the calculation results of sensitivity coefficients of cast iron mechanical properties  $K_i$  to dimensional evaluation  $D_0$ ,  $D_1$ ,  $D_2$ ,  $D_{100}$ ,  $D_{-100}$  of the structure calculated according to the formula (2).

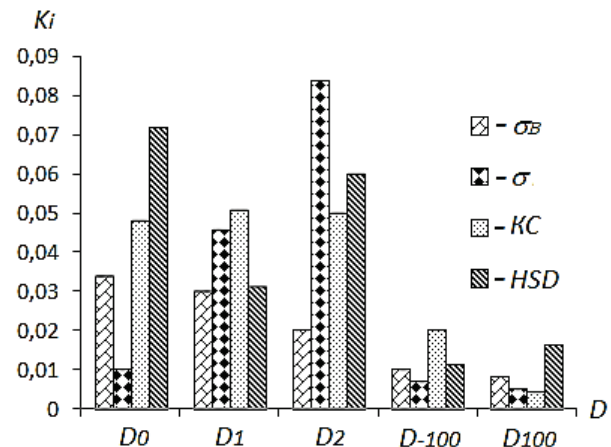


Figure 4 Sensitivity of Cast Iron Mechanical Properties to Dimensions of Graphite

Relatively high sensitivity indexes among those under consideration demonstrate strength characteristics ( $\sigma_B$  and  $\sigma$ ) and hardness  $HSD$  to dimensions  $D_0$ ,  $D_1$ ,  $D_2$  of cementite (Fig. 5) and graphite of spherical form (Fig. 4). This sensitivity results from influence of cementite  $Fe_3C$  in cast iron alloy on increase in its hardness and strength, stabilization of pearlite, expansion in number of basic strengthening phase, wear resistance increase and reduce of plastic and antifricition properties. Upon the increase of graphite quantity in the cast iron structure, its strength, hardness and wear resistance reduce. Influence of graphite with spherical form on the mechanical properties is proven by sensitivity of these characteristics to dimensional

evaluation (Fig. 4). For the ultimate strength sensitivity index to fractal dimension  $D_0$  of cementite is 0.06; to informational dimension  $D_1$  – 0.07 (Fig. 5). Sensitivity indexes for the ultimate bending strength  $\sigma$  to cementite dimension  $D_0$  and  $D_2$  are 0.09 and 0.08 respectively (Fig. 5), and to graphite dimension  $D_2$  is 0.084 (Fig. 4). Sensitivity coefficients between impact strength indexes  $KC$ , cementite dimensions  $D_0$ ,  $D_2$  (Fig. 5) and pearlite matrix  $D_2$  (Fig. 6) are defined within 0.07, which also confirms the influence of these structure elements on plastic properties of cast iron.

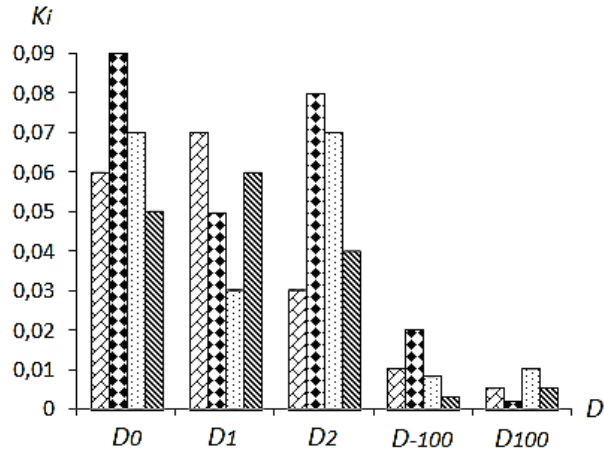


Figure 5 Sensitivity of Cast Iron Mechanical Properties to Dimensions of Cementite

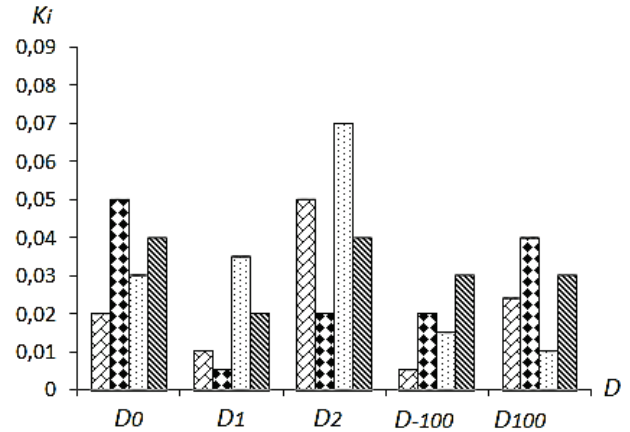


Figure 6 Sensitivity of Cast Iron Mechanical Properties to Dimensions of Pearlite

The above results indicate the influence of the structural elements form, expressed in fractal dimension, and their distribution in volume, expressed in the information and correlation dimensions on the mechanical properties of the metal.

Sensitivity indexes  $\sigma_B$ ,  $\sigma$ ,  $KC$  and  $HSD$  to dimensions  $D_{-100}$  and  $D_{100}$  of cementite and graphite are relatively lower compared to dimensions  $D_0$ ,  $D_1$ ,  $D_2$  (Figs. 4-6), which indicates small correlation between them.

Relations between the most sensitive dimensions of the cast iron structure elements and its mechanical properties (Fig. 7) as well as the relevant regression Eqs. (3)-(6) are shown below.

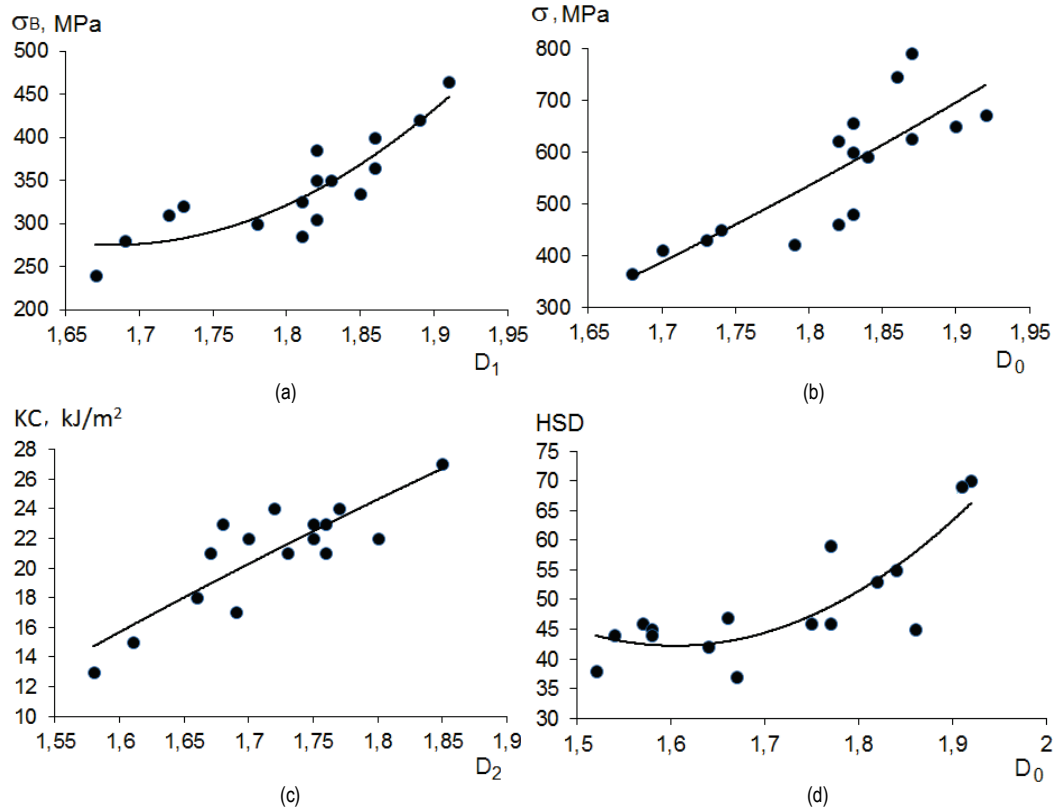


Figure 7 Dependence of Mechanical Properties on Cementite (a-c) and Graphite (d) dimensions

$$\sigma_B = 3284,30 \cdot D_1^2 - 11043 \cdot D_1 + 9558,40 \quad R^2 = 0,77 \quad (3)$$

$$\sigma = 1535,90 \cdot D_0 - 2226,80 \quad R^2 = 0,68 \quad (4)$$

$$KC = 44,20 \cdot D_2 - 54,91 \quad R^2 = 0,72 \quad (5)$$

$$HSD = 241,76 \cdot D_0^2 - 775,92 \cdot D_0 + 664,79 \quad R^2 = 0,70 \quad (6)$$

Improvement of the cast iron mechanical properties  $\sigma_B$ ,  $\sigma$ ,  $KC$  (Figs. 7a-7c) is caused by influence of such technological factors as chemical composition, heat removal rate during cooling down of cast iron rolls. They influence not only the relation of structure elements but also their geometrical configuration, which is registered by the multifractal spectrum of Renyi dimensions.

Limits of graphite inclusions serve as microstress concentrators and increase of its contents weaken metal matrix of cast iron, which is indicative of influence on mechanical properties of cast iron either composition, sizes, distribution of graphite or form of such inclusions. The increase of hardness  $HSD$  from 35 to 70 units is connected with the increase of carbon content from 3.00 to 3.40%. And growth of fractal dimension of graphite to 1.93 (Fig 6d) is caused by the change of its form (Fig. 1) to a spherical one because of increase of Mg inclusions from 0.035 to 0.056%.

#### 4 CONCLUSION

As a result of implementation of the cast iron quality estimation method, the following results have been obtained:

- 1) For the prediction of mechanical properties of roll-foundry iron, it is effectually to use dimensional evaluations  $D_0$ ,  $D_1$ ,  $D_2$  of graphite and cementite, which is proven by the determined sensitivity between them.
- 2) Relatively high sensitivity among the indexes under consideration – ultimate strength, ultimate bending strength and impact strength – is recorded for dimensions  $D_0$ ,  $D_1$ ,  $D_2$  of cementite, hardness sensitivity to fractal dimension  $D_0$  of graphite.
- 3) Statistical dimensions of graphite and cementite  $D_{-100}$ ,  $D_{100}$  have relatively low sensitivity to the mechanical properties in the analyzed scale ( $\times 300$ ,  $\times 400$ ).
- 4) The results indicate the influence of the structural elements form, expressed in fractal dimension, and their distribution in volume, expressed in the information and correlation dimensions on the mechanical properties of the metal.

The proposed method allows to evaluate the quality of cast iron on the basis of the dimensional values analysis characterizing the most sensitive elements of its structure and enables evaluation of mechanical properties of materials based on determination of their sensitivity to dimensions of structure elements from the multifractal Renyi spectrum.

#### 5 REFERENCES

- [1] Kos, Ž., Gotal Dmitrović, L., & Klymenko, Ie. (2017). Developing a model of a strain (deformation) of a damaged reinforced 150 concrete pillar in relation to a linear load capacity. *Tehnički glasnik - Technical Journal*, 11(4), 150-154.
- [2] Aniskin, A., Orešković, M., & Kozina, G. (2017). The effects of particles orientation on lateral pressure within the confined vertical walls. *Tehnički vjesnik*, 24(4), 1349-1253. <https://doi.org/10.17559/TV-20160826121746>
- [3] Mishutn, A., Kroviakov, S., Pishev, O., & Soldo, B. (2017). Modified expanded clay light weight concretes for thin-walled reinforced concrete floating structures. *Tehnički glasnik - Technical Journal*, 11(3), 121-124.
- [4] Kroviakov, S. & Mishutn, A. (2017). Production technology of modified expanded clay lightweight concrete for floating structures. *The Scientific Journal of Cihan University – Sulaimanyia*, 1(4), 2-10.
- [5] Dubrov, Yu., Bol'shakov, V., & Volchuk, V. (2015). *Paths to Identification of Periodic Multicriteria Technologies*. Saarbrücken, Deutschland: Palmarium Academic Publishing. (in Russian)
- [6] Mandelbrot, B. B. (1982). *The Fractal Geometry of Nature*. New York–San Francisco: Freeman.
- [7] Bolshakov V., Volchuk V., Dubrov Yu. (2016). *Fractals and properties of materials*. Saarbrücken, Deutschland: Lambert Academic Publishing.
- [8] Volchuk, V. M. (2017). On the Application of Fractal Formalism for Ranging Criteria of Quality of Multiparametric Technologies. *Metallofizika i Noveishie Tekhnologii, International Scientific and Technical Journal of the Institute of Metal Physics*. G.V. Kurdyumov National Academy of Sciences of Ukraine, 39(7), 949-957. (in Russian) <https://doi.org/10.15407/mfint.39.07.0949>
- [9] Bolshakov, V. I.; Volchuk, V. M.; & Dubrov, Yu. I. (2016). *Fundamentals of fractal modeling*. Kyiv, Ukraine: PH "Akademperiodyka" National Academy of Sciences of Ukraine.
- [10] Rényi, A. (1970). *Probability Theory*. Amsterdam, Netherlands: North-Holland.
- [11] Bolshakov, V. I. & Dubrov, Yu. I. (2002). An estimate of the applicability of fractal geometry to describe the language of qualitative transformation of materials. *Journal of Reports of the National Academy of Sciences of Ukraine*, 4, 116-121. (in Russian)
- [12] Volchuk, V. M. (2015). Determining the sensitivity of the multifractal characteristics of metals, *Bulletin of Prydniprov'ska State Academy of Civil Engineering and Architecture, Ukrainian. Journal of Technical Sciences, Constructions and Architectures*, 12, 10-14. (in Russian)



**Authors' contacts:**

**Volodymyr VOLCHUK**, PhD, Assoc. Prof.

Prydniprov's'ka State Academy of Civil Engineering and Architecture  
Department of materials science,  
24a Chernyshevskyst., Dnipro, Ukraine  
volchuky@gmail.com

**Ievgenii KLYMENKO**, PhD, Full Professor, vice-rector

Odessa State Academy of Civil Engineering and Architecture,  
4 Didrihsona st., Odessa, Ukraine  
klimenkoew57@gmail.com

**Sergii KROVIKOV**, PhD, Assist. Prof.

Odessa State Academy of Civil Engineering and Architecture,  
4 Didrihsona st., Odessa, Ukraine  
skrovyakov@ukr.net

**Matija OREŠKOVIĆ**, PhD

Sveučilište Sjever, Sveučilišni centar Varaždin, Odjel za graditeljstvo  
Jurja Križanića 31b, 42000 Varaždin, Croatia  
moreskovic@unin.hr

# TRANSPORT EMISSIONS AND ELECTRIC MOBILITY IN PRIVATE TRANSPORT IN THE REPUBLIC OF SLOVENIA

Simon MUHIČ, Ante ČIKIĆ, Jadran PIŠTAN, Marinko STOJKOV, Mladen BOŠNJAKOVIĆ

**Abstract:** Since the ratification of the Kyoto Protocol more and more emphasis is laid on reducing greenhouse gas emissions. The article analyses the feasibility of introducing electric vehicles into traffic rather than vehicles with internal combustion engines. From standpoint of emission sources use of electricity for transport is analysed with stress on private cars and typical emissions from power sector by energy conversion in Slovenia. Results of research shows that electric car has a little more than twice better efficiency of the primary energy use, taking into account only efficiency in the energy chain. Electric mobility brings a more efficient use of energy in road transport with demand to reduce emission at power generation. So presented number can vary greatly, depending on the electrical energy source. In the present research problems connected with immediate initiation of the electric cars are not analysed.

**Keywords:** electric mobility; electric vehicles; emissions; transport

## 1 INTRODUCTION

Energy use in the transport sector in Slovenia represents around 40 % of total energy use. For this purpose, mainly imported petroleum products are used. Introduction of alternative fuels, emphasizing electric mobility, is a prioritized task in the field of transport, as well as in the current proposed orientations for preparing the new energy concept of the Republic of Slovenia.

In the last decade, transport took over the first place among the sectors regarding the energy use, namely in 2002, it represented 32 % of end energy use in Slovenia. Today it has grown to just above 40 %. The end energy use in 2007 amounted to 4954 *ktoe*. In the period from 1992 to 2007, it increased by 49 %; the majority of growth occurred in 1997 and it continues to rise. Transport energy use is almost exclusively (99 %) based on fossil fuels, resulting in a constant increase of the greenhouse gas emissions [1].

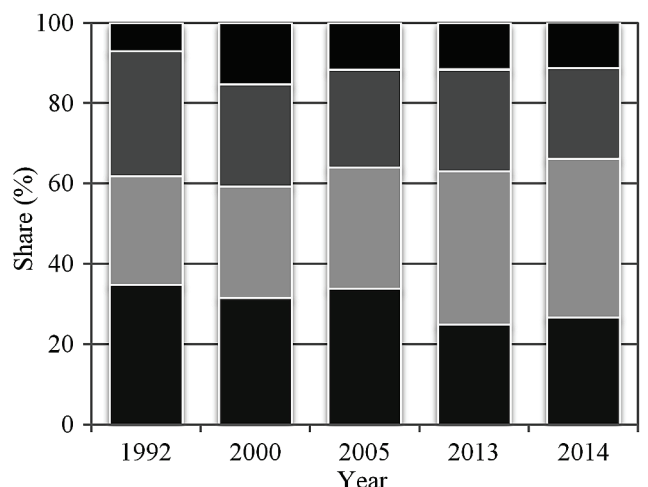
Nowadays, electric drive cars are no longer rare, since all automotive concerns and a significant number of institutes engage in their development, but although a lot has been written and spoken about the electric cars, electric transport is still a distant vision, at least on Slovenian roads, as only a small number of electric representatives can be found [2].

In 2014, 153 electric vehicles (EV) were registered in Slovenia, i.e. only around 0,01 % of all vehicles [2] of which 133 were private cars, however, at the end of 2015, from 1437444 registered vehicles 599 were electric, which amounts to approximately 0,04 % of all vehicles [3]. From the statistics it can be identified that electrically powered vehicles are on the rise, but according to the national energy programme, by 2020 the number of them should represent 2,7 % of vehicle fleet. Introduction of alternative fuels, putting an emphasis on electric mobility, is a prioritized task in the field of transport, as well as in the current proposed orientations for preparing the new energy concept of the Republic of Slovenia [4].

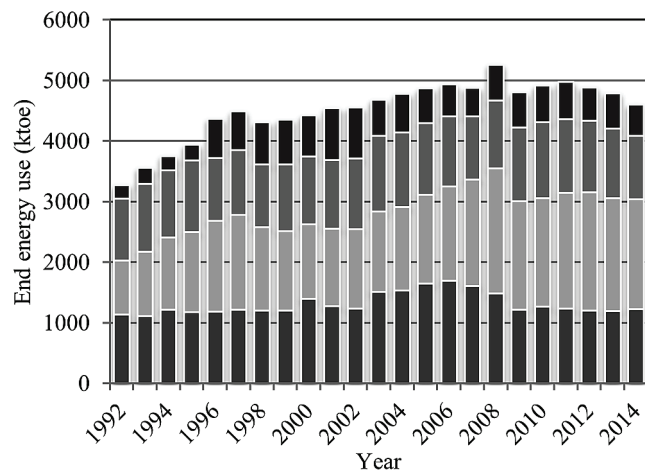
Fig. 1 shows the shares in energy use by sectors in Slovenia since 1992 and how it has been increasing over the years until today. The increase can also be linked with the previously mentioned data on the increase in the number of registered vehicles. It is visible that the share of the end energy use in transport is 39,5 % for the year 2014 [1].

It can be concluded that replacing the energy source for just over 40 % of the end energy use represented by transport today would have a significant effect on emissions. As a result, we could expect lower emissions and less harmful impact on the natural and urban environment. Nevertheless, the change that would occur in this case must not to be overlooked. The primary energy from mainly imported fossil fuels of petroleum origin is replaced with electrical energy. At the same time, we face the problem of emissions in the conversion of fuels into electrical energy. The future society will have to be based on a high proportion of renewable energy sources (RES) for supplying energy. This is necessary to control climate change and to boost competitiveness and reliability of the energy supply [5]. The main problem is motor transport, where a positive trend of reducing emissions due to the advancement in vehicle fleet is seen, however, because of the increasing number of vehicles these effects are diminishing. Due to the increased number of motor vehicles and numerous migrations, the use of motor fuels has risen and consequently, the emissions have as well. It is assumed that the growing transport is a heavy burden for the environment; that it is in the interest of all to reduce the emissions from transport; that initiation of different technologies in transport is needed, and with the correct attitude, electric transport would mean larger energy independence and more stable economy [6]. The greenhouse gases from transport in Slovenia increased from 1986 to 2012 by 185 %; as well as elsewhere in Europe the greenhouse gas (GHG) emissions from transport are higher than the overall growth. In the area of the first EU member states, from 1990 to 2012, the GHG emissions increased by

9 %, moreover, in the whole current EU area by 14 % (in Slovenia in the same period by 111 %). The most greenhouse gas emissions in transport are caused by road transport, which generates 99,2 %. A relatively high proportion of transport emissions in relation to total emissions (31 % in 2012) and not enough strict measures for their reduction complicate the commitment of Slovenia to achieve the Kyoto Protocol commitments [7]. Fig. 1 shows shares of sectors in the end energy use in period 1992 – 2014.



■ Other ■ Households ■ Transport ■ Manufacturing and construction  
Figure 1 Shares of sectors in the end energy use [1]



■ Manufacturing and construction ■ Transport ■ Households ■ Other  
Figure 2 The end energy use across sectors [1]

Fig. 2 shows total end energy use in "ktoe" in Slovenia in the same period. With the National Energy Efficiency Action Plan 2014-2020 (AN URE 2020), according to the requirements of Energy Efficiency Directive 2012/27/EU, Slovenia has set an indicative target for improving energy efficiency by 2020, concluding that primary energy use will not surpass 7125 million toe in 2020, meaning it may not exceed the 2012 data for more than 2 %, and sets the national target of improving energy efficiency by 20 % until 2020 [8].

## 2 ENERGY IN TRANSPORT

Through membership in the European Union, Slovenia has committed itself to achieving of the target values for emissions of greenhouse gases defined in the Kyoto Protocol. Transport is the sector in which the most of fossil fuels is spent. In 2012, the energy use in transport amounted to 1953 ktce. According to the previous year, it increased by almost 2 %, and by 59 % in comparison to the year 2000; in comparison to the year 1992, it was higher by 120 %. In 2008, when the maximum in the observed period was reached, it decreased by 6 %. By far the most energy was used by road transport, which in 2012 represented more than 97 % of the total use. The share of transport regarding the total end energy use in Slovenia, which in 1992 amounted to 24,4 %, in 2002 increased to 31,6 %. Energy use in transport is almost exclusively in 99 % based on fossil fuels, among which in 2011 the diesel fuel strongly dominated with 65,0 %, followed by the petrol fuel with 30,8 %. Liquid fuels, the usage of which is still increasing in the transport sector, remain the most important energy source with 51 % share. Unlike the transport, energy use in industry is decreasing.

In the current state of technology, motorcycles, private cars and small delivery vehicles are already suitable for transition to electric drive. In 2010 in Slovenia, these types of vehicles represented 85 % of all motor vehicles in road transport, their fuel use amounted to 73,5 % of total use in road transport, and the share of CO<sub>2</sub> emissions was 73,9 % [9]. The mentioned shares and numbers point out that, based on new technologies, e-mobility plays an important role in protecting the environment and ensuring the sustainable energy use.

Table 1 Structure of energy use in transport [10]

		2000	2005	2010	2012	2013
Cars	%	73,6	67,4	61,9	62,2	62,1
Freight vehicles	%	19,5	26,4	32,9	33,6	33,6
Buses	%	2,7	2,4	1,9	1,3	1,2
Motorcycles	%	0,1	0,3	0,4	0,4	0,4
Railways	%	1,9	1,9	1,3	1,2	1,2
Airplanes	%	2,1	1,6	1,6	1,3	1,5

Tab. 1 shows the structure of energy use in transport in Slovenia in period 2000 – 2013. For example during 2013 private vehicles represent 62,1 % of energy use in transport, which is 33 % of the end energy use. Tab. 2 shows the sources of distributed electrical energy in 2014 and information on emissions, as well as the radioactive waste per kW-h produced in Slovenia. The majority of electrical energy is from fossil fuels (47,86 %) and of nuclear origin (38,76 %) [11] and only 13,37 % of electrical energy comes from renewable energy sources.

Tab. 3 shows the quantities of electrical energy on the power plants threshold in Slovenia in period 2012 – 2014. The last column shows the part produced for Croatia. The total production in Slovenia is thus the sum of production in the first column and the last column.

**Table 2** The share of electrical energy sources [11]

Fossil fuels	47,86 %
Coal and lignite	40,17 %
Natural gas	4,71 %
Petroleum products	0,17 %
Unidentifiable	2,81 %
Nuclear fuel	38,76 %
Renewable energy sources	13,37 %
Hydropower	11,58 %
Wind	0,05 %
Solar energy	0,89 %
Wood biomass	0,00 %
Geothermal energy	0,32 %
Landfill gas	0,13 %
Sewage treatment plant gas	0,00 %
Biogas	0,38 %
Biodiesel	0,01 %
Unidentifiable	0,01 %
Total	100,00 %

The end use of energy, i.e. the end energy use or the energetic end use is the energy, used in industry sectors

**Table 4** Emissions from electrical energy conversion [14]

Gas	Unit of measurement	2009	2010	2011	2012	2013	2014
CO <sub>2</sub>	kg CO <sub>2</sub> /kW·h	0,480	0,491	0,516	0,497	0,450	0,316
CH <sub>4</sub>	kg CH <sub>4</sub> /kW·h	0,00016	0,00015	0,00016	0,00016	0,00013	0,00011
N <sub>2</sub> O	kg N <sub>2</sub> O/kW·h	0,00188	0,00190	0,00204	0,00197	0,00178	0,00137
Total GHG	kg CO <sub>2</sub> -eq/kW·h	0,483	0,493	0,519	0,499	0,452	0,317

**Table 5** Emissions in 2013 in Slovenia from energy use across sectors [15]

Unit	Non-energy related sources	Electricity and heat production (incl. fugitive emissions)	Industry and construction (energy use of fuels)	Transport	Other (wide use)	Total
kt CO <sub>2</sub> -eq	3287,6	6230,9	1641,5	5459,1	1546,7	18165,8
%	18,1	34,3	9,0	30,1	8,5	100,0

General average of emissions of all individual greenhouse gases (GHG) and the carbon dioxide equivalent per kW·h in Slovenia from 2009 to 2014 amounts to 0,460 g [13]. Tab. 4 shows the carbon dioxide equivalent (CO<sub>2</sub>-eq), which is a product of the quantity (mass) of individual greenhouse gasses, multiplied by their global warming potential. The obtained value enables the impact of different greenhouse gasses to be combined in the same unit, representing the unified carbon footprint. It is measured with unit of carbon dioxide equivalent (CO<sub>2</sub>-eq).

Tab. 5 shows emissions across sectors [15]. Energy-related greenhouse gas emissions are caused by fuel combustion in electrical energy sources, heating, transport, processing industries and construction, as well as in services and households. In addition, the emissions which are not generated directly by fuel combustion, but are connected to energy, i.e. fugitive emissions, which are generated by coal mining (collieries), transport and natural gas distribution, as well as by flue gas desulphurisation.

Electrical energy in Slovenia is generating the approximate average of 0,43 kg of CO<sub>2</sub> emissions per kWh of energy produced [13]. In the 2012 study, the CARB (California Air Resource Board) department performed the analysis by calculating the energy demands and CO<sub>2</sub> equivalent emissions of a traditionally used – conventional petrol vehicle (CV), a combination of electric motor and internal combustion engine - hybrid vehicle (HV), and also

(construction and processing), transport, households and by other users (services and other use), and does not include the conversion and transmission losses, the energy sector's own use and non-energy related use. Also, capacity of power plants in Slovenia is in slightly increase during observed period, from 3351 MW in 2012 till 3453 MW in 2014.

**Table 3** Quantities of electrical energy (EE) and installed capacity of power plants in Slovenia [12]

Year	Production (GW·h)	End use (GW·h)	Capacity (MW)	Croatia 1/2 EE from NPP Krško (GW·h)
2014	13456	12560	3453	3030
2013	12599	12587	3434	2518
2012	12083	12540	3351	2622

a battery electric vehicle (BEV) throughout their lifecycle. The study was founded as a support to the California Climate Change Legislation. The results of used hybrid model are calculated by weighted-average parameters of CV and BEV. Archive data used in the paper are based on the California GREET model, ANL (Argonne National Laboratory) findings and scientific sources in peer-reviewed literature. Several cases of the models are tested as sensitivity analyses on variation of input parameters and initial assumptions such as carbon emissions of petrol and electricity, different portions of electric rated power, electric battery rated power and reliability and fuel use. The calculations of techno-economic parameters (efficiency) of each vehicle type are performed and it is easy to see that HV is the best vehicle in efficiency and CO<sub>2</sub> equivalent emissions. The calculations of total present value costs of all types of vehicles are performed too and as a result the HV are the cheapest during their lifetime, CV are in the middle and as the most expansive are BEV.

The most important aim of this research is to define the environmental influence of each type of vehicles, considering the lifetime energy use, CO<sub>2</sub> equivalents emissions and also air pollution emissions. Considering environmental influence, the BEV are vehicles with the least overall impact, HV are in the middle and CV are vehicles with most significant influence [16]. The results of the study are presented in Fig. 3.

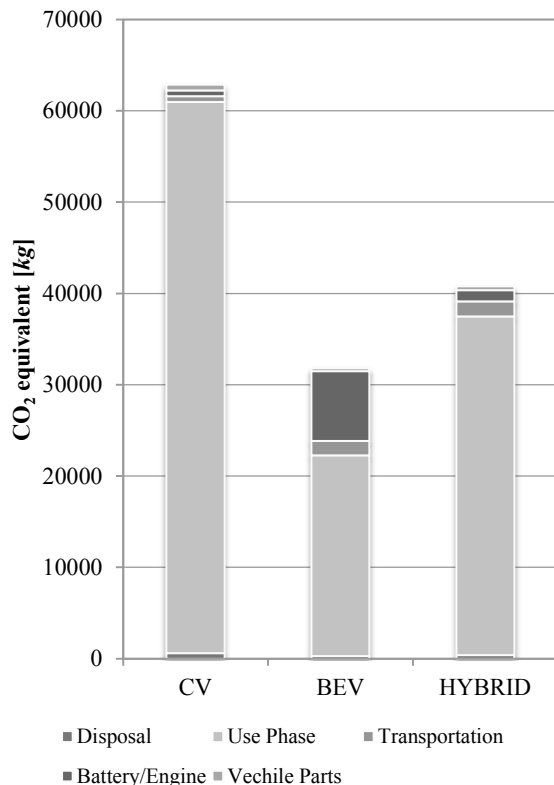


Figure 3 Emissions of the vehicles according to lifecycle phases [16]

As presented in the Fig. 3, the impact of electric vehicles on transport emissions - in the phase where they are driven directly by electrical energy or driven by hybrid motors is meter of research.

### 2.1 Example of an Electric Vehicle for Emission Calculation

In this case scenario, model is used to find optimal size of the system for power supply for period from 1<sup>st</sup> June to 31<sup>st</sup> August. Different values of loss of load probability (LOLP) in this case scenarios are assumed. Optimal size of the off-grid system for following values of LOLP is determined: 0,00; 0,01; 0,02; 0,03; 0,04; 0,05; 0,06; 0,07; 0,08; 0,09; 0,10, and 0,15, respectively.

### 2.2 Emission Impacts of e-Mobility Introduction

Tab. 6 shows the average mileage in Slovenia. Considering that the average electric car needs 0,2 kWh/km, calculation gives need of 2530,6 kW·h/year for each car.

Table 6 The average mileage of private cars [20]

	All fuel	Petrol	Diesel
Average (km)	12653	10235	16879

If it is assumed replacing the total number of classic cars with the electric versions, it can be calculated how much electrical energy would be needed in total at the EV charging stations, neglecting any additional losses. For the entire fleet of private cars on 31 December 2014 (1068362 cars), we would need 2703,6 GW·h/year. The annual use of energy to power the entire fleet of electric cars means 20 % of the annual production of electrical energy on the power plants threshold (without energy produced in Nuclear Power Plant for Republic of Croatia), or 21,5% of the end energy use. This definitely means that the energy use would increase by the mentioned percentage, from current 12560 GW·h on 15264 GW·h, which would, of course, be more than the current production.

If it is assumed that the structure of energy sources for production of additional capacity is about the same as it was in 2013, the increase in CO<sub>2</sub> emissions at electrical energy conversion could be calculated. Thus, for electric vehicles 1222 kt of CO<sub>2</sub> per year would be emitted. Considering that approximately 62% of the transport energy represents private cars, it can be assumed that they also cause as many emissions, amounting to the total emission of 3390,1 kt of CO<sub>2</sub> per year. Using these calculated data, we can now evaluate, that the emissions would be 64% lower than they are today, taking into account only emissions from private cars.

## 3 DISCUSSION

In the Republic of Slovenia, the share of energy from renewable sources, which actually fully justifies the feasibility of introducing electric vehicles, is a bit over 13%. The importance of renewable energy sources in the case of electric vehicles is inversely proportional to the harmful emissions; the greater is the share of renewable energy sources, the lower is the share of harmful emissions. Table 7 shows the status of emissions assuming the introduction of electric vehicles. Decreasing emissions in private transport for 1745,9 kt CO<sub>2</sub> represents only 9,6 % of reduction of total emissions according to the data from the year 2013, and the fact that at the introduction of complete electric mobility in private transport, private cars still represent only around 8 % of the sources of emissions.

Table 7 GHG emissions considering electric cars

	Non-energy related sources	Electricity and heat production (incl. fugitive emissions)	Industry and construction (energy use of fuels)	Transport	Transport – only private vehicles	Other (wide use)	Total
2013 kt CO <sub>2</sub> -eq	3287,6	6230,9	1641,5	2069,0	3390,1	1546,7	18165,8
Introducing EV kt CO <sub>2</sub> -eq	3287,6	6230,9	1641,5	2069,0	1222,0	1546,7	16419,9

Results can be also evaluated through the aspect of primary energy efficiency. For comparison a classic vehicle

is selected on the one hand, with the internal combustion engine and the average efficiency. On the other hand, an

electric vehicle is selected for comparison, which uses thermal power plant as a source of energy. Taking into account the efficiencies according to the energy chain [21, 22, 23] and traffic modelling [24], the differences between electric vehicles and vehicles with internal combustion engines are identified. Despite the significantly higher efficiency of the first, the difference is actually relatively small, mainly because of losses when converting energy in the power plant, and due to losses in battery conversions. Thus, it can be concluded that the electric car has a little more than twice better efficiency of the primary energy. In our calculation it is not considered the possible energy recovery through regenerative braking system, which, according to some estimates [21], increases the efficiency of the vehicle itself by 17 %. When dealing with efficiencies, of course it has to pay attention to the correct interpretation, since estimating emissions through the energy efficiency is valid only as long as the chemical energy of fossil fuels is used. In the case of the use of renewable energy sources, which have relatively poor energy efficiency, this comparison is not purposeful.

#### 4 CONCLUSION

E-mobility or the introduction of electric vehicles brings a more efficient use of energy in road transport. Electric vehicles reduce greenhouse gas emissions. At the current structure of electrical energy conversion in Slovenia, CO<sub>2</sub> emissions of a simple battery electric vehicle are 64 % lower than in a classic drive vehicle. This number can vary greatly depending on the electrical energy source. Electric vehicles are also an advantage for local emissions. Residents of some Slovenian cities are exposed to serious concentrations of NO<sub>2</sub> and dust particles PM<sub>10</sub>, which largely originate from transport. Excessive contamination with dust particles in Slovenian cities is a serious environmental problem, which is why the European Commission initiated the procedure at the EU Court of Justice against Slovenia for violating the environmental protection.

According to the obtained results, a partial reduction in emissions of greenhouse gasses is needed. However, analyzed problem is very dependent on future investments in renewable sources; moreover electrical energy application cannot be possible without serious global alliances and collaborations.

Transport driven by electrical energy from own sources would of course mean an increased financial, political and technological independence, and can function as some sort of a lift for the standard of Slovenia. Economically speaking, society could gain a lot, because there would be no more imported primary energy from petroleum products, coming from elsewhere; closely related is also the independency from foreign sources and supply which can at the same time also mean less political influence from the outside. Nevertheless, energy independence is also preferred by the EU.

The immediate introduction of the electric cars presents a problem also due to the load of the power grid. A drastic

increase in the number of electric cars, by taking into account the current configuration of the electrical energy system, would also represent a problem for the distribution.

#### 5 REFERENCES

- [1] Agencija Republike Slovenije za okolje. Raba končne energije po sektorjih: Kazalci okolja v Sloveniji. [http://kazalci.arso.gov.si/?data=indicator&ind\\_id=717](http://kazalci.arso.gov.si/?data=indicator&ind_id=717). (2016, January 18)
- [2] Statistični urad Republika Slovenija, medijsko središče, SI-STAT. <http://www.stat.si/StatWeb/prikazi-novico?id=5227&idp=22&headerbar=19>. (2015, May 28)
- [3] Republika Slovenija Ministrstvo za infrastrukturo. Energetski koncept Slovenije, Portal energetika, Direktorat za energijo. <http://www.Energetika-portal.si/dokumenti/strateski-razvojni-dokumenti/energetski-koncept-slovenije/>. (2015)
- [4] Agencija RS za okolje. Izpusti toplogrednih plinov iz prometa: Kazalci okolja v Sloveniji, Institut Jožef Stefan. [http://kazalci.arso.gov.si/?data=indicator&ind\\_id=627](http://kazalci.arso.gov.si/?data=indicator&ind_id=627). (2014, September 9).
- [5] Česen, M., Staničič, D., Urbančič, A., Levstek, M., Babuder, M., Beravs, F., Kopač, J., Lah, T., Merše, S., Nemac, F., Stojanovič, B., Svoljšak, M., Škornik, S., Volfand, J., & Žebeljan, D. (2009). Obnovljivi viri energije (OVE) v Sloveniji (pp. 37-48 and 127-131). Celje: Fit media d.o.o., ISBN 978-961-6283-34-2.
- [6] Agencija za energijo. Elektromobilnost. [http://www.agenrs.si/documents/10926/20705/PUB\\_20121211\\_Elektromobilnost\\_VFfinal-Rev\\_1\\_1790.pdf](http://www.agenrs.si/documents/10926/20705/PUB_20121211_Elektromobilnost_VFfinal-Rev_1_1790.pdf). (2012, December 11)
- [7] Senočetnik, A. Pogoji so, električnih avtomobilov pa je zdaj še zelo malo. <http://www.gorenjskiglas.si/article/20160409/C/160409774/1038/po-goji-so-elektricnih-avtomobilov-pa-je-zdaj-se-zelo-malo>. (2016, April 9)
- [8] Ministrstvo za infrastrukturo Republike Slovenije. Akcijski načrt za energetske učinkovitost za obdobje 2014–2020. (2015). Ljubljana: s.n.
- [9] Agen. Poraba končne energije v prometu: Kazalci okolja v Sloveniji. [http://kazalci.arso.gov.si/?data=indicator&ind\\_id=680](http://kazalci.arso.gov.si/?data=indicator&ind_id=680). (2013, September)
- [10] Agencija Republike Slovenije za okolje. Energetska učinkovitost in raba energije v sektorjih rabe končne energije: Kazalci okolja v Sloveniji. Jožef Stefan Institute. See [http://kazalci.arso.gov.si/?data=indicator&ind\\_id=724](http://kazalci.arso.gov.si/?data=indicator&ind_id=724). (2015, November 14)
- [11] Energija plus d.o.o. Sestava primarnih virov za proizvodnjo električne energije. <http://www.energijaplus.si/za-dom/pomoc-in-podpora/sestava-primarnih-virov-za-proizvodnjo-elektrike>. (2014)
- [12] Ministrstvo za infrastrukturo. Statistika. Portal Energetika, Statistični urad RS. <http://www.energetika-portal.si/statistika/>. (2014).
- [13] GEN energija. Nizkoogljična proizvodnja električne energije: Proizvodnja, GEN energija. <http://www.gen-energija.si/proizvajamo/trajnostna-proizvodnja>. (2015).
- [14] Institut Jožef Stefan. Izpusti CO<sub>2</sub>/TGP na enoto električne energije. Center za energetske učinkovitost. <http://www.rcp.ijs.si/ceu/sl/izpusti-co2tgp-na-enoto-elektricne-energije>. (2016).
- [15] Agencija Republike Slovenije za okolje. Izpusti toplogrednih plinov energetskega izvora: Kazalci okolja v Sloveniji. Institut Jožef Stefan. [http://kazalci.arso.gov.si/?data=indicator&ind\\_id=705](http://kazalci.arso.gov.si/?data=indicator&ind_id=705). (2016, January 18).
- [16] Mediamatters for America, California Air Resources Board.

- Experts Respond To Distortions Of Electric Car's Environmental Benefits. <http://mediamatters.org/blog/2013/03/13/experts-respond-to-distortions-of-electric-cars/193040>. (2013, March 13).
- [17] SUZUKI. Splash 2007 – Present: Autoevolution. [http://www.autoevolution.com/cars/suzuki-splash-2007.html#aeng\\_suzuki-splash-2007-10](http://www.autoevolution.com/cars/suzuki-splash-2007.html#aeng_suzuki-splash-2007-10). (2013).
- [18] German E cars GmbH. Elektrifizierte Personenwagen. <http://www.german-e-cars.de/Personen-wagen.357.0.html?&L=0%3C%2Fref>. (2010).
- [19] Laurent, J. M. The Stromos: For Germans Who Can't Wait for an Electric Car. Plugincars. <http://www.plugincars.com/stromos-german-e-cars-old-school-those-who-dont-want-wait-107199.html>. (2011, May 17). See
- [20] Statistični urad Republike Slovenije. Povprečno število prevoženih kilometrov in poraba goriva osebnih avtomobilov. Podatkovni portal SI-STAT. [http://pxweb.stat.si/pxweb/Dialog/varval.asp?lang=2&ma=1815420S&path=../Database/Okolje/18\\_energetika/07\\_18154\\_poraba\\_gospodinjstva/&ti=](http://pxweb.stat.si/pxweb/Dialog/varval.asp?lang=2&ma=1815420S&path=../Database/Okolje/18_energetika/07_18154_poraba_gospodinjstva/&ti=). (2014).
- [21] U.S. Department of Energy. Where the Energy Goes: Electric Cars. Fueleconomy. <https://www.fueleconomy.gov/feg/atvev.shtml>. (2016).
- [22] Grobljar, D. (2009). *Ogrevanje hibridnih in električnih vozil*. Fakulteta za pomorstvo in promet, Portorož, UDK 629.331(043.2).
- [23] Markowitz, M. Wells to wheels: electric car efficiency. Energy Matters. See <https://matter2energy.wordpress.com/2013/02/22/wells-to-wheels-electric-car-efficiency/>. (2013, February 22).
- [24] Kurnaz, İ. (2016). Urban traffic modeling with microscopic approach using cellular automata. *Technical Gazette*, 23(6), 1565-1570. <https://doi.org/10.17559/TV-20140601114314>

#### Authors' contacts:

**Simon MUHIČ**, Ph.D. Associate Professor  
Faculty of Technologies and Systems  
Na Loko 2, 8000 Novo mesto, Slovenia  
+386 7393 0019, [simon.muhic@guest.arnes.si](mailto:simon.muhic@guest.arnes.si)

**Ante ČIKIĆ**, Ph.D. Associate Professor  
Mechanical Engineering Faculty in Slavonski Brod  
Trg Ivane Brlić Mažuranić 2  
35000 Slavonski Brod, Croatia  
+385 35493444, [acikic@vtsbj.hr](mailto:acikic@vtsbj.hr)

**Jadran PIŠTAN**, B.Sc.  
Faculty of Technologies and Systems  
Na Loko 2, 8000 Novo mesto, Slovenia  
+386 7393 0019, [jadran.pistan@yahoo.com](mailto:jadran.pistan@yahoo.com)

**Marinko STOJKOV**, Ph.D., Full Professor  
Mechanical Engineering Faculty in Slavonski Brod  
Trg Ivane Brlić Mažuranić 2  
35000 Slavonski Brod, Croatia  
+385 35493444, [mstojkov@sfsb.hr](mailto:mstojkov@sfsb.hr)

**Mladen BOŠNJAKOVIĆ**, Ph.D., Senior lecturer  
College of Slavonski Brod  
Dr. Mile Budaka 1  
35000 Slavonski Brod, Croatia  
+385 35492634, [mladenb@vusb.hr](mailto:mladenb@vusb.hr)



# OPTIMIZATION OF MACHINING PARAMETERS IN FACE MILLING USING MULTI-OBJECTIVE TAGUCHI TECHNIQUE

Yusuf FEDAI, Funda KAHRAMAN, Hediye KIRLI AKIN, Gokhan BASAR

**Abstract:** In this research, the effect of machining parameters on the various surface roughness characteristics (arithmetic average roughness ( $R_a$ ), root mean square average roughness ( $R_q$ ) and average maximum height of the profile ( $R_z$ )) in the milling of AISI 4140 steel were experimentally investigated. Depth of cut, feed rate, cutting speed and the number of insert were considered as control factors;  $R_a$ ,  $R_z$  and  $R_q$  were considered as response factors. Experiments were designed considering Taguchi  $L_9$  orthogonal array. Multi signal-to-noise ratio was calculated for the response variables simultaneously. Analysis of variance was conducted to detect the significance of control factors on responses. Moreover, the percent contributions of the control factors on the surface roughness were obtained to be the number of insert (71.89 %), feed (19.74 %), cutting speed (5.08%) and depth of cut (3.29 %). Minimum surface roughness values for  $R_a$ ,  $R_z$  and  $R_q$  were obtained at 325 m/min cutting speed, 0.08 mm/rev feed rate, 1 number of insert and 1 mm depth of cut by using multi-objective Taguchi technique.

**Keywords:** milling; optimization; surface roughness; Taguchi

## 1 INTRODUCTION

Machining processes like turning, milling, drilling and grinding, etc., have been commonly used in the manufacturing industries. Milling is one of the basic machining processes using rotary tools to remove material from a workpiece by feeding the tools into the workpiece at a certain direction [1]. Milling is a system consisting of a workpiece, cutting tool, machine tool, fixture and cutting parameters. The machinability of a material is defined by measuring factors such as tool life, cutting force and surface roughness. Surface roughness is a commonly encountered problem in machined surfaces. The quality of the surface plays a very important role in the performance of the milling as a milled surface of good quality significantly improves fatigue strength, corrosion resistance or creep life. Surface roughness is determined using  $R_a$ ,  $R_z$  and  $R_q$  measurements [2, 3].

At the present time, there have been many investigation progressions in surface roughness modeling and optimization of the machining parameters. Kivak [4] studied the effect of cutting tools, cutting speed and feed rate on the surface roughness and flank wear in milling of Hadfield steel using Taguchi method (TM). Stipkovic Filho et al. [5] developed a mathematical model for surface roughness as a function of cutting speed, feed and cutting depth in face milling of AISI 4140 hardened steel using response surface methodology (RSM). Sarıkaya et al. [6] researched the influence of machining parameters on surface roughness and tool life in face milling process of AISI D3 steel with carbide coated inserts using TM. Ghani et al. [7] optimized machining conditions in end milling process AISI H13 hardened steel using TM. Gopalsamy [8] used TM to find optimal process parameters on surface roughness and tool life for end milling hardened steel. Ab. Rashid et al. [9] applied artificial neural network and multiple regression method for modeling and optimizing of surface roughness. Patwari et al. [10] modelled and optimized machining parameters for surface roughness in end milling of medium

carbon steel by using RSM and genetic algorithm. Baek et al. [11] optimized machining parameters in face milling operation of AISI 1041 steel. Benardos and Vosniakos [12] predicted surface roughness in CNC face milling using neural networks and Taguchi's design of experiments. Routara et al. [13] investigated the influence of cutting parameters: spindle speed, depth of cut and feed rate on the surface roughness of aluminum, brass and AISI 1040 steel in CNC end milling using RSM. Chhabada and Ambekar [14] used grey relational analysis to multi-response optimization of machining parameters on CNC milling of EN 19 alloy steel with TiAlN coated cutter. Mansour and Abdalla [15] used RSM for modeling surface roughness in end milling of EN 32 case hardening steel. Gologlu and Sakarya [16] investigated the effects of cutter path strategies on surface roughness of pocket milling of 1.2738 steel based on TM. Gupta and Sood [17] studied the effects of machining parameters on cutting force and surface roughness in turning of AISI 4340 steel using uncoated carbide insert. Taguchi technique and the utility concept were used for the determination of the optimal performance characteristics. They found that cooling condition has a dominant effect on the performance characteristics.

In this study, the effect of machining parameters on the various surface roughness characteristics;  $R_a$ ,  $R_q$  and  $R_z$  in the milling of AISI 4140 steel with TiAlN+TiN, PVD-coated, R 390-11 T308M-PM 1030 solid carbide insert were experimentally investigated. Optimal machining parameters were determined using multi-objective Taguchi technique and a confirmation experiment was conducted to test the success of the optimization.

## 2 MATERIALS AND METHODS

Experiments were conducted in dry cutting conditions by using a SPINNER MVC1000 model CNC milling machine. The workpiece material used was AISI 4140 steel in the form of a 260 × 150 × 25 mm block. The chemical composition and mechanical properties of AISI 4140 steel

are given in Table 1. R 390-020B20-11M tool holder and a TiAlN+TiN, PVD-coated, R 390-11 T308M-PM 1030 solid carbide insert were used. The experimental set up is displayed in Fig. 1. The surface roughness characteristics;  $R_a$ ,  $R_z$  and  $R_q$  values of workpieces were measured by MITUTOYO SJ-400 transportable surface roughness tester. The cut off length and evaluation length were constant at 0.8 mm and 4 mm respectively. Surface roughness measurements were made three times on the surfaces of workpieces, and their average roughness parameters were determined. Experiments were conducted according to the Taguchi  $L_9$  orthogonal design matrix and the results were evaluated using Minitab 17 software.

**Table 1** The chemical compositions and mechanical properties of AISI 4140 workpiece material

Chemical compositions (wt.%)					
C	Si	Mn	P	S	Ti
0.378	0.223	0.688	0.015	0.007	0.007
Al	Cr	Mo	Ni	V	Co
0.018	0.970	0.199	0.032	0.010	0.009
Mechanical properties					
Tensile strength	Yield strength	Elongation (%)	Brinell Hardness	Elastic modulus	Poisson ratio
655 MPa	415 MPa	25.70	197 HB	190-210 GPa	0.27-0.30

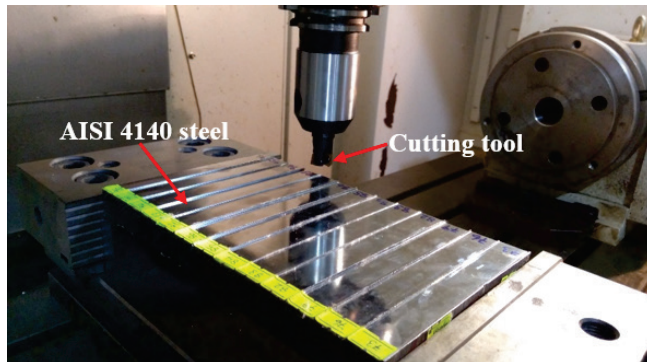


**Figure 1** Experimental set up for milling tests

### 3 EXPERIMENTAL RESULTS AND DISCUSSION

Taguchi technique has been widely used in engineering analysis. This technique exhibits a systematic way that is simple and effective in order to optimize designs for cost, performance and quality [18, 19]. Although the traditional Taguchi technique is successfully applied in the optimization of single response problems, it is not used to solve multi-response problems [20, 21].

Multi objective Taguchi method was proposed by Tong et al. [22] and Anthony [23]. This method transforms multiple responses to single response by simply adding normalized quality loss values for analyzing multiple quality characteristics together. Fig. 2 demonstrates the flow chart for the multi objective optimization.

In this study, depth of cut (mm), feed rate (mm/rev), cutting speed (m/min) and number of insert (pieces) were chosen as input parameters; the surface roughness characteristics  $R_a$  ( $\mu\text{m}$ ),  $R_q$  ( $\mu\text{m}$ ) and  $R_z$  ( $\mu\text{m}$ ) were chosen as output parameters. Specified parameters and their levels

are given in Tab. 2. Taguchi  $L_9$  orthogonal array and experimental results were given in Tab. 3.

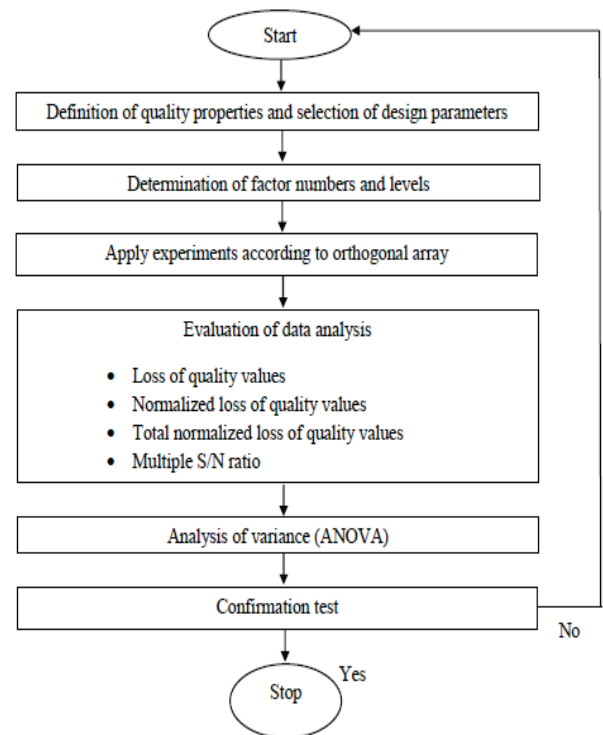


**Figure 2** Flow chart for multi-objective optimization

**Table 2** Control factors and their levels

Symbol	Factor	Unit	Level 1	Level 2	Level 3
A	doc	mm	0.5	1	1.5
B	f	mm/rev	0.08	0.12	0.16
C	V	mm/min	175	250	325
D	N	(pieces)	1	2	3

#### Evaluation of data analysis:

Multiple responses are transformed to single response using the Taguchi quality loss function. This optimization procedure is given below and explained.

#### 1. Compute the quality loss ( $L_{ij}$ )

Quality loss can be classified into three categories: “larger-is-better”, “smaller-is-better” and “normal-is-better”. In this study, the “smaller-is-better” category was selected for obtaining optimum machining parameters. Quality loss values for these responses were calculated using Eq. (1) and shown in Tab. 4.

$$L_{ij} = \frac{1}{n_i} \sum_{k=1}^{n_i} y_{ijk}^2 \quad (1)$$

where  $n_i$  is the number of experiment repetition for the  $i^{\text{th}}$  response,  $y_{ijk}$  is the observed value for the  $i^{\text{th}}$  response in the  $k^{\text{th}}$  repetition of the  $j^{\text{th}}$  experiment and  $L_{ij}$  is the loss function of the  $i^{\text{th}}$  response in the  $j^{\text{th}}$  experiment.

## 2. Establish the multi S/N ratio (MSNR):

## Step 1: Calculation of Normalized Quality Loss

$$C_{ij} = \frac{L_{ij}}{L_i^*} \quad (2)$$

$$L_i^* = \max \{L_{i1}, L_{i2}, \dots, L_{ij}\}$$

where  $C_{ij}$  is the Normalized Quality Loss,  $L_{ij}$  is the quality loss and  $L_i^*$  is the maximum quality loss among the experimental runs. Normalized quality loss values for these

responses were computed by using Eq. (2) and summarized in Tab. 5.

## Step 2: Calculation of Total Normalized Quality Loss

$$TNQL_j = \sum_{i=1}^m w_i C_{ij} \quad (3)$$

where  $TNQL_j$  is Total Normalized Quality Loss,  $w_i$  is the weight of  $i^{\text{th}}$  a normalized response ( $i = 1, 2, \dots, m$ ).  $m$  is the number of response factors.

Table 3  $L_9$  orthogonal design matrix and experimental results for  $Ra$ ,  $Rz$  and  $Rq$ 

Trial No	$doc$ (mm)	$f$ (mm/rev)	$V$ (m/min)	$N$ (pieces)	$Ra$ 1 ( $\mu\text{m}$ )	$Ra$ 2 ( $\mu\text{m}$ )	$Ra$ 3 ( $\mu\text{m}$ )	Ave. $Ra$ ( $\mu\text{m}$ )	$Rz$ 1 ( $\mu\text{m}$ )	$Rz$ 2 ( $\mu\text{m}$ )	$Rz$ 3 ( $\mu\text{m}$ )	Ave. $Rz$ ( $\mu\text{m}$ )	$Rq$ 1 ( $\mu\text{m}$ )	$Rq$ 2 ( $\mu\text{m}$ )	$Rq$ 3 ( $\mu\text{m}$ )	Ave. $Rq$ ( $\mu\text{m}$ )
1	0.5	0.08	175	1	0.19	0.16	0.20	0.183	1.35	1.39	1.36	1.367	0.24	0.24	0.26	0.247
2	0.5	0.12	250	2	0.25	0.27	0.30	0.273	1.90	1.95	1.85	1.900	0.31	0.36	0.38	0.350
3	0.5	0.16	325	3	1.20	1.22	1.21	1.210	4.90	5.00	5.10	5.000	1.34	1.38	1.36	1.360
4	1	0.08	250	3	0.46	0.52	0.50	0.493	2.32	2.47	2.41	2.400	0.54	0.60	0.61	0.583
5	1	0.12	325	1	0.13	0.16	0.14	0.143	0.90	0.82	0.88	0.867	0.16	0.18	0.20	0.180
6	1	0.16	175	2	0.48	0.53	0.47	0.493	2.70	3.00	2.90	2.867	0.61	0.60	0.65	0.620
7	1.5	0.08	325	2	0.22	0.23	0.21	0.220	1.60	1.55	1.45	1.533	0.28	0.30	0.27	0.283
8	1.5	0.12	175	3	1.03	1.08	1.06	1.057	4.40	4.35	4.25	4.333	1.15	1.25	1.13	1.177
9	1.5	0.16	250	1	0.29	0.28	0.31	0.293	1.90	1.80	2.00	1.900	0.38	0.35	0.40	0.377

Table 4 Quality loss values for  $Ra$ ,  $Rz$  and  $Rq$ 

Exp. No	Quality Loss (dB)		
	$Ra$	$Rz$	$Rq$
1	0.0339	1.8767	0.0609
2	0.0751	3.6967	0.1239
3	1.4642	25.0467	1.8499
4	0.2448	5.7867	0.3423
5	0.0217	0.7667	0.0343
6	0.2459	8.3667	0.3882
7	0.0485	2.3800	0.0804
8	1.1186	18.8067	1.3873
9	0.0869	3.6367	0.1432

$TNQL_j$  values have been determined by using Eq. 3. Then for each response, a weight ( $w_i$ ) was assigned, to indicate its importance relative to other responses. In this case each response has a different importance and weight. Weighting factors have been selected as  $w_1 = 0.333$ ,  $w_2 = 0.333$ ,  $w_3 = 0.333$  for surface roughness. Multi signal-to-noise ratio ( $MSNR$ ) was calculated by using Eq. 4.  $TNQL_j$  and  $MSNR_j$  values were given in Tab. 6.

Table 5 Normalized quality loss values for  $Ra$ ,  $Rz$  and  $Rq$ 

Exp. No	Normalized quality loss values		
	$Ra$	$Rz$	$Rq$
1	0.0232	0.0749	0.0329
2	0.0513	0.1476	0.0670
3	1.0000	1.0000	1.0000
4	0.1672	0.2310	0.1850
5	0.0148	0.0306	0.0185
6	0.1679	0.3340	0.2099
7	0.0331	0.0950	0.0435
8	0.7640	0.7509	0.7499
9	0.0593	0.1452	0.0774

## Step 3: Determine the multi S/N ratio (MSNR)

$$MSNR_j = -10 \log(TNQL_j) \quad (4)$$

Table 6  $TNQL$  and  $MSNR$  values

Exp. No	$TNQL$	$MSNR$ (dB)
1	0.0437	13.598
2	0.0886	10.524
3	1.0000	0.000
4	0.1944	7.113
5	0.0213	16.713
6	0.2373	6.248
7	0.0572	12.426
8	0.7549	1.221
9	0.0940	10.269
Average $MSNR$		8.679

Table 7 Main effects of factors on  $MSNR$ 

Factor	$MSNR$ (dB)			
	Level			Max-Min
	1	2	3	
$doc$	8.041	<b>10.024*</b>	7.972	2.052
$f$	<b>11.045*</b>	9.486	5.506	5.540
$V$	7.022	9.302	<b>9.713*</b>	2.691
$N$	<b>13.527*</b>	9.733	2.778	10.749
*Optimal level				

## 3. Determine the optimal factor/level combinations

The effect of the control factors on the  $MSNR$  was obtained from Tab. 7. For the surface roughness parameters  $Ra$ ,  $Rz$  and  $Rq$ , the  $MSNR$  graphs of the control factors are shown in Fig. 3. The best factor / level combination was identified as  $A_2B_1C_3D_1$ . The optimum levels of different control factors minimum surface roughness are A at level 2

(1 mm) and B at level 1 (0.08 mm/rev), C at level 3 (325 m/min), D at level 1 (1).

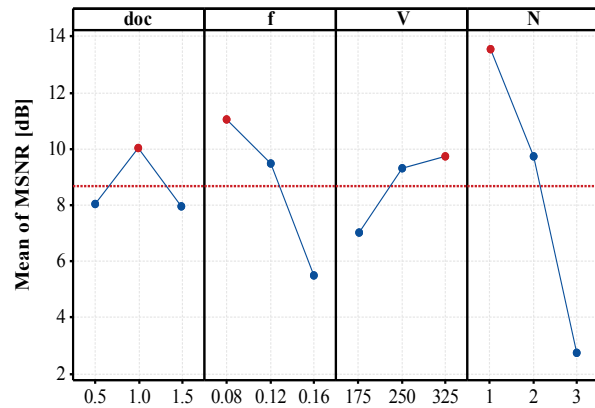


Figure 3 MSNR graph of control factors

#### 4. Variance analysis (ANOVA)

ANOVA was performed to calculate the effective factors on the surface roughness results and the contribution of these factors in the milling process (Tab. 8). From the ANOVA chart, the surface roughness parameters  $Ra$ ,  $Rz$  and  $Rq$  appear to be the most important factor in the feed rate. When the effect of the factors as a percentage is examined, it is seen that the effect of number of insert is 71.89%, the effect of the feed rate is 19.74%, the effect of the cutting speed is 5.08%, and the effect of the depth of cut is 3.29%. In conclusion, according to the ANOVA table, the most important factor to consider for surface roughness has been found to be the number of insert.

Table 8 ANOVA for MSNR

Factors	Degree of freedom (DOF)	Sum of squares (SS)	Mean square (MS)	Percent contribution (PC)
<i>doc</i>	2	8.150	4.075	3.29
<i>f</i>	2	48.964	24.482	19.74
<i>V</i>	2	12.607	6.303	5.08
<i>N</i>	2	178.300	89.150	71.89
Total	8	248.020		100

#### 5. Confirmation experiment

The final step of the optimization process is to test the condition giving the optimal values to verify that the proposed improvement has been met. Verification test results are given in Tab. 9. In this work, the optimum result for the surface roughness as a result of milling process was reached under the experimental conditions  $A_2B_1C_3D_1$  test conditions. Eq. (5) was used to calculate  $Ra$ ,  $Rz$  and  $Rq$  of surface roughness values at optimal milling conditions determined by Taguchi technique. The estimated value of the MSNR at the optimum parameter levels ( $\eta_{opt}$ ) is calculated.

$$\eta_{opt} = \eta_m + \sum_{i=1}^p (\eta_{mi} - \eta_m) \quad (5)$$

where  $\eta_{opt}$  is the predicted MSNR,  $\eta_m$  is the overall average of the MSNR,  $\eta_{mi}$  is the average MSNR at the optimum level, and  $p$  is the number of the input factors that significantly influence the quality characteristic.

Table 9 Confirmation test results

Surface roughness	Random parameters	Optimum process parameters	
		Predicted	Experimental
Level	$A_2B_1C_2D_3$	$A_2B_1C_3D_1$	$A_2B_1C_3D_1$
$Ra$ ( $\mu m$ )	0.493		0.117
$Rz$ ( $\mu m$ )	2.400		0.933
$Rq$ ( $\mu m$ )	0.583		0.143
MSNR (dB)	7.113	18.273	17.359

It is seen that an improvement of 10.246 (dB) in the MSNR when the optimal process parameter ( $A_2B_1C_3D_1$ ) is used instead of the random parameter ( $A_2B_1C_2D_3$ ). The results obtained from the confirmation experiments reflect the success of the multi-response optimization.

#### 4 CONCLUSIONS

This study presented multi objective Taguchi technique to optimize performance parameters of AISI 4140 steel. The multiple quality characteristics were considered simultaneously using Taguchi quality loss function. The findings of the investigation are summarized as follows:

- The optimal levels of the machining parameters for minimum surface roughness for  $Ra$ ,  $Rz$  and  $Rq$  values were obtained to be 325 m/min cutting speed, 0.08 mm/rev feed rate, 1 mm depth of cut and 1 number of insert.
- $Ra$ ,  $Rz$  and  $Rq$  have been decreased down to 0.117  $\mu m$ , 0.933  $\mu m$  and 0.143  $\mu m$ , respectively against the random values of  $Ra$ ,  $Rz$  and  $Rq$  of 0.479  $\mu m$ , 2.400  $\mu m$  and 0.583  $\mu m$ , respectively.
- The percent contribution of the control factors on the multiple quality characteristics was obtained to be number of insert (71.89%), feed rate (19.74%), cutting speed (5.08%), and depth of cut (3.29%) with ANOVA. The results show that the number of insert was found to be the significant factor among process parameters. The confirmation test conducted to determine optimal combination of machining parameters of AISI 4140 steel.
- Confirmation test results show that the increase of the MSNR ratio from the random input parameters to the optimal performance parameter was obtained to be 10.246 dB. These results show that the multi response optimization technique by using a Taguchi quality loss function can significantly improve the quality performance characteristics of the milling process.

#### 5 REFERENCES

- Groover, M. P. (2010) *Principles of modern manufacturing 4<sup>th</sup> edition*, John Wiley & Sons.
- Kalpakjian, S. (1995) *Manufacturing Engineering and Technology 3<sup>rd</sup> edition*. Reading: Addison-Wesley.

- [3] El-Hofy, H. A. G. (2005) *Advanced Machining Processes: Nontraditional and Hybrid Machining Processes 1st edition*, McGraw-Hill.
- [4] Kivak, T. (2014). Optimization of surface roughness and flank wear using the Taguchi method in milling of Hadfield steel with PVD and CVD coated inserts. *Measurement*, 50, 19-28. <https://doi.org/10.1016/j.measurement.2013.12.017>
- [5] Stipkovic Filho, M., Stipkovic, M. A., Bordinassi, É. C., Delijaicov, S., & de Almeida, S. L. R. (2018). Experimental Numerical Model of Roughness in Finishing Face Milling of AISI 4140 Hardened Steel. In *Improved Performance of Materials* (pp. 83-91). Springer, Cham. [https://doi.org/10.1007/978-3-319-59590-0\\_8](https://doi.org/10.1007/978-3-319-59590-0_8)
- [6] Sankaya, M., Yilmaz, V., & Dilipak, H. (2016). Modeling and multi-response optimization of milling characteristics based on Taguchi and gray relational analysis. *Proceedings of the Institution of Mechanical Engineers, Part B: Journal of Engineering Manufacture*, 230(6), 1049-1065. <https://doi.org/10.1177/0954405414565136>
- [7] Ghani, J. A., Choudhury, I. A., & Masjuki, H. H. (2004). Performance of P10 TiN coated carbide tools when end milling AISI H13 tool steel at high cutting speed. *Journal of Materials Processing Technology*, 153, 1062-1066. <https://doi.org/10.1016/j.jmatprotec.2004.04.353>
- [8] Gopalsamy, B. M., Mondal, B., & Ghosh, S. (2009). Taguchi method and ANOVA: An approach for process parameters optimization of hard machining while machining hardened steel. *Journal of Scientific and Industrial Research*, 68, 686-695.
- [9] Ab. Rashid, M. F. F., Gan, S. Y., & Muhammad, N. Y. (2009). Mathematical modeling to predict surface roughness in CNC milling. *World Academy of Science, Engineering and Technology*, 53, 393-396.
- [10] Patwari, M. A. U., Amin, A. K. M. N., & Arif, M. D. (2011). Optimization of surface roughness in end milling of medium carbon steel by coupled statistical approach with genetic algorithm. *Special Issue of the International Journal of the Computer, the Internet and Management*, 19.
- [11] Baek, D. K., Ko, T. J., & Kim, H. S. (2001). Optimization of feedrate in a face milling operation using a surface roughness model. *International Journal of Machine Tools and Manufacture*, 41(3), 451-462. [https://doi.org/10.1016/S0890-6955\(00\)00039-0](https://doi.org/10.1016/S0890-6955(00)00039-0)
- [12] Benardos, P. G. & Vosniakos, G. C. (2002). Prediction of surface roughness in CNC face milling using neural networks and Taguchi's design of experiments. *Robotics and Computer-Integrated Manufacturing*, 18(5-6), 343-354. [https://doi.org/10.1016/S0736-5845\(02\)00005-4](https://doi.org/10.1016/S0736-5845(02)00005-4)
- [13] Routara, B. C., Bandyopadhyay, A., & Sahoo, P. (2009). Roughness modeling and optimization in CNC end milling using response surface method: effect of workpiece material variation. *The International Journal of Advanced Manufacturing Technology*, 40(11-12), 1166-1180. <https://doi.org/10.1007/s00170-008-1440-6>
- [14] Chhabada, M. V. & Ambekar, S. D. (2016). Multi-response optimization of machining parameters on CNC milling of EN 19 Alloy Steel with TiAlN coated milling cutter using GRA. *International Journal for Scientific Research & Development*, 4(5), 98-103.
- [15] Mansour, A. & Abdalla, H. (2002). Surface roughness model for end milling: a semi-free cutting carbon casehardening steel (EN32) in dry condition. *Journal of Materials Processing Technology*, 124(1-2), 183-191. [https://doi.org/10.1016/S0924-0136\(02\)00135-8](https://doi.org/10.1016/S0924-0136(02)00135-8)
- [16] Gologlu, C. & Sakarya, N. (2008). The effects of cutter path strategies on surface roughness of pocket milling of 1.2738 steel based on Taguchi method. *Journal of materials processing technology*, 206(1-3), 7-15. <https://doi.org/10.1016/j.jmatprotec.2007.11.300>
- [17] Gupta, M. K. & Sood, P. K. (2016). Optimizing multi characteristics in machining of AISI 4340 steel using Taguchi's approach and utility concept. *Journal of The Institution of Engineers (India): Series C*, 97(1), 63-69. <https://doi.org/10.1007/s40032-015-0201-1>
- [18] Ross, P. J. (1988) *Taguchi Techniques for Quality Engineering*, McGraw Hill, New York.
- [19] Phadke, M. S. (1989) *Quality Engineering Using Robust Design*, Prentice-Hall, Englewood Cliffs, NJ.
- [20] Terzi, U. & Baynal, K. (2005). Concurrent optimization of multi response quality characteristics based on Taguchi method, *35<sup>th</sup> International Conference on Computers and Industrial Engineering*, 2, 1929-1934.
- [21] Mohamed, M. A., Manurung, Y. H., & Berhan, M. N. (2015). Model development for mechanical properties and weld quality class of friction stir welding using multi-objective Taguchi method and response surface methodology. *Journal of Mechanical Science and Technology*, 29(6), 2323-2331. <https://doi.org/10.1007/s12206-015-0527-x>
- [22] Tong, L. I., Su, C. T., & Wang, C. H. (1997). The optimization of multi-response problems in the Taguchi method. *International Journal of Quality & Reliability Management*, 14(4), 367-380. <https://doi.org/10.1108/02656719710170639>
- [23] Antony, J. (2001). Simultaneous optimisation of multiple quality characteristics in manufacturing processes using Taguchi's quality loss function. *The International Journal of Advanced Manufacturing Technology*, 17(2), 134-138. <https://doi.org/10.1007/s001700170201>

#### Authors' contacts:

**Yusuf FEDAI**, Assist. Prof. Dr.  
Osmaniye Korkut Ata University  
Department of Manufacturing Engineering,  
80000, Osmaniye, Turkey  
E-mail: yusuffedai@osmaniye.edu.tr

**Funda KAHRAMAN**, Assoc. Prof. Dr.  
Mersin University  
Department of Mechatronics Engineering,  
80000, Mersin, Turkey  
E-mail: fkahraman@mersin.edu.tr

**Hediye KIRLI AKIN**, Assist. Prof. Dr.  
Osmaniye Korkut Ata University  
Department of Manufacturing Engineering,  
80000, Osmaniye, Turkey  
E-mail: hediyeakin@osmaniye.edu.tr

**Gokhan BASAR**, Res. Assist.  
Osmaniye Korkut Ata University  
Department of Manufacturing Engineering,  
80000, Osmaniye, Turkey  
E-mail: gokhanbasar@osmaniye.edu.tr

# A PRELIMINARY STUDY FOR EARLY BREAST CANCER DETECTION WITH MICROWAVES

Emine AVŞAR AYDIN

**Abstract:** Breast cancer is the most common type of cancer in female all over the world. Early detection and treatment gives a chance to overcome this cancer. In breast cancer detection, there are many methods such as X-ray mammography, Magnetic Resonance Imaging, and Ultrasound Imaging. However, existing these methods have limitations such as X-rays, disturbing pressure on the breast, and high cost of devices, etc. Because of all the reasons mentioned, microwave breast imaging has the potential to overcome from some of the limitations of conventional breast cancer screening systems. The physical basis breast cancer detection by microwaves depends on the difference between the dielectric properties of normal and malignant breast tissue. Microwave breast cancer imaging is also a noninvasive method and it has low cost. Therefore, microwave imaging technology for breast cancer detection has attracted much attention by many researchers in these days. By using Computer Simulation Technology Microwave Studio and Antenna Magus Software, breast model with tumor and antennas were generated in this study. The presence of the tumor was investigated using a receiver and a transmitting antenna. While the transmitting antenna was stationary, the receiving antenna was moved to different positions. S11 (return loss) results were evaluated. This study is a preliminary study to determine the location and characteristic features of the tumor. Furthermore, this study will show that scanning methods will determine the location and size of the tumor at higher accuracy and the reconstruction of the reflected waves will allow to clearly determining the location of the tumor.

**Keywords:** antenna design; breast cancer; computer simulation technology (CST); dielectric properties; microwaves

## 1 INTRODUCTION

The breast cancer, which is especially common among women, occurs on the breast tissue covering the wide area between collarbone and armpit and extending on the chest muscles including the chest. Breast cancer emerges from occurrences of mutations and abnormal changes on genes that control the growth and regeneration of cells. Healthy cell, which has the ability of knowing the way and time of division, multiplies uncontrollably by losing this ability due to gene problems and generates cancerous tissues. Unhealthy tissue formation usually occurs at the tip of the breast lobules or milk channels [1].

A study in 2009 has shown that deaths in Turkey are mostly due to cardiovascular disorders and cancer and also women with cancer have the most breast cancer [2, 3]. Again according to the same research, deaths caused by cancer are expected to rise to the first place from 2015. Early diagnosis is important for reduction of cancer-related deaths and treatment. While early stage diagnosis is to help of the cancer treatment, delay of diagnosis reduces chances of treatment [4].

Widespread and primary method used for the screening of breast cancer is X-ray mammography which uses low power X-rays. The breast is compressed for better imaging and exposed to ionizing X-rays even if low-power in X-ray mammography. This method is painful due to compression and there is a possibility of damaging the tissue because it uses ionizing X-rays. [5].

Magnetic resonance imaging (MRI) is an alternative method to X-ray mammography in breast cancer imaging. MRI overcomes the disadvantages of X-ray mammography and can produce successful results about the presence of the tumor in the tissue. But it cannot demonstrate the same success in terms of whether the tumor is good or bad. [5].

Another method used in breast cancer detection is Ultrasound imaging (USI) in which transient waves are used. In USI, imaging is done by collecting back-reflections from the sound waves sent into the tissue. USI consists of disadvantages due to the pressure application with measuring probe and the necessity of using coupling gel to increase the amount of wave penetrating into the tissue by preventing the reflection of sound waves.

Microwave imaging is seen as an alternative method to the above mentioned X-mammography, MRI and USG methods [6-9]. The advantage of microwave imaging is that it allows imaging without the need for any compression or pressure application at lower frequencies than X-rays. With increasing momentum in recent years, microwave imaging located at the center of interest of researchers is still in the research and development phase and prototypes have begun to be created by various research groups [10, 11].

In the literature, there are some theoretical and simulation studies. Li et al. [12] presented co-focal microwave imaging algorithm. In the presented study [12], malignant tumor with a diameter of 2mm at the bottom of 3.1 cm deep is placed to developed two-dimensional, anatomically realistic, MRI-derived FDTD (finite difference time Domain, finite differences in time domain) model and developed image creation algorithm is applied. As a result of the application, the tumor is found to be 6 mm in diameter and 3.3 cm deep.

The method presented by Xie et al. [13] as multistatic adaptive microwave imaging (MAMI) demonstrates high resolution and low side lobe performance. The characteristics of the method in presented study are shown on a three dimensional breast model simulated by the FDTD method.

Another study in the literature is by Zhou [14]. In microwave imaging studies based on broadband profiles, electric field data scattered from multiple objects in a target



are collected and a filtered imaging algorithm is applied to these data. Simulation results confirm with measurement results [14].

In this article, the presence of the tumor was investigated using a receiver and a transmitting antenna. While the transmitting antenna was stationary, the receiving antenna was moved to different positions. This study is a preliminary study to determine the location and characteristic features of the tumor.

## 2 MATERIAL AND METHOD

The physical basis for microwave imaging lies in the significant contrast in the dielectric properties between the normal breast tissue and the malignant tissue at microwave frequencies [15]. Microwave imaging (MWI) techniques consist of tomography based and radar based imaging. Communication of through breast is saved by microwave tomography. At the same time, an electrical property map of the region of interest is created using radar-based imaging [16, 17]. By transmitting electromagnetic waves through the female breast, the scattered field is obtained on the breast in MWI method. While the transmitting antennas are fed by the electromagnetic signals, the receiving antennas collect the electromagnetic signals and define by scattering parameters "S-parameters".

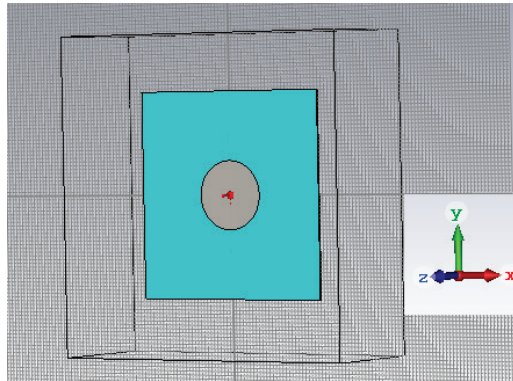


Figure 1 Antenna structure in Antenna Magus Software

Table 1 Features of used antenna

Parameter	Values
Dielectric substrate	2.0
Antenna length	54.2428 mm
Antenna width	54.2428 mm
Antenna height	1 mm
Diameter of patch antenna	18.08095 mm
Feed-pin radius	0.25 mm
Coaxial diameter	1.15128 mm

### 2.1 Antenna Model

A circular pin-fed linearly polarized microstrip patch antenna was preferred in this paper. This antenna was put into Computer Simulation Technology (CST) platform from Antenna Magus Software, a tool for modeling and designing antennas (Fig. 1). The reason for choosing this antenna in this study is its low cost, low profile, lightweight, and high efficiency [17]. Features of the antenna are shown

in Tab. 1. On the other hand, microstrip patch antenna with breast model was designed in CST and simulation was performed in CST Design Studio.

### 2.2 Breast Model

As shown in Fig. 2, the breast has hemispherical model and the dimensions of the breast tissues and tumor are shown in Tab. 2. The dielectric properties of each tissue are shown in Tab. 2 [11]. One of the dielectric properties is the conductivity ( $\sigma$ ), other is the relative permittivity ( $\epsilon_r$ ).

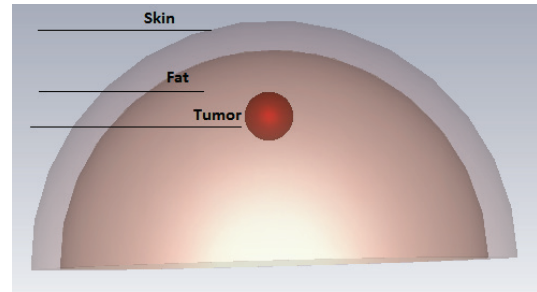


Figure 2 Breast structure in CST Microwave Studio

Table 2 Features of breast structure

Tissue Portion	Size
Breast Diameter	100 mm
Skin Thickness	2 mm
Tumor Radius	5 mm

Table 3 Dielectric properties of breast tissues and tumor

Tissue Portion	Conductivity (S/m)	Relative Permittivity
Skin	1.49	37.9
Fat	0.14	5.14
Tumor	1.4	50

## 3 RESULTS

In this article, the presence of the tumor was investigated using a receiver and a transmitting antenna. As shown in Figure 3 that while the transmitting antenna was stationary, the receiving antenna was moved to different positions.

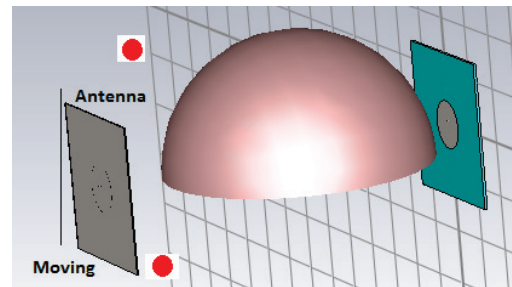


Figure 3 Data collection process using the receiving circular patch antenna moving vertically along two red dots antenna as the transmitting antenna is stationary

As shown in Fig. 3, the receiver antenna was moved up from the bottom of the breast structure to generate scatter signals. S11 (return loss) results were obtained at each antenna position from the bottom of breast structure to top. Graphics (a, b, c, d, e, and f) in Fig. 4 represent different positions of receiving antenna. When the antenna is in the same position as



the tumor or different position, the results vary. For instance; b graphic shows that the antenna is in the same position as the tumor and also is different from others. On the other hand, Fig. 5 shows two signals at the same position from two simulation models (one of them is with tumor, other is without tumor). It is clear that two signals' magnitude can be recognized.

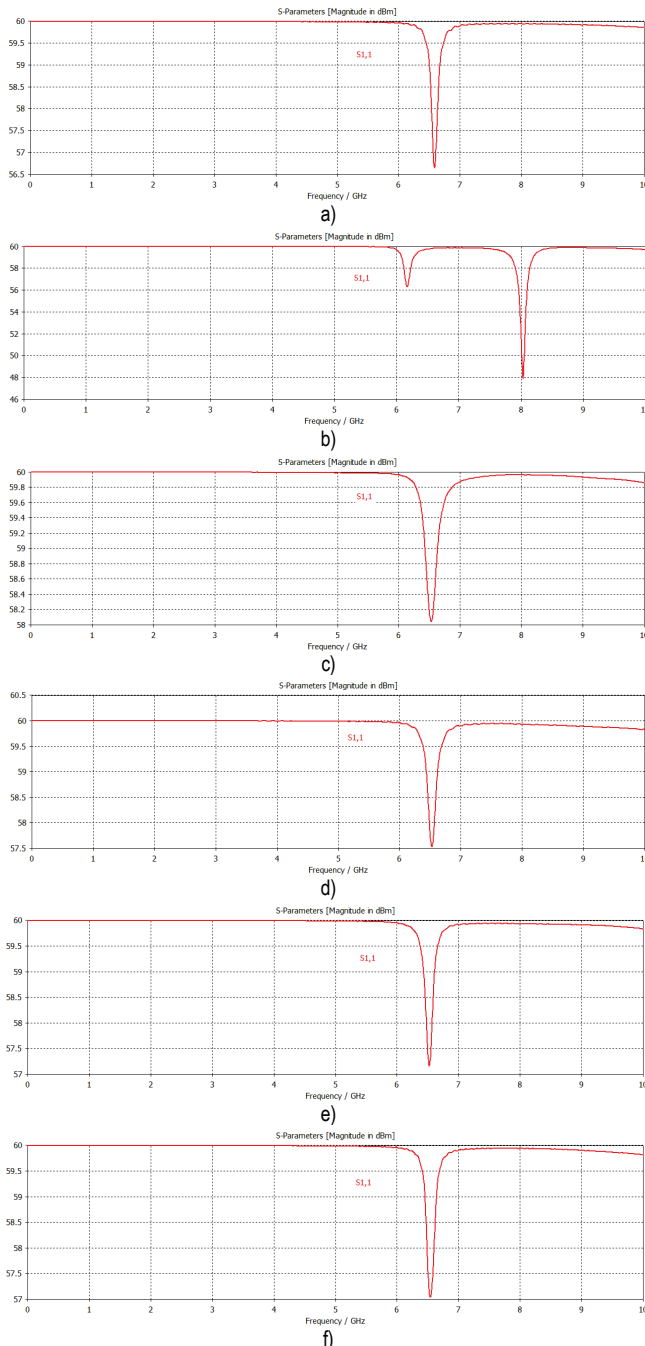


Figure 4 The S11 results (return loss) in frequency domain for each different position

In a study, the S11 simulations with and without tumors were compared at some antenna positions [18]. The positions where the antenna is on the axis of a tumor, S11 of the two simulations with tumor and without tumor were differentiated, in the same sub-band of 6 to 8 GHz, (Fig. 6).

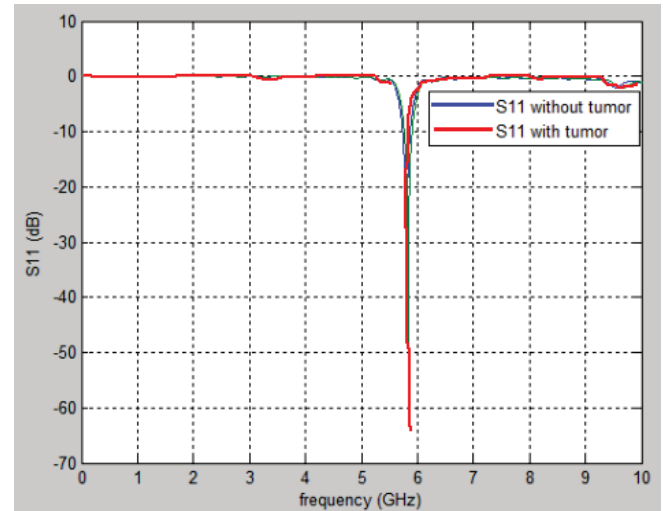


Figure 5 The magnitude of two signals (with tumor and without tumor)

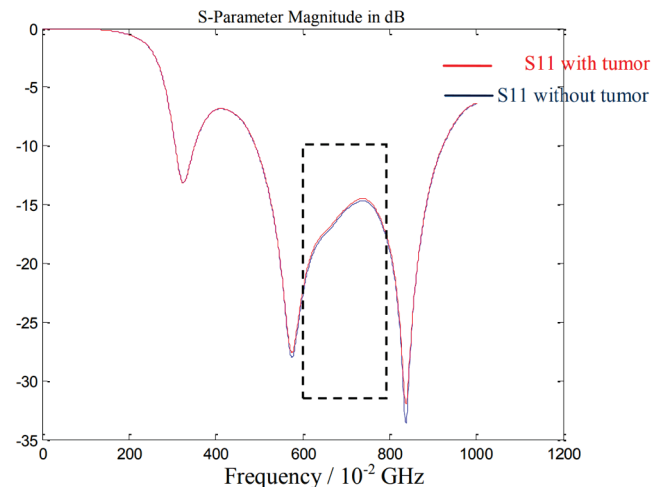


Figure 6 Comparison of two S11 (with and without tumors) the antenna is placed away from the axis the tumor [18]

#### 4 CONCLUSION

In this study, a microwave imaging system was preferred to detect breast cancer. CST software was used to create a life-like breast phantoms and a circular pin-fed linearly polarized microstrip patch antenna which generates a microwave signal. The receiver antenna was moved up from the bottom of the breast structure to generate scatter signals. This movement repeated for breast model with tumor and without tumor. The difference between tumor and without tumor showed that microwave imaging system is successful for breast cancer detection. In future work, a viable 3D image reconstruction process will be applied and will be repeated experimentally at the same time. This study will show that scanning methods will determine the location and size of the tumor at higher accuracy and the reconstruction of the reflected waves will allow to clearly determining the location of the tumor.

#### 5 REFERENCES

- [1] Meme Kanseri, Wikipedia, [http://tr.wikipedia.org/wiki/Meme\\_kanseri](http://tr.wikipedia.org/wiki/Meme_kanseri), Feb. 2014.

- [2] Kanser Kayıtcılığı, Türkiye Halk Sağlığı Kurumu Kanseri Daire Başkanlığı, <http://www.kanser.gov.tr/daire-faaliyetleri/kanser-kayitciligi/108-t%C3%BCrkiye-kanser-kayitciigi.html#sthash.rW1OWNI4.dpuf>, Dec. 2013.
- [3] Gültekin, M. (2013). *Kanser Dairesi Faaliyetleri*.
- [4] Kanser Türleri: Meme Kanseri, Türkiye Halk Sağlığı Kurumu Kanseri Daire Başkanlığı, <http://www.kanser.gov.tr/kanser/kanser-turleri/49-memekanseri.html#sthash.RFWV7MIA.dpuf> (2013).
- [5] Hassan, A. M. & El-Shenawee, M. (2011). Review of electromagnetic techniques for breast cancer detection. *IEEE Reviews in Biomedical Engineering*, 4, 103-118. <https://doi.org/10.1109/RBME.2011.2169780>
- [6] Xu, M., Thulasiraman, P., & Noghanian, S., (2011). Microwave Tomography for Breast Cancer Detection on Cell Broadband Engine Processors. *J. Parallel Distrib. Comput.*, 72, 1106-1116. <https://doi.org/10.1016/j.jpdc.2011.10.013>
- [7] Santorelli, A. & Popovic, M. (2011). SAR Distribution in Microwave Breast Screening: Results with TWTLTLA Wideband Antenna. *Intelligent Sensors, Sensor Networks and Information Processing (ISSNIP)* / Adelaide, 11-16. <https://doi.org/10.1109/ISSNIP.2011.6146531>
- [8] Lazaro, A., Girbau, D., & Villarino, R. (2010). Simulated and Experimental Wavelet-based Detection of Breast Tumor using a UWB Radar. *40<sup>th</sup> European Microwave Conference* / Paris, 373-376.
- [9] Zhang, D. & Mase, A. (2011). Ultrashort-Pulse Radar System for Breast Cancer Detection Experiment: Imaging in Frequency Band. *Microwave Conference Proceedings (CJMW)* / Hangzhou, 1-3.
- [10] Meaney, P. M., Fanning, M. W., Li, D., Poplack, S. P., & Paulsen K. D. (2000). A Clinical Prototype for Active Microwave Imaging of the Breast. *IEEE Transactions on Microwave Theory and Techniques*, 48(11), 1841-1853. <https://doi.org/10.1109/22.883861>
- [11] Klemm, M., Craddock, I. J., Leendertz, J. A., Preece, A., Gibbins, D. R., Shere, M., & Benjamin, R. (2010). Clinical Trials of a UWB Imaging Radar for Breast Cancer. *Antennas and Propagation (EuCAP), 2010 Proceedings of the Fourth European Conference on*.
- [12] Li, X. & Hagness S. C. (2001). A Confocal Microwave Imaging Algorithm for Breast Cancer Detection. *IEEE Microwave and Wireless Components Letters*, 11(3), 130-132. <https://doi.org/10.1109/7260.915627>
- [13] Xie, Y., Guo, B., Xu, L., Li, J., & Stoica, P. (2006). Multistatic Adaptive Microwave Imaging for Early Breast Cancer Detection. *IEEE Transactions on Biomedical Engineering*, 53(8), 1647-1657. <https://doi.org/10.1109/TBME.2006.878058>
- [14] Zhou, Y. (2010). Microwave Imaging based on Wideband Range Profiles. *Progress in Electromagnetics Research Letters*, 19, 57-65. <https://doi.org/10.2528/PIERL10100608>
- [15] Xie, Y., Guo, B., Xu, L., Li, J., & Stoica, P. (2006). Multistatic adaptive microwave imaging for early breast cancer detection. *IEEE Trans. Biomed. Eng.*, 53(8), 1647-1657. <https://doi.org/10.1109/TBME.2006.878058>
- [16] Bahramiabarghouei, H., Porter, E., Santorelli, A., Gosselin, B., Popovi, M., & Rusch, L. A. (2015). Flexible 16 antenna array for microwave breast cancer detection. *IEEE Trans. Biomed. Eng.*, 62(10), 2516-2525. <https://doi.org/10.1109/TBME.2015.2434956>
- [17] Eltigani, F. M., Yahya, M. A. A., & Osman, M. E. (2017). Microwave Imaging System for Early Detection of Breast Cancer. *2017 International Conference on Communication, Control, Computing and Electronics Engineering (ICCCCEE)* / Khartoum, Sudan. <https://doi.org/10.1109/ICCCCEE.2017.7866083>
- [18] Chouiti, S. M., Merad, L., & Meriah, S. M. A Microwave Imaging Technique Implementation for Early Detection of Breast Tumors. *Advances in Circuits, Systems, Signal Processing and Telecommunications*, pp. 233-236.

**Author's contact:****Emine AVŞAR AYDIN**

Adana Science and Technology University,  
Department of Aeronautical Engineering  
Adana Bilim ve Teknoloji Üniversitesi,  
Gültepe Mh., Sarıçam/Adana, Turkey  
eaydin@adanabtu.edu.tr  
rasvaenime@gmail.com

# SUCCESS MEASUREMENT OF BUSINESS PROCESSES

Ivica KANIŠKI, Ivan VINCEK

**Abstract:** A business process is an activity or set of activities that accomplish a specific goal of an organization. In almost every organization there are three important pillars that keep the whole organization together - people, processes and technology. All three are linked and if one of them does not work well, others can easily collapse. Success Measurement is a complex activity that includes at least four disciplines: economics, IT, management and accounting, implying the process of quantifying the effectiveness and effectiveness of an action. Success Measurement is a dynamic system that supports the decision-making process by collecting and analyzing information.

**Keywords:** analysis of business processes; business processes; measuring success; program tools

## 1 INTRODUCTION

The effectiveness and overall business results of any business organization largely depend directly on the way in which business processes are managed, i.e. the business relations and all business activities necessary for the realization of the set organizational goals.

Market environment and heavy competition in business direct many organizations in terms of the necessity of the existence of business marketing in the market of business consumption and it being conditioned by quality management of business processes.

It is necessary to implement radical and significant changes in a company's business conduct that will result with lower expenses and shorter production cycle, accompanied by the quality of goods or services. Those changes are directed at the reforming, restructuring and innovation of business processes by the use and support of IT.

## 2 BUSINESS PROCESSES

Business processes can be described as a sequence of logically connected activities that use resources of a company and that have an end goal of satisfying the customers' needs for goods or services of a certain quality and price, in an adequate time frame and simultaneous realization of certain values. [1]

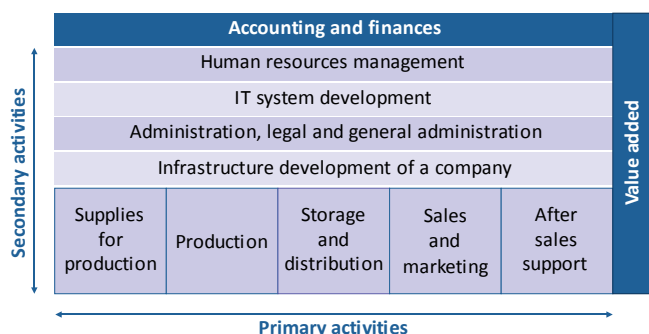


Figure 1 Porter's chain of values

We can measure the efficiency of a process carried out in time and the expenses required to turn the input values of a process into an output result.

Processes are elements of each company, but they are rarely described or analyzed. In organizations that are not production oriented, processes are not clearly defined and it is difficult to describe them precisely.

### 2.1 Analysis of Business Processes

The business process analysis is especially useful for attaining goals related to consumers, and for efficiency and profitability. Moreover, the whole business process analysis can be helpful in checking whether control systems are in place to lower the risks, i.e. risk exposure.

The business process analysis is primarily performed in order to determine:

- activities that do not add value,
- redundant activities or tasks (repeated in different parts of organization or repeated because of errors)
- sequential activities and tasks that can be conducted at the same time, i.e. that can overlap,
- activities performed only based on experience (which can be very dangerous because the business practice is not documented),
- imbalance between directional processes and enabling processes
- inadequate use of technology,
- insufficient training, education and staff knowledge/experience,
- modes of giving feedback,
- liaisons between missing processes,
- unnecessary reports,
- inadequate rules and procedures. [2]

The business process analysis often uses: the comparison of documentation procedures, business process mapping, whole process observation, root cause analysis, critical path analysis, matrix analysis, correlation matrix, Pareto analysis, force-field analysis, process restriction

analysis, cultural factor analysis, analysis of added value, scenario analysis, etc. [2]

Regardless of the choice of its conduct, the analysis of a specific business process mainly begins with the analysis of current activities. It needs to be stressed that it is more difficult to carry out the analysis of an existing process than to create a new process, because the existing process does not necessarily need to be logical or make sense, while the proposed business process is generally logical.

The analysis of an existing process attempts to determine its quality, its bottleneck, weak areas and areas critical for improvement. Quality analysis includes the consideration of all activities within a given process and the identification of the modes of measuring all other processes that contribute to the success of a certain process. [2]

## 2.2 Business Performance Perception Framework

The defined matrix, the framework of how we perceive a company's success, can be seen on three levels and from three different perspectives: goals and success measurement, design and its implementation and the management's practice. With the help of a matrix, nine different elements were identified that need to be taken into consideration when improving business processes.

Besides the process level, both the organizational and individual level need to be emphasized and attention must be paid to the fact that the approach focused exclusively on the process level or the perspective of measuring the success and business processes management is not whole. Performance indicators of all three levels need to be taken into account as a whole.

**Table 1** Framework for the business performance perception

	Objectives and performance measurement	Design and usage	Management practice
Organizational level	Organizational objectives and the measuring of organizational success	Organizational design and its use	Managing an organization
Processual level	Process objectives and the measuring of the success of a process	Process design and its application	Process management
Individual level	Individual objectives and the measuring of individual success	Design of activities and its application	Managing activities

## 2.3 Business Controlling

Often, in times of economic crisis, a need appears for making an extra effort to solve certain difficulties in a company's business caused by external or internal factors. It is because of such character of the art of controlling that its main function is aimed at achieving the highest possible business efficiency. [6]

Because of market globalization, throughout the last few decades, there was a significant turn in the way companies conduct their business. Consumers' needs are getting more and more demanding regarding the price, but also quality.

Markets saturated with unlimited amounts of goods and services offered come as a turning point in the way of managing and designing business strategies for companies.

One of the most significant problems of contemporary companies' expansion and development is a decrease in the transparency of the business conduct as a whole and less coherence of individual organizational units. It is more and more difficult to manage companies that have grown in such a way.

Controlling is a function of leadership without which it is difficult to imagine a contemporary company. It solves the ever increasing problems of coordination and integration.

One of the reasons for the occurrence of controlling could be the separation of the ownership function from the function of management, which leads to difficulties in communication and leadership. One of the reasons why controlling appeared as such could be the emergence of the need for a faster business decision-making. It is this multidisciplinary feature of controlling that implies the need for a more precise definition of it. The primary role of controlling is the merging of different parts of a company into a whole unit with the goal of creating a comprehensive perspective of its overall business conduct. It links partial organizational functions into a single unit to maximize the effectiveness and efficiency of a company.

The outset for the execution of controlling is based on the company's accounting, spreading out onto all other organizational elements with the goal of creating a compact unit.

Although the concept of controlling changed over time, it can be said that controlling came into existence based on the accounting concept. [2]

## 2.4 Role of Controlling in a Company

Although controlling relates to business operations of a company as a whole, a large portion of it consists of a plan and analysis. Due to controlling, management should be informed of everything that takes place with the goal of better quality decision-making. In large companies, situations often occur where each department works independently and partially also independently sets certain goals, which can lead to incoherently set goals. The role of controlling in such a company is connecting those departments in order to create unique goals and plans. [2]

One of the most important goals of controlling is planning business operations. Planning helps to anticipate certain outcomes in business operations which helps decrease possible risks to the lowest level possible. Planning operations significantly increases the chances of attaining goals. Although there are different levels of planning, the ones that stand out as the most significant ones would be: strategic, tactics and operational planning.

By means of planning, different organizational units meet through partial operational plans of the whole company. The main task of controlling is to align partial plans by taking into account all important information gathered within and outside the company. In order to successfully align partial plans, controlling has to find the causes of mutual misalignment. Besides the mentioned, controlling also has the role to check the reality of proposed plans.

Nowadays, a good quality informational system represents a base for the quality functioning of controlling. Considering the fact that controlling has the role to pick the most crucial information for decision-making, a good quality informational system can represent an insurmountable link in quality decision-making and reporting. One can say that accounting is the center of informational systems within a company. The goal of controlling is to pick the accounting information that are crucial for quality decision-making.

The role of controlling in a company can be the formulating of new or the restructuring of the already existing organizational structure for an easier and more complete flow of important data and information to the staff in charge with it. The organization of a company has to be set up in a way that facilitates the realization of specified value systems to the maximum.

### 3 MEASURING THE SUCCESS OF BUSINESS OPERATIONS

The fundamental goal of a company's existence and business operations is business success. An important factor that is related to business success and that needs to be pointed out is the idea of measuring the performance and the success of business operations. To measure the success of business operations means to have a clearly defined scale of values and a tool that will be used to measure success.

Efficacy is stated as a principle and an aggregate index of the correlations between the output and input. When mentioned in the context of companies, efficacy stands for the success of a company related to its use of the resources available, regardless of how resources have been allocated.

Efficiency, performance or productivity stands for achieving the basic goals of a company. The idea of efficiency as a measure includes the evaluation of whether the company manages to unify its many goals and to what extent. It is related to the idea of strategic company management. [3]

#### 3.1 Financial Indicator Analysis

In the business operations' analysis, there are many methods, techniques and the variant quality of information that are at the disposal of various interest groups. For that reason, it can be concluded that financial analysis is all but unified. It is a fact that the object of interest for financial analysis is the company itself, therefore it is important to discern whether the analysis is carried out externally or internally, which will depend on who is in charge with it and in whose interest it is for the analysis to be done. It

could be owners, investors, creditors or all other interest groups.

**Table 2** Illustration of the earning power indicator formation

Indicator	Numerator	Denominator
Return on sale (ROS)	Income (net or gross)	Revenue (turnover)
Return on investment (ROI, ROA)	Income (net or gross)	Total funds
Return on equity (ROE)	Net income	Own equity

When talking about external analysis, carried out by the financial analysts performing the role of the future or current owners or investors of a company, it is most often carried out exactly by the financial indicators, that have their base calculation in the externally (publicly) available data, which is, of course, limited. On the contrary, internal analysis is conducted by the company's manager, who has all the existing data at his disposal.

The use of financial indicators can be systematically divided into:

- comparison of the company's performance throughout a particular period of time,
- comparison of various companies,
- comparison of different industries. [3]

The indicators that are calculated by using the data of financial reports can be divided into a few categories, normally into the following groups:

- earning power indicators,
- activity indicators,
- liquidity indicators,
- indicators of financing and company indebtedness.

##### 3.1.1 Earning Power Ratio

The indicators of the earning power of a company have always been and still are an important objective of the business operations' success analysis as part of the financial report analysis.

Taking this into consideration, it can be concluded that only the companies that have a big earning power can win new business domains and markets, create new work posts, and at the same time assure their owners that the rate of return will be at least at the level of a certain risk (in the form of dividends, bonus rate pay or in the form of the stocks or share value increase).

However, earning power is one of those company features that is very difficult to specify and measure.

The return on sale, return on investment and return on equity are the indicators we get by using the financial report data. They are the indicators of the company's income, deficit and balance. [3]

##### 3.1.2 Activity Ratio

Activity ratio measures how successful a company was in managing the assets it has. The ratios from this group are also called turnover ratios and they can be calculated as a relation between the revenue and any kind of funds. To do

that, turnover data from the revenue report is used, as well as the funds' status reported in the balance sheet or the averages of certain forms of assets.

The most calculated ones are the turnover ratio of the funds invested, turnover ratio of the long-term assets, current assets or the turnover ratio of one of the entries of short-term assets i.e. claims, inventory or cash.

$$\text{Asset turnover ratio} = \frac{\text{total revenue}}{\text{total assets}}$$

$$\text{Inventory turnover ratio} = \frac{\text{total revenue}}{\text{inventory}}$$

$$\text{Receivable turnover ratio} = \frac{\text{total revenue}}{\text{receivables}}$$

Ratios of the duration of the receivable turnover ratio, inventory turnover ratio, asset turnover ratio and the duration of the accounts payable are very important because they indicate the speed at which cash flow takes place in a company. It is both the liquidity and the profitability of company business operations that depend on the average speed of cash flow. The cash flow cycle deals with all the components of a company, but it is especially focused on four entries in the balance and those are: cash, cash equivalents, inventory, receivables and the accounts payable. Money and money equivalents are linked to forms such as inventory and receivables and that is why, from the cash flow perspective, it is important for those entries to be as small as possible, i.e. for the time of their link to be as short as possible. [3]

### 3.1.3 Liquidity Ratio

Liquidity stands for the ability of a certain kind of asset to turn into money. Another meaning of the term is the ability of a company to settle all the received short-term liabilities.

Liquidity ratios are a part of the so-called ratios of the horizontal financial structure because they put into relation certain parts (short-term assets) with other parts (short-term liabilities) and with the goal of defining the company's ability to keep its liquidity. There are a few indicators of liquidity, the two most common are the so-called current ratio and quick ratio. [3]

The current ratio of liquidity is calculated:

$$\text{Current ratio} = \frac{\text{short term assets}}{\text{current liabilities}}$$

Current ratio is the proportion of short-term and current assets and the short-term or current liabilities.

Quick ratio is calculated:

$$\text{Quick ratio} = \frac{\text{cash} + \text{marketable securities} + \text{accounts receivable}}{\text{current liabilities}}$$

### 3.1.4 Ratio of the Financing and Using of Financial Leverage

Financing ratios show the importance of the owner structure of financing and interest charge, as well as other

fixed remunerations that arise as a consequence of using external sources of financing. The most common ratios of this group are:

- Debt-to-asset ratio,
- Debt-to-equity ratio,
- Coverage ratio. [3]

$$\text{Debt-to-asset ratio} = \frac{\text{total debt}}{\text{total assets}}$$

The debt-to-asset ratio shows what level of risk the company's creditors are subject to considering the financial structure of a source, and it shows what the fixed interest charge that burdens a company's business operations is.

$$\text{Debt-to-equity ratio} = \frac{\text{total debt}}{\text{equity}}$$

The debt-to-equity ratio can also be calculated as a relation between the long-term liabilities and the majority of the ownership equity because such a ratio is convenient for the optimization of the company's financial structure.

$$\text{Debt-to-equity ratio} = \frac{\text{long-term liabilities}}{\text{equity}}$$

## 3.2 Measuring Success by Relative Ratios of Success

When measuring the global (total) results of a company, we have to discern different influences so that economics could adequately interpret that the effects of each one of the necessary element influences by its effect on the end result. At the starting point of the contemporary idea business success, there is the idea of the economic principle or the principle of the least assets, which expresses tendency to:

- Accomplish the maximum effect (outputs, income, returns, profits) by using the resources at the disposal (sources, inputs, expenses, assets, investments or the so-called sacrifice);
- Accomplish the desired effects through a minimal investment of resources. [3]

Measuring success through manufacturing, cost-effectiveness and profitability of labor gives the necessary data about different results. This information will be especially needed if it is known that other companies with identical global results accomplish higher wages or dividends, or the faster rate of development (because they are capable of extracting funds for the development of an investment). Not only is the goal to attain the data of the causes of the results' variance, but also to measure the need which has to be taken to make them relatively bigger.

### 3.2.1 Labor PRODUCTIVITY

The influence of human labor on the productivity of a company is called labor productivity or just productivity. Namely, labor productivity is the relationship between the total value of the output and labor hours invested into creating those outputs.



The simplest formula or the outset for calculating productivity is:

$$\text{Labor productivity} = \text{total output} / \text{labor hours}$$

The numerator of the abovementioned formula can also be:

- product quantity (pieces, tons, meters etc.),
- sales transactions (expressed in amount or money)
- transfer of goods, people and information,
- number of overnight stays in tourism, etc. [3]

### 3.2.2 Cost-Effectiveness

When dealing with cost-effectiveness, it is necessary to analyze individual segments of business operations or each individual input needed for getting the desired outputs for a company to come into market with.

Taking cost-effectiveness as a comprehensive expression of efficiency, it needs to be linked to the idea of economizing, which could be best defined as the rational management or rational, economic treatment of all elements that have an impact on achieving results and realizing income. Consequently, one can say that a comprehensive expression of efficiency can be explained as a relation between the total income and total expenses that occurred with the goal of making income. The relation is:

$$E = \frac{\sum \text{income}}{\sum \text{expenses}} \quad [3]$$

The quotient of this ratio shows how many kuna of income have been realized compared to each kuna spent. That is a significant indicator and it says a lot about the success of a business operation. The quotient expressed by an absolute number is enough of an indicator whether the business is economical or not.

If the quotient is:

- higher than 1, the business is economical,
- lower than 1, the business is uneconomical,
- equal to 1, the business is on the verge of being economical – there is no financial result. [3]

### 3.2.3 Return on Assets

The realization of income, i.e. profit, is the motive that inspires every entrepreneur to realize his or her business ideas and profit by initiating business processes. As the conditions in which business operations of companies take place may vary, the results will be different, too. By determining the ratio of the return on assets (income) and investments or expenses needed for the profit to come into realization, we measure the profitability or rentability. Profitability, as a part of an analysis, can be seen as a principle or indicator of success by the help of relative indexes of success. [3]

As a principle, it shows the rationality of a business process by attempting to achieve the maximum business profit with the assets invested (principal funds, capital), i.e.

by realizing the profit with the minimum investments, assets or one's own capital. As an index, profitability reflects the realistic state of the ratio between the profit and the assets invested. Operationally, it shows how many money units of a business profit are gained per unit of assets invested or how many units of assets need to be invested to achieve one unit of business profit. [3]

The general pattern of measuring rentability is the ratio between the profit (income) and capital:

$$\text{Asset profitability} = \frac{\text{income}}{\text{assets}} \times 100$$

When we put total expenditure of a company (i.e. expenses) into the denominator, we get a return on assets.

$$\text{Return on assets} = \frac{\text{business income}}{\text{business expenses}} \times 100$$

Accordingly, it is only the assets' profitability that can be considered the real indicator of profitability as it indicates how many units of business results are realized per each monetary unit of invested assets. [3]

## 3.3 Measuring Success in Terms of Value Based Management (VBM)

A lack of the coherence of goals in different interest groups in a company should be solved by applying value based management (VBM).

To achieve a viable value creation, a manager's success should be measured by means of criteria that can be directly linked to creating a value for owners. In a certain sense, VBM represents a mixture of different economic disciplines and subjects. For instance, the goal of increasing value for the company's owners was taken from financing, together with the discounted cash flow technique. The principle of value creation as a result of investing in the company's activities in which the company has comparative advantages before the potential and existing competition was taken from the field of business strategies. It was from accounting that the adjusted basic structure of financial reports was taken.

VBM is a combination of principles, convictions and processes that make it possible for a company to be successful in fighting the competition from the outside and the institutional imperatives within a company. From a general point of view, VBM can be defined as an integrated system of management and control which measures and supports the creation of values. [3]

Important features of VBM:

- Management – VBM represents a system of controlling and managing, i.e. a certain set of tools used in unifying resources and tasks with the purpose of achieving certain goals,
- Concept – basic values of the concept are definitely and permanently conducted through all levels of an organization,
- Maximizing the company owner's values – basic purpose of VBM is to create as much as possible of a

net value by allocating the company's resources to the most valuable investments, which includes predicting and focusing on the future results of a business. [3]

VBM is an integrating process of improving the operational and strategic decision-making of a company as a whole. In a company that has accepted the concept of managing focused on value, the managing processes such as planning and the estimation of success offer the decision makers certain data and encouragement that help them conduct the measures that lead to the basic goal of business, the growth of value.

The procedure of setting the goals of VBM is based on the next principles:

- goals need to include the financial and non-financial aspects and need to be based on the quality components of a particular business activity,
- goals have to be adjusted to the level of managing that they are being set for,
- mutual time inter-relatedness of goals is necessary, too, i.e. for the long-term goals to be the continuation of the long-term ones. [3]

The biggest error that can arise when assessing the success of management and consequently awarding the managers is connecting the managers' success to the accounting results, instead of evaluating the success related to the realization of a certain strategy or the specific indicators of a certain activity.

The following principles apply for the system of business success evaluation:

- rating the success of a specific business unit – each unit in a company is assessed based on its own success indicators,
- relating success assessment to the short-term and long-term goals of a specific business unit,
- combining the financial and operational criteria based on value factors,
- introduction of indicators that operate as systems of an early forewarning of a possible crisis. [3]

VBM can be seen as a continuous process which begins with strategic planning so as to achieve the comparative advantages that will generate the growth of economic profits and the shareholders' yield. The economic features of an industrial environment in which a company makes business determine the form of financial reports of a company which are reflected through the analysis of the traditional criteria of success.

#### 4 PROGRAM TOOLS FOR BUSINESS PROCESSES

The goal of all program tools for modeling and of the analysis of business processes is to document and analyze the existing business processes and propose improvement based on that analysis.

Tools for modeling and the analysis of business processes are program solutions that managers, IT experts, analysts and end users apply for creating the models of

business processes in an organization, for storing the data of those models and their analysis. From the functionality point of view, those tools enable the documentation and analysis of the existing situation and the documentation of the proposal of the improvement and analysis of the expected effects of the proposed changes. [1]

Program tools for managing business processes differ in capabilities, reliability and the adjustment with the IT standards. They also differ in prices and that is why making a decision on which one to choose is very difficult.

Producers of the tools for managing business processes implement different strategies so as to achieve the biggest possible success on the market. Some producers adjust their program solutions to the specifications of certain businesses, and some develop universal program solutions, applicable to all companies. [1]

#### 5 CONCLUSION

It is most important to point out that the success of making business has to be attuned to the business strategy of a company. Business indicators are the inevitable tools of examining and exploring a company's business efficacy. The right choice is possible only in case when the mission, vision and goal projects get clearly defined by the management.

Because of the global competition on the market, companies can achieve the competitive advantage only by offering cheaper and better quality products and services, for which efficient and innovative business processes are needed. Performing business processes is in the focus of the attention of the management and their strategy. For that reason, business processes become the core of a company's functioning, because it is all about processes before products or services.

Companies that want to be successful have to embrace the principles of business orientation. Process orientation is not a synonym for the process organizational structure. It determines understanding the course of business and it is only the first step in the process-oriented organizational structure.

For a successful conduct of projects, it is very important to apply the appropriate program tools. The decision of the choice of the optimal program tool depends on the quality and the options of a tool, but also on the goals of a project. Even the best tools can turn out to be very bad if we try to apply them to the environment that does not have enough knowledge to use them or understand them.

The more different methods there are built into a tool, the better; more options are offered, but at the same time they are more complex and expensive.

#### 6 REFERENCES

- [1] Bosilj Vukšić, V. & Kovačić, A. (2004). *Upravljanje poslovnim procesima*. Sinergija nakladništvo, Zagreb.
- [2] Bosilj Vukšić, V., Hernaus, T., & Kovačić, A. (2008). *Upravljanje poslovnim procesima: Organizacijski i informacijski pristup*. Školska knjiga, Zagreb.

- [3] Dvorski, S. & Kovšca, V. (2011). *Ekonomija za poduzetnike*. Tiva tiskara, Varaždin.
- [4] Marić, G. (2006). *Upravljanje poslovnim procesima*. Školska knjiga, Zagreb.
- [5] Žugaj, M. & Cingula, M. (1992). *Temelji organizacije*. Foing, Varaždin.
- [6] Nidžara Osmanagić, B. (2007). *Kontroling – Abeceda poslovnog uspjeha*. Školska knjiga, Zagreb.
- [7] [http://agririsk.agr.hr/Upravapdf/Poslovni\\_pokazatelji.pdf](http://agririsk.agr.hr/Upravapdf/Poslovni_pokazatelji.pdf) (Accessed on 15.08.2017)
- [8] [http://www.agr.unizg.hr/cro/nastava/oduli/doc/87437\\_pokazatelji\\_uspjesnosti.pdf](http://www.agr.unizg.hr/cro/nastava/oduli/doc/87437_pokazatelji_uspjesnosti.pdf) (Accessed on 15.08.2017)

**Authors' contacts:**

**Ivica Kaniški, mag.oec.**

Ante Starčevića 38, G. Knežinec  
42204 Turčin, Croatia  
099/372-0774  
[ivica.kaniski@gmail.com](mailto:ivica.kaniski@gmail.com)

**Ivan Vincek, mag.oec.**

Jurketinec 60, 42243 Maruševac, Croatia  
091/501-8171  
[ivanvincek92@gmail.com](mailto:ivanvincek92@gmail.com)

# MATRICES IN COMPUTER GRAPHICS

Nataša LONČARIĆ, Damira KEČEK, Marko KRALJIĆ

**Abstract:** In this article, the usage of matrices and matrix operations in computer graphics is shown. A brief overview of geometric transformations in computer graphics is given. The "Matrix - Computer Graphics" application software is created for the representation and easier understanding of relations between geometric transformations and matrix calculus.

**Keywords:** computer graphics; geometric transformations; matrices; "Matrix - Computer Graphics" application software

## 1 INTRODUCTION

Computer graphics is a computing field that involves the creating, storing and processing of image content via computer. It has a wide application in science, engineering, art and especially in the field of entertainment, movies and video games. [3, 2] Computer graphics began to progress in the 1960s when the first interactive creation of graphic content was enabled, and since then it has been developing incredibly quickly [6]. It is important to note that computer graphics applications are used for various educational purposes. For example, computer graphics applications can, in the education process, help people with learning difficulties [10], assist students in understanding computer science algorithms [4], as well as increasing students' interest in programming and computer graphics [1].

## 2 2D TRANSFORMATIONS

The fundamental part of computer graphics are geometric transformations that can change the position, size, orientation and shape of an object. Basic geometric transformations in a 2D plane are called 2D transformations and those are translation, rotation, scaling, reflection and shear. Furthermore, each of the well-known transformations is briefly explained in [11], [9].

Before considering the abovementioned transformations, it should be noted that for any point  $T(x, y)$  in a 2D plane, a column vector or row vector representation can be used. In this article, column vector representation is used, i.e. point  $T$  is represented as  $T = \begin{bmatrix} x \\ y \end{bmatrix}$ .

### 2.1 Translation

Translation is a geometric transformation that moves the current point  $T = \begin{bmatrix} x \\ y \end{bmatrix}$  to the point  $T' = \begin{bmatrix} x' \\ y' \end{bmatrix}$  for a given vector  $\vec{t} = t_x\vec{i} + t_y\vec{j} = \begin{bmatrix} t_x \\ t_y \end{bmatrix}$ . Translation is shown in Fig. 1.

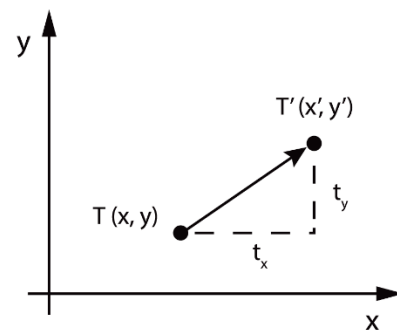


Figure 1 Translation

Therefore, point  $T'$  can be written as:

$$T' = T + \vec{t} \quad (1)$$

and in matrix notation as:

$$\begin{bmatrix} x' \\ y' \end{bmatrix} = \begin{bmatrix} x \\ y \end{bmatrix} + \begin{bmatrix} t_x \\ t_y \end{bmatrix}. \quad (2)$$

### 2.2 Rotation

Let  $O(0,0)$  and  $\theta$  be a point and an angle given respectively. Rotation around the point  $O(0,0)$  by the angle  $\theta$  is a transformation that maps every point  $T$  in the plane to the point  $T'$  in such a manner that the following properties are true:

$$|OT| = |OT'| \text{ and } \angle TOT' = \theta$$

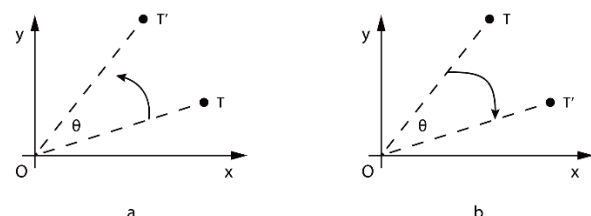


Figure 2 Rotation

By convention, rotation by the positive angle  $\theta$  goes counter-clockwise (Fig. 2a), while rotation by the negative angle  $\theta$  goes clockwise (Fig. 2b).

Rotation of the point  $T(x, y)$  located at the angle  $\phi$  from the horizontal  $x$  coordinate with a distance  $r$  from the origin of the coordinate system leads to a new point  $T'(x', y')$ . By using standard trigonometry, coordinates of the point  $T(x, y)$  can be expressed as:

$$x = r \cos \phi \quad (3)$$

$$y = r \sin \phi \quad (4)$$

Similarly, coordinates of the point  $T'(x', y')$  can be expressed as:

$$x' = r \cos(\phi + \theta), \quad (5)$$

$$y' = r \sin(\phi + \theta). \quad (6)$$

By using the equations (3) and (4), as well as addition formulas, the following formulas can be obtained:

$$x' = r \cos \phi \cos \theta - r \sin \phi \sin \theta = x \cos \theta - y \sin \theta, \quad (7)$$

$$y' = r \cos \phi \sin \theta + r \sin \phi \cos \theta = x \sin \theta + y \cos \theta, \quad (8)$$

which can be, in a matrix form, written as:

$$\begin{bmatrix} x' \\ y' \end{bmatrix} = \begin{bmatrix} \cos \theta & -\sin \theta \\ \sin \theta & \cos \theta \end{bmatrix} \cdot \begin{bmatrix} x \\ y \end{bmatrix}. \quad (9)$$

### 2.3 Scaling

Scaling is a mapping that expands or compresses each point coordinate. The scaling of each coordinate is determined by the scaling factor  $S$ . If the scaling factors for each coordinate are different, scaling is disproportionate. If the scaling factors are the same for all coordinates, scaling is proportional. For the point  $T(x, y)$  and the scaling factor  $S_x$  and  $S_y$  that scales the point  $T(x, y)$  in the  $x$  and  $y$  direction respectively, the following coordinates of the point  $T'$  are obtained:

$$x' = S_x \cdot x, \quad (10)$$

$$y' = S_y \cdot y. \quad (11)$$

In the matrix form, equations (10) and (11) can be written as:

$$\begin{bmatrix} x' \\ y' \end{bmatrix} = \begin{bmatrix} S_x & 0 \\ 0 & S_y \end{bmatrix} \cdot \begin{bmatrix} x \\ y \end{bmatrix}. \quad (12)$$

For example, for the scaling factors  $S_x = S_y = 2$ , the scaling process of the square is shown in Fig. 3.

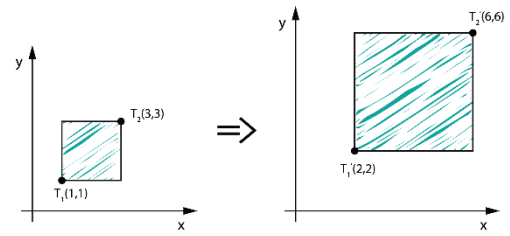


Figure 3 Proportional scaling of the square

### 2.4 Reflection

Reflection is a special case of a scaling where the size of the object does not change. For the scaling factors  $S_x = -1$  and  $S_y = 1$ , reflecting is about the  $y$  axis. If the scaling factors are  $S_x = 1$  and  $S_y = -1$ , there is a reflection about the  $x$  axis. For the scaling factors  $S_x = S_y = -1$ , reflection is about the  $x$  and  $y$  axes. In Fig. 4, reflections about the  $x$  and  $y$  axes of Super Mario, the main character in the Super Mario video games as an original object, are shown.

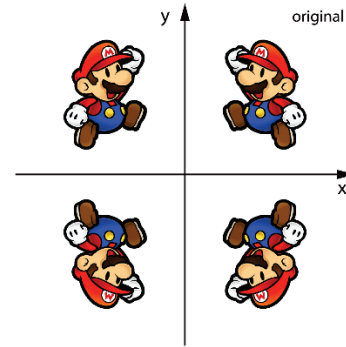


Figure 4 Reflection

### 2.5 Shear

Skewing the object with respect to the  $x$  or  $y$  axis is called shear transformation. Skewing by the angle  $\alpha$  with respect to the  $x$  axis and by the angle  $\beta$  with respect to the  $y$  axis is illustrated in Fig. 5.

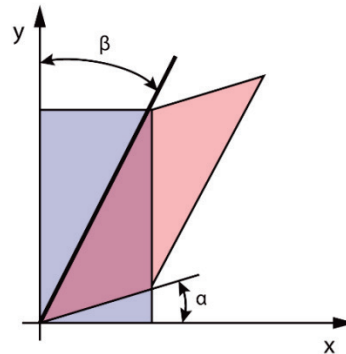


Figure 5 Shear

Coordinates of the point  $T'(x', y')$  can be defined as:

$$x' = x + y \cdot \tan \beta, \quad (13)$$

$$y' = y + x \cdot \tan \alpha. \quad (14)$$

In the matrix form, point  $T'$  can be represented as:

$$\begin{bmatrix} x' \\ y' \end{bmatrix} = \begin{bmatrix} 1 & \tan \beta \\ \tan \alpha & 1 \end{bmatrix} \cdot \begin{bmatrix} x \\ y \end{bmatrix} \quad (15)$$

## 2.6 Homogeneous Coordinate System

The process of implementing several successive transformations is, by using Cartesian coordinates, computationally more extensive. Namely, it can be noticed that to perform translation, matrix addition is carried out, while to perform other transformations, only matrix multiplication is carried out. In order to treat all transformations in the same manner, i.e. to reduce them to matrix multiplication, homogeneous coordinates are introduced. Thus, each Cartesian point  $T(x, y)$  can be converted into homogeneous coordinates  $T(x, y, w)$ , and a coordinate system with this point representation is called a homogeneous coordinate system. Although triples of coordinates commonly display a point in space, here they represent a point in the plane or 2D point. Two sets of homogeneous coordinates,  $(x, y, w)$  and  $(x', y', w')$ , represent the same point if one is a multiple of the other. For example, coordinates  $(1, 2, 3)$  and  $(2, 4, 6)$  represent the same point. It can be concluded that one point in homogeneous coordinates can be displayed in infinitely many ways, that is, one whole class of triples of coordinates represents the same point in the plane. This class of triples of coordinates which represent one point in the plane  $(t_x, t_y, t_w)$ , where  $t \neq 0$ , actually represents a line in the 3D space. It should be noted that at least one homogeneous coordinate must be different from zero, meaning that the point  $(0, 0, 0)$  is not allowed. If the coordinate  $w \neq 0$ , each of them can be divided by  $w$ , which is why the point  $T$  can be written as:

$$T(x, y, w) = T\left(\frac{x}{w}, \frac{y}{w}, 1\right) = (x_w, y_w, 1) \quad (16)$$

All such points form a plane with the equation  $w = 1$  in the 3D space. In the case of  $w = 0$ , it is a point in infinity, which will not be considered in more detail.

The usage of homogeneous coordinates is of great importance in computer graphics. Homogeneous coordinates provide a uniform mathematical tool for all transformations, where matrix transformation through homogeneous coordinates must be in the  $3 \times 3$  form [8].

In that sense, homogeneous translation matrix becomes:

$$M_{tr} = \begin{bmatrix} 1 & 0 & t_x \\ 0 & 1 & t_y \\ 0 & 0 & 1 \end{bmatrix}, \quad (17)$$

where translation is reduced to a matrix multiplication:

$$\begin{bmatrix} x' \\ y' \end{bmatrix} = \begin{bmatrix} x \\ y \end{bmatrix} + \begin{bmatrix} t_x \\ t_y \end{bmatrix} \rightarrow \begin{bmatrix} x' \\ y' \\ 1 \end{bmatrix} = \begin{bmatrix} 1 & 0 & t_x \\ 0 & 1 & t_y \\ 0 & 0 & 1 \end{bmatrix} \cdot \begin{bmatrix} x \\ y \\ 1 \end{bmatrix} \quad (18)$$

Furthermore, the homogeneous translation matrix is:

$$M_{tr} = \begin{bmatrix} 1 & 0 & t_x \\ 0 & 1 & t_y \\ 0 & 0 & 1 \end{bmatrix}, \quad (19)$$

homogeneous rotation matrix:

$$M_{ro} = \begin{bmatrix} \cos \phi & -\sin \phi & 0 \\ \sin \phi & \cos \phi & 0 \\ 0 & 0 & 1 \end{bmatrix}, \quad (20)$$

homogeneous scaling matrix:

$$M_{sc} = \begin{bmatrix} S_x & 0 & 0 \\ 0 & S_y & 0 \\ 0 & 0 & 1 \end{bmatrix} \quad (21)$$

and homogeneous shear matrix:

$$M_{sh} = \begin{bmatrix} 1 & \tan \beta & 0 \\ \tan \alpha & 1 & 0 \\ 0 & 0 & 1 \end{bmatrix}. \quad (22)$$

In order to conduct several sequences of the transforms, all these transformations must be compound. After the implementation of all transformations, for example scaling, rotation and translation over the point  $T$  in this original order, and the coordinates of the point  $T'$  could be calculated in the following way:

$$T' = M_{tr} \cdot M_{ro} \cdot M_{sc} \cdot T, \quad (23)$$

i.e. they could be calculated by multiplying the homogeneous scaling matrix, homogeneous rotation matrix and homogeneous translation matrix, respectively, into a single matrix.

## 3 "MATRIX – COMPUTER GRAPHICS"

In high school or at the faculty level education, matrix calculus is an integral and significant part of the mathematics curriculum for students. One of the possible ways of matrix operation implementation is computer graphics.

In order to better illustrate the relations between geometric transformations and the matrix calculus described in the previous section, the "Matrix - Computer Graphics" application software that provides a simple interface for studying 2D graphics is created. This application software is written in C#, an object-oriented programming language. One can find more about C#, for example, in [5,7]. The "Matrix – Computer Graphics" application is available at: [http://www.mediafire.com/file/pgv2jkrp0gqg47/Matrix\\_-\\_Computer\\_Graphics.exe](http://www.mediafire.com/file/pgv2jkrp0gqg47/Matrix_-_Computer_Graphics.exe) or



[http://www.mediafire.com/file/84b4dhwonqcb78c/Matrix\\_-\\_Computer\\_Graphics.zip](http://www.mediafire.com/file/84b4dhwonqcb78c/Matrix_-_Computer_Graphics.zip)

Using the "Matrix - Computer Graphics" application you can easily apply one of the abovementioned transformations on the desired object. Students can easily draw the desired object in the coordinate system and optionally, by using the determined matrices, apply the corresponding geometric transformations. One of the possibilities is to optionally enter data in the upper matrices for the corresponding transformation (translation, rotation, scaling or shear) of the drawn object, or to directly insert only the rotation angle or shear angles of the drawn object with respect to the  $x$  or  $y$  axis in the two lower matrices as shown in Fig. 6.

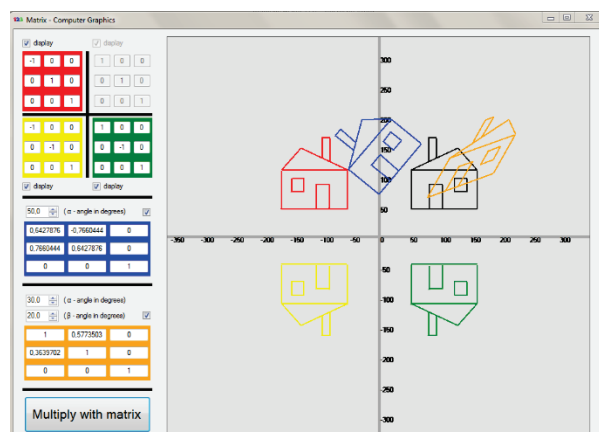


Figure 6 "Matrix - Computer Graphics" example

## 4 CONCLUSION

Computer graphics is an unavoidable part of everyday life. As it is widely known, computer graphics is present in computer games, films, television commercials, as well as in various branches of the industry. In this paper, authors tried to get closer to the students who are dealing with computer science, especially computer graphics, the mathematical background of computer graphics in which the term matrix is in the center. Although computer graphics is nowadays usually 3D, in this paper the authors looked only at 2D transformations in order to show, in a simpler way, the relationship between the matrix calculus and geometric transformations used in computer graphics. For this purpose, the "Matrix - Computer Graphics" application gives a contribution in the visualization and easier learning of relationships between the matrices and their applications on display and positioning, as well as on transforming different objects on a computer.

## 5 REFERENCES

- [1] Bruno, J., Jan, V., & Slaby, A. (2009). Computer Graphics in Computer Science Education. *Problems of Education in the 21<sup>st</sup> Century*, 11, 60-68.
- [2] Hearn, D. D., Baker, M. P., & Carithers, W. (2014). *Computer Graphics with Open GL*, 4<sup>th</sup> Edition. Pearson Education Limited.
- [3] Hughes, J. F., van Dam, A., McGuire, M., Sklar, D. F., & Foley, J. D. (2014). *Computer Graphics: Principles and Practice*, 3<sup>rd</sup> Edition. Addison-Wesley.
- [4] Naps, T. L. (2005). JHAYÉ: Supporting Algorithm Visualization. *IEEE Computer Graphics and Applications*, 25(5), 49-55. <https://doi.org/10.1109/MCG.2005.110>
- [5] Petricek, T. & Skeet, J. (2010). *Real-World Functional Programming: With Examples in F# and C#*, 1<sup>st</sup> Edition. Manning Publications.
- [6] Salomon, D. (2011). *The computer graphics manual*, Volume 2. Springer-Verlag London Limited. <https://doi.org/10.1007/978-0-85729-886-7>
- [7] Sharp, J. (2013). *Microsoft Visual C# 2013 Step by Step (Step by Step Developer)*, 1<sup>st</sup> Edition. Microsoft Press.
- [8] Skala, V. (2006). Length, Area and Volume Computation in Homogeneous Coordinates. *International Journal of Image and Graphics*, 06(04), 625-639. <https://doi.org/10.1142/S0219467806002422>
- [9] Srivastav, M. K. (2016). Transformation of an Object in Computer Graphics: A Case Study of Mathematical Matrix Theory. *Elixir Comp. Engg.* 100, 43396-43399.
- [10] Vera, L., Campos, R., Herrera, G., & Romero, C. (2007). Computer graphics applications in the education process of people with learning difficulties. *Computers & Graphics*, 31, 649-658. <https://doi.org/10.1016/j.cag.2007.03.003>
- [11] Vince, J. (2010). *Mathematics for Computer Graphics*, 3<sup>rd</sup> Edition. Springer-Verlag London Limited. <https://doi.org/10.1007/978-1-84996-023-6>

### Authors' contacts:

**Nataša LONČARIĆ**, Lecturer  
Tehnička škola Čakovec  
Športska 5, 40000 Čakovec, Croatia  
e-mail: [naloncario@unin.hr](mailto:naloncario@unin.hr)

**Damira KEČEK**, Senior Lecturer  
University North, University Center Varaždin  
104. brigade 3, 42000 Varaždin, Croatia  
e-mail: [dkecek@unin.hr](mailto:dkecek@unin.hr)

**Marko KRALJIĆ**, Student  
Faculty of Organization and Informatics  
Pavlinska 2, 42000 Varaždin, Croatia

14pt  
14pt  
**ARTICLE TITLE ONLY IN ENGLISH (Style: Arial Narrow, Bold, 14pt)**

14pt  
**Ivan HORVAT, Thomas JOHNSON (Style: Arial Narrow, Bold, 11pt)**

**Abstract:** Article abstract contains maximum of 150 words and is written in the language of the article. The abstract should reflect the content of the article as precisely as possible. TECHNICAL JOURNAL is a trade journal that publishes scientific and professional papers from the domain(s) of mechanical engineering, electrical engineering, civil engineering, multimedia, logistics, etc., and their boundary areas. This document must be used as the template for writing articles so that all the articles have the same layout. (Style: Arial Narrow, 8pt)

8pt  
**Keywords:** keywords in alphabetical order (5-6 key words). Keywords are generally taken from the article title and/or from the abstract. (Style: Arial Narrow, 8pt)

10pt

10pt

## 1 ARTICLE DESIGN

(Style: Arial Narrow, Bold, 10pt)

10pt

(Tab 6 mm) The article is written in Latin script and Greek symbols can be used for labelling. The length of the article is limited to eight pages of international paper size of Letter (in accordance with the template with all the tables and figures included). When formatting the text the syllabification option is not to be used.

10pt

### 1.1 General guidelines

(Style: Arial Narrow, 10pt, Bold, Align Left)

10pt

The document format is Letter with margins in accordance with the template. A two column layout is used with the column spacing of 10 mm. The running text is written in Times New Roman with single line spacing, font size 10 pt, alignment justified.

Article title must clearly reflect the issues covered by the article (it should not contain more than 15 words).

Body of the text is divided into chapters and the chapters are divided into subchapters, if needed. Chapters are numbered with Arabic numerals (followed by a period). Subchapters, as a part of a chapter, are marked with two Arabic numerals i.e. 1.1, 1.2, 1.3, etc. Subchapters can be divided into even smaller units that are marked with three Arabic numerals i.e. 1.1.1, 1.1.2, etc. Further divisions are not to be made.

Titles of chapters are written in capital letters (uppercase) and are aligned in the centre. The titles of subchapters (and smaller units) are written in small letters (lowercase) and are aligned left. If the text in the title of the subchapter is longer than one line, no hanging indents.

10pt

Typographical symbols (bullets), which are being used for marking an item in a list or for enumeration, are placed at a beginning of a line. There is a spacing of 10pt following the last item:

- Item 1
- Item 2
- Item 3

10pt

The same rule is valid when items are numbered in a list:

1. Item 1
2. Item 2
3. Item 3

10pt

### 1.2 Formatting of pictures, tables and equations

(Style: Arial Narrow, 10pt, Bold, Align Left)

10pt

Figures (drawings, diagrams, photographs) that are part of the content are embedded into the article and aligned in the centre. In order for the figure to always be in the same position in relation to the text, the following settings should be defined when importing it: text wrapping / in line with text.

Pictures must be formatted for graphic reproduction with minimal resolution of 300 dpi. Pictures downloaded from the internet in ratio 1:1 are not suitable for print reproduction because of unsatisfying quality.

10pt

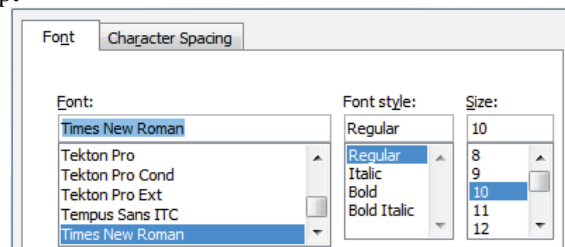


**Figure 1** Text under the figure [1]  
(Style: Arial Narrow, 8pt, Align Centre)

10pt

The journal is printed in black ink and the figures have to be prepared accordingly so that bright tones are printed in a satisfactory manner and are readable. Figures are to be in colour for the purpose of digital format publishing. Figures in the article are numbered with Arabic numerals (followed by a period).

Text and other data in tables are formatted - Times New Roman, 8pt, Normal, Align Center.

When describing figures and tables, physical units and their factors are written in italics with Latin or Greek letters,

while the measuring values and numbers are written upright.

10pt

**Table 1** Table title aligned centre  
(Style: Arial Narrow, 8pt, Align Centre)

	1	2	3	4	5	6
ABC	ab	ab	ab	ab	ab	ab
DEF	cd	cd	cd	cd	cd	cd
GHI	ef	ef	ef	ef	ef	ef

10 pt

Equations in the text are numbered with Arabic numerals inside the round brackets on the right side of the text. Inside the text they are referred to with equation number inside the round brackets i.e. “.... from Eq. (5) follows ....” (Create equations with MathType Equation Editor - some examples are given below).

10pt

$$F_{\text{avg}}(t, t_0) = \frac{1}{t} \int_{t_0}^{t_0+t} F(q(\tau), p(\tau)) d\tau, \quad (1)$$

10pt

$$\cos \alpha + \cos \beta = 2 \cos \frac{\alpha + \beta}{2} \cdot \cos \frac{\alpha - \beta}{2}. \quad (2)$$

10pt

Variables that are used in equations and also in the text or tables of the article are formatted as *italics* in the same font size as the text.

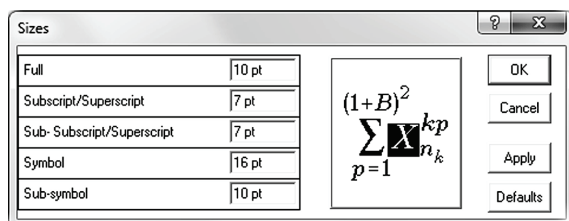


**Figure 2** The texts under figures  
(Style: Arial Narrow, 8pt, Align Centre)

Figures and tables that are a part of the article have to be mentioned inside the text and thus connected to the content i.e. „, ... as shown in Fig. 1...” or „data from Tab. 1...” and similar.

10pt

## 2 PRELIMINARY ANNOTATION

10pt

Article that is offered for publication cannot be published beforehand, be it in the same or similar form, and it cannot be offered at the same time to a different journal. Author or authors are solely responsible for the content of the article and the authenticity of information and statements written in the article.

Articles that are accepted for publishing are classified into four categories: original scientific papers, preliminary communications, subject reviews and professional papers.

**Original scientific papers** are articles that according to the reviewer and the editorial board contain original theoretical or practical results of research. These articles need to be written in such a way that based on the information given, the experiment can be repeated and the

results described can be achieved together with the author's observations, theoretical statements or measurements.

**Preliminary communication** contains one or more pieces of new scientific information, but without details that allow recollection as in original scientific papers. Preliminary communication can give results of an experimental research, results of a shorter research or research in progress that is deemed useful for publishing.

**Subject review** contains a complete depiction of conditions and tendencies of a specific domain of theory, technology or application. Articles in this category have an overview character with a critical review and evaluation. Cited literature must be complete enough to allow a good insight and comprehension of the depicted domain.

**Professional paper** can contain a description of an original solution to a device, assembly or instrument, depiction of important practical solutions, and similar. The article need not be related to the original research, but it should contain a contribution to an application of known scientific results and their adaptation to practical needs, so it presents a contribution to spreading knowledge, etc.

Outside the mentioned categorization, the Editorial board of the journal will publish articles of interesting content in a special column. These articles provide descriptions of practical implementation and solutions from the area of production, experiences from device application, and similar.

10pt

## 3 WRITING AN ARTICLE

10pt

Article is written in the English language and the terminology and the measurement system should be adjusted to legal regulations, standards (ISO 80 000 series) and the SI international system of units. The article should be written in third person.

**Introduction** contains the depiction of the problem and an account of important results that come from the articles that are listed in the cited literature.

**Main section of the article** can be divided into several parts or chapters. Mathematical statements that obstruct the reading of the article should be avoided. Mathematical statements that cannot be avoided can be written as one or more addendums, when needed. It is recommended to use an example when an experiment procedure, the use of the work in a concrete situation or an algorithm of the suggested method must be illustrated. In general, an analysis should be experimentally confirmed.

**Conclusion** is a part of the article where the results are being given and efficiency of the procedure used is emphasized. Possible procedure and domain constraints where the obtained results can be applied should be emphasized.

10pt

## 4 RECAPITULATION ANNOTATION

10pt

In order for the articles to be formatted in the same manner as in this template, this document is recommended for use when writing the article. Finished articles written in MS Word for Windows and formatted according to this

template must be submitted using our The Paper Submission Tool (PST) (<https://tehnickiglasnik.unin.hr/authors.php>) or eventually sent to the Editorial board of the Technical Journal to the following e-mail address: [tehnickiglasnik@unin.hr](mailto:tehnickiglasnik@unin.hr)

The editorial board reserves the right to minor redaction corrections of the article within the framework of prepress procedures. Articles that in any way do not follow these authors' instructions will be returned to the author by the editorial board. Should any questions arise, the editorial board contacts only the first author and accepts only the reflections given by the first author.

10pt

## 5 REFERENCES (According to APA)

10pt

The literature is cited in the order it is used in the article. Individual references from the listed literature inside the text are addressed with the corresponding number inside square brackets i.e. "... in [7] is shown ...". If the literature references are web links, the hyperlink is to be removed as shown with the reference number 8. Also, the hyperlinks from the e-mail addresses of the authors are to be removed. In the literature list, each unit is marked with a number and listed according to the following examples (omit the subtitles over the references – they are here only to show possible types of references):

9pt

- [1] See <http://www.bibme.org/citation-guide/apa/>
- [2] See [http://sites.umuc.edu/library/libhow/apa\\_examples.cfm](http://sites.umuc.edu/library/libhow/apa_examples.cfm)
- [3] (Style: Times New Roman, 9pt, according to APA)
- [4] Amidzic, O., Riehle, H. J., & Elbert, T. (2006). Toward a psychophysiology of expertise: Focal magnetic gamma bursts as a signature of memory chunks and the aptitude of chess players. *Journal of Psychophysiology*, 20(4), 253-258. <https://doi.org/10.1027/0269-8803.20.4.253>
- [5] Reitzes, D. C., & Mutran, E. J. (2004). The transition to retirement: Stages and factors that influence retirement adjustment. *International Journal of Aging and Human Development*, 59(1), 63-84. Retrieved from <http://www.baywood.com/journals/PreviewJournals.asp?Id=0091-4150>
- [6] Jans, N. (1993). *The last light breaking: Life among Alaska's Inupiat Eskimos*. Anchorage, AK: Alaska Northwest Books.
- [7] Miller, J., & Smith, T. (Eds.). (1996). *Cape Cod stories: Tales from Cape Cod, Nantucket, and Martha's Vineyard*. San Francisco, CA: Chronicle Books.
- [8] Chaffe-Stengel, P., & Stengel, D. (2012). *Working with sample data: Exploration and inference*. <https://doi.org/10.4128/9781606492147>
- [9] Freitas, N. (2015, January 6). People around the world are voluntarily submitting to China's Great Firewall. Why? Retrieved from [http://www.slate.com/blogs/future\\_tense/2015/01/06/tencent\\_s\\_wechat\\_worldwide\\_internet\\_users\\_are\\_voluntarily\\_submitting\\_to.html](http://www.slate.com/blogs/future_tense/2015/01/06/tencent_s_wechat_worldwide_internet_users_are_voluntarily_submitting_to.html)

(Style: Times New Roman, 9pt, according to APA)

10pt

10pt

### Authors' contacts:

8pt

**Full Name, title**  
Institution, company  
Address  
Tel./Fax, e-mail

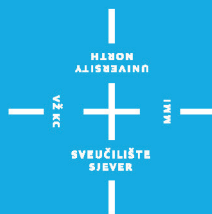
8pt

**Full Name, title**  
Institution, company  
Address  
Tel./Fax, e-mail



TEHNIČKI GLASNIK / TECHNICAL JOURNAL – GODIŠTE / VOLUME 12 – BROJ / NUMBER 2

LIPANJ 2018 / JUNE 2018 – STRANICA / PAGES 62-123



**Sveučilište  
Sjever**

SVEUČILIŠTE SJEVER / UNIVERSITY NORTH – CROATIA – EUROPE

ISSN 1846-6168 (PRINT) / ISSN 1848-5588 (ONLINE)

TEHNICKIGLASNIK@UNIN.HR – [HTTP://TEHNICKIGLASNIK.UNIN.HR](http://tehnickiglasnik.unin.hr)